ENHANCING FOAM STABILITY BY THE USE OF SURFACTANTS MIXTURES FOR EOR PURPOSES

A Dissertation

by

MOHAMMED ABDULLAH M ALMOBARKY

Submitted to the Office of Graduate and Professional Studies of
Texas A&M University
in partial fulfillment of the requirements for the degree of

DOCTOR OF PHILOSOPHY

Chair of Committee,	David S. Schechter
Committee Members,	Jerome Schubert
	Hadi Nasrabadi
	Berna Hascakir
	Mahmoud El-Halwagi
Head of Department,	A. Daniel Hill

December 2017

Major Subject: Petroleum Engineering

ABSTRACT

This experimental research investigates the opportunity to enhance the oil recovery by enhancing the foam stability by the use of surfactants mixtures in comparison with individual surfactants. The mixtures were prepared with commercially available individual surfactants. They were also tested and compared with the individual surfactants in terms of foam stability in presence and absence of crude oil, mobility reduction, and enhancing the oil recovery.

The screening and comparison processes were achieved in four experimental stages: preliminary experimental work, static tests combined with both interfacial tension measurements and bubbles sizes, dynamic tests for mobility control evaluation and core flooding experiments for oil recovery.

Shaking tests showed that binary surfactants mixtures perform better when a good foamability agent was mixed with a good foam-oil stabilizer. Observations indicated that mixtures are better in foam stability in presence and absence of crude oil, lower in CMC, lower in $\sigma_{g/w}$ and $\sigma_{o/w}$, generated higher foam viscosity in porous media and produced more oil than individual surfactants.

In comparison with AAS anionic surfactant, mobility results showed a 5.12-fold decrease in mobility using AAS-IOS mixture, 6.32-folds using AAS-AAS mixtures, and 3.42-folds using AAS-nonionic mixture. Moreover, AAS produced 2.5% additional oil recovery compared with 7.5% with AAS-IOS, and 7.48% with AAS-AAS mixture.

Mobility control evaluation in the high permeability, in-house built, glass beads pack resulted in higher foam viscosity when using individual surfactants. However, the mixtures proved better performance in low permeability porous media at low shear rate. The contradictory behaviors were related to the differences in micellar stabilities of the individual surfactants and their mixtures.

For mobility control of $ScCO_2$, two anionic surfactants were examined and compared in terms of mobility reduction and in-situ foam viscosity. The newly developed complex nanofluid (CNF) surfactant generated higher foam viscosities at all conditions with and without salinity than that of AOS surfactant. In comparison with 27.54% additional oil recovery of $ScCO_2$ injection, AOS/$ScCO_2$ co-injection produced 1% more oil recovery, and CNF/$ScCO_2$ co-injection produced 8% addition oil recovery.

DEDICATION

I dedicate this dissertation to

My GOD for giving me the opportunity to live, worship and for all the blessings throughout my whole life.

My parents whom I am grateful for their love, selflessness, and believing in me;

My sister may ALLAH rest her soul in peace.

Special dedication to

My wife, Norah, for her patience and support,

My sons and daughter, Abdullah, Abdullaziz and Hanan,

My siblings, Turki and Amani,

My brothers and sisters, Maryam, Razan, Wijdan, Bayan, and Ahmed;

May ALLAH make your lives full of happiness, success, and prosperity.

ACKNOWLEDGEMENTS

I am truly grateful for the chair of the committee, Professor David S. Schechter, for his significant help, support, and guidance to make this work better. I would like also to thank the committee members: Professor Jerome Schubert, Professor Hadi Nasrabadi, Professor Berna Hascakir, and Professor Mahmoud El-Halwagi.

I am thankful for King Saud University in Riyadh, my employer in Kingdom of Saudi Arabia for their help and support in my scholarship.

My deepest thanks for Mr. John Maldonado for being always available for any requirements in the laboratories of the Petroleum Engineering department at Texas A&M University.

Being one proud aggie, thank you all Texas A&M faculty, staff, and students.

CONTRIBUTORS AND FUNDING SOURCES

This dissertation was fulfilled under the supervision of the chair of the committee, Professor David S. Schechter, and with the help of the committee members including Professor Jerome Schubert, Professor Hadi Nasrabadi, Professor Berna Hascakir; and Professor Mahmoud El-Halwagi.

The laboratory and research experimental devices were funded by Professor David S Schechter.

Experimental setup was prepared in cooperation with Zuhair Al-Yousef. The laboratory safety requirements were made available in cooperation with John Maldonado, the facilities coordinator in the Department of Petroleum Engineering, Texas A&M University.

The student completed all other experimental work in this dissertation independently.

The scholarship and tuition fees with graduate studies were funded by King Saud University in the Kingdom of Saudi Arabia.

NOMENCLATURE

A	Area per molecule at the air-water interface
AE	Alcohol ethoxylate
AEGS	Alcohol ethoxy glyceryl sulfonate
AES	Alcohol ethoxy sulfate
AESo	Alcohol ethoxy ethyl sulfonate
AOS	Alpha olefin sulfonate
API	American Petroleum Institute Oil Gravity
B	Bridging coefficient
bbl/day	barrel per day
BF	Betaine foaming agent
BP	British Petroleum, Oil Industry Company
BPR	Back pressure regulator
C	Concentration
C/W	CO_2 water interfaces
CMC	Critical Micelle Concentration
CO_2	Carbon Dioxide
CPC	Cetylpyridinium chloride
dA	Different in Surface Area
dG	Difference in Surface Free Energy

DI	Deionized water
E	Entering coefficient
EIA	Energy Information Administration
EO	Ethylene oxide
EOR	Enhanced Oil Recovery
FA-SAGD	Foam Assisted Steam Assisted Gravity Drainage
FHL	Foam half-life
FL	Foam column length
FL1	Foam height after 1-hr
FL2	Foam height after 2-h.
G/O	Gas-Oil interface
G/W	Air water interfaces
hfi	initial foam height
HLB	Hydrophilic Lipophilic Balance
hr.	hour
ID	Inside diameter
IFT	Interfacial tension
IOS	Internal olefin sulfonate
K	Permeability
$k_{r,displaced}$	Relative Permeability of the Displaced Fluid
$k_{r,Displacing}$	Relative Permeability of the Displacing Fluid
L	Lamellae number

M	Mobility Ratio
Mbbl/day	Million barrels per day
ml	Milliliter
MRF	Mobility Reduction Factor
N_2	Nitrogen
NBU	North Burbank Unit Crude oil
O/W	Oil-water interfaces
OBR	Overburden pressure
OD	Outside Diameter
OOIP	Original Oil In Place
OPES	Octylphenol ethoxyethylsulfonate
P	Pressure
Pc^*	Limiting Capillary Pressure
PEF	Polymer enhanced foam
PEG	Polyethylene Glycol
PO	Polypropylene oxide
POE	Polyoxyehtylene
PPM	Part per million
PV-inj	Pore volumes injected
S	Spreading coefficient
SAG	Surfactant Alternating Gas
SAGD	Steam Assisted Gravity Drainage

SB-1	Synthetic brine 1
SB-2	Synthetic brine 2
$ScCO_2$	Super critical CO_2
S_{or}	Residual oil saturation
S_{wi}	Irreducible water saturation
T	Time
WAG	Water Alternating Gas
XRD	X-Ray Diffraction
B	Interaction parameter
γ	Surface Tension
ΔP	Pressure drop
$\mu_{displaced}$	Viscosity of the Displaced Fluid
$\mu_{Displacing}$	Viscosity of the Displacing Fluid
μ_{foam}	Foam viscosity
$\sigma_{g/o}$	Gas-oil or air-oil surface tension
$\sigma_{g/w}$	Gas-water or air-water surface tension
$\sigma_{o/w}$	Oil-water surface tension
τ_1	Fast relaxation time
τ_2	Slow relaxation time
φ	Porosity
Γ	The amount of surfactants per unit area of the liquid-air interface
∇P^{min}	Minimum pressure gradient

TABLE OF CONTENTS

Page

Page

LIST OF FIGURES

Page

Page

Page

Page

Page

Page

Page

LIST OF TABLES

Page

Page

Page

CHAPTER I

INTRODUCTION

I.1 Dissertation Overview

Foam, in this study, is used as a mobility control agent to enhance the oil recovery. The surfactants mixtures were prepared by mixing individual surfactants. Both mixtures and individual surfactants were compared in terms of foam stability, mobility control, and enhancing oil recovery.

Chapter 1 provides an introduction that includes an overview of the oil recovery stages of oil reservoirs, fundamentals and definitions for EOR processes, foam in EOR applications and the study's objectives.

Chapter 2 provides a literature review and basic principles about foam application in EOR industry. It starts with a brief introduction about the surfactants as the main element in the foam system. Then, the foam definition is introduced and the surfactant role in foam stabilization or thin-film stability as well. After that, the applications of foam to assist the EOR processes which include foam generation and placement inside the porous media. Moreover, one separate section is provided about the use of surfactants mixtures in EOR as well as in enhancing the foam stability. Finally, a brief description covers the main challenges facing the foam applications in assisting EOR processes.

Chapter 3 includes lists of the materials, chemicals, and instruments utilized throughout the study. Moreover, it also shows the schematic diagrams of the experimental

setups and the protocols, in details, by which those experiments were performed. Finally, a flow chart showing the milestone or the methodology to achieve this research's objectives.

Chapter 4 introduces the results and discussions for the preliminary work. It includes a fast screening experimental process to understand the foamability and foam stability for the individual surfactants under investigation. It also provides the chemical stability of the surfactants in a synthetic reservoir brine solution. Then, it compares the foamability and foam stability for the individual surfactants and their mixtures at 1:1 mixing ratio.

Chapter 5 introduces the results and discussions of more comprehensive experimental investigation for the chosen mixtures during the preliminary work. Each chosen mixture was examined and compared with its individual surfactants in separate section. The comparisons were achieved in terms of foamability and foam stability in absence and presence of crude oil. Moreover, the comparisons and observations were explained by measuring the interfacial properties, performing mobility reduction evaluation and investigating the oil recovery by conducting core-flooding experiments.

Chapter 6 introduces the conclusions and recommendations based on the results of this research.

I.2 Oil Recovery Challenges

There are normally three main stages of oil recovery in an oil reservoir: primary, secondary and tertiary. In primary recovery, there are different mechanisms that displace

oil through the porous media toward the production wells such as water influx, solution gas drive, or gas cap drive that all depends on the reservoir pressure. The next stage in oil recovery is the secondary recovery in which the reservoir pressure is maintained by water or gas injection which also displaces oil toward the production wells (Green and Willhite 1998). After the primary and secondary recovery stages, nearly two-thirds of oil is left behind as an immobile oil due to a combination of physical, chemical, and geological reasons such interfacial tension (i.e. capillary forces) and reservoir's heterogeneity.

In tertiary stage, a variety of EOR processes can be employed to extract more oil (Green and Willhite 1998). Green and Willhite (1998) defined the EOR as any process includes injection of liquid or gas that does not exist naturally in the reservoir to interact with rock and/or hydrocarbons to extract and displace more oil. These interactions might result in interfacial tension reduction between oil and water and wettability alteration when using a carefully selected surfactant in surfactant flooding EOR process. Another example is the heavy oil reservoirs in which steam injection is employed as an EOR process to reduce the oil viscosity and extract more oil.

Different classifications were proposed for EOR methods. The US Department of Energy divided them into three main types: chemical injection processes, gas injection processes, and thermal recovery processes. Green and Willhite (1998) divided them into five types: chemical, miscible, thermal, mobility control, and microbial EOR. Taber et al. (1997) screened many laboratory studies, field projects and pilots for EOR applications. They found the most successful EOR processes are steam flooding as the best, chemical

flooding processes especially polymers for mobility control, and the most applied method of the EOR processes is the CO_2 flooding.

The need for EOR is inevitable due to the significant economic and technical challenges facing the oil industry. BP review (2016) predicted that the global consumption of energy has doubled than that of the year 2014. China oil imports grew by +6.3% and India by +8.1% (BP review, 2016). EIA (2016) reported a projected increase by 48% in the global oil consumption by 2040. At shorter term predictions, the global oil demand was 95.6 Mbbl/day in 2016 and will increase to 101.6 Mbbl/day by the year 2021. Moreover, their predictions showed an increase in both oil consumption and supply to 2018, but the consumption is increasing at a faster rate (EIA, 2016). Nowadays, mature oil fields are responsible for a significant amount of oil production, and EOR methods are suggested as a must to choose to face the challenges concerning the oil production decline and increasing demand (Manrique et al. 2010). All predictions for future oil consumption and demand confirms the importance to enhance the oil production capacity from matured oil reservoirs to meet the global increase in demand for energy. It is compelling to engineer new technologies or to enhance the currently available ones to extract as much as possible from the oil remaining underground.

Oil displacement processes such as EOR in petroleum reservoirs include two approaches for improving the oil sweep efficiency: microscopic and macroscopic efficiencies. Processes that occur in pores scale are called microscopic. Surfactant flooding, for instance, enhances the microscopic sweep efficiency by the interactions that

occur in microscale levels that induce lower oil-water interfacial tension and wettability alteration (Green and Willhite 1998).

Gas injection EOR methods include injecting CO_2, N_2, hydrocarbon gases, or flue gas. In fact, CO_2 miscible flooding is one of the most globally applied EOR methods according to Taber et al (1997). Furthermore, it was successfully applied in many field projects with impressive ability to enhance the oil recovery (Dong, Huang, and Srivastava 2000). In general, gas injection EOR processes are dramatically affected by viscous fingering, gas channeling, and gravity override that results in poor volumetric sweep efficiency, macroscopic efficiency, and low oil recovery, see **figure 1** (Borchardt et al. 1985; Healy, Holstein and Batycky 1994; Hadlow 1992; Farajzadeh et al. 2012). Another factor that affects oil displacement efficiency is the reservoir heterogeneity due to the presence of natural fractures, faults, and different vertical and horizontal permeability (Ahmed 2000).

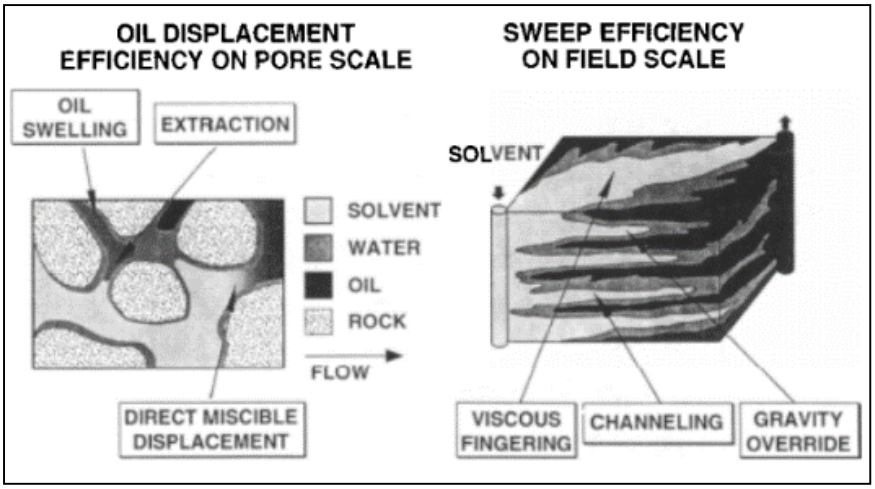

Figure 1: Viscous fingering, channeling, and gravity override impact in miscible flooding (Reprinted from Healy et al. 1994)

Despite the fact that the EOR processes are showing better performance than both primary and secondary recovery stages, but oil recovery using EOR encounters many technical challenges as follows:

1. EOR processes are very expensive;
2. High-temperature requirements and heat loss limitations in thermal flooding processes (Ali, 2003).
3. The need to increase the viscosity of the chemicals in chemical flooding processes with the addition of polymers which increases the cost dramatically.
4. The surfactant loss due to the adsorption at the reservoir rock is also a significant challenge.
5. Gas gravity segregation and viscous fingering are the most significant limiting factors for gas injection EOR processes (Sahimi et al., 2006; Green and Willhite, 1998), see figure 1.
6. A common challenge for all EOR processes is the irreversibility when it fails to enhance the oil recovery. There is no method to retrieve the injected chemicals. Moreover, none of these EOR processes can be universally applied at any reservoir. Each process has its limitations, and the selection must be achieved carefully and accurately based on the reservoir's petrophysical and fluids properties, and conditions. The influences on the injected EOR fluids in rocks and/or fluids properties are irreversible which makes EOR processes applications, in general, involve high-risk (Amro, Al Mobarky, and Al-Homaidhi 2007).

For gas injection processes, different methods and applications were proposed to overcome the gravity segregation and viscous fingering due to the low viscosity and density of the injected fluids: Water-Alternating-Gas (WAG), foam assisted EOR processes, and thickening agents to increase the gas viscosity (Casteel and Djabbarah, 1988; Enick et al., 2012).

The use of foam for mobility control has been successfully applied in laboratory scale as well as field scale (Turta and Singhal, 2002). Foam is a proven technology that successfully increases the viscosity of gases such as N_2 or CO_2, decreases the mobility of the displacing fluid, and leads to better sweep efficiency and higher oil recovery (Falls et al., 1988). Surfactant or foaming-agent plays a significant rule in foam technology (Borchardt et al., 1985). Moreover, many studies emphasized the importance of the chemical structure of surfactant and provided surfactant selection criteria (Borchardt et al., 1985; Nikolov et al., 1986).

The mobility control is usually described by a value called the mobility ratio. The mobility ratio is defined as the ratio of the mobility of the displacing fluid to the mobility of the displaced fluid, see **equation 1** (Green and Willhite 1998). For effective mobility control, M less than unity is favorable. It can be easily recognizable that increasing the displacing fluid viscosity or decreasing the reservoir oil viscosity will decrease M to the desired favorable conditions.

$$M = \frac{k_{r,\,Displacing} \,/\, \mu_{Displacing}}{k_{r,\,displaced} \,/\, \mu_{displaced}} \qquad (1)$$

I.3 Research Objectives

The objectives of this research are:

1. To examine different types of commercially available surfactants in terms of their ability to generate and stabilize foam at ambient and reservoir conditions;
2. To enhance the foamability and foam stability of the individual surfactants in absence and in presence of crude oil at ambient and reservoir conditions by the use of surfactants mixtures;
3. To demonstrate the possible mechanisms by which the surfactants mixtures enhance the foamability and foam stability in comparison with the individual surfactants;
4. To investigate the ability of the newly developed mixtures of surfactants, in comparison with the individual surfactants, to provide better mobility control and higher oil recovery;
5. To compare a newly developed anionic foaming agent with a commercially available anionic surfactant for the application of foam for mobility control in supercritical CO_2 EOR.

CHAPTER II

LITERATURE REVIEW

Foam stabilizing mechanisms are considerably dependent on the surfactant selected to perform as a foaming agent in foam for mobility control. The objective of this chapter is to introduce a literature review on foam definitions, stabilizing mechanisms, foam generation in porous media, foam for mobility control, field applications. The literature review also includes the importance of surfactants in foam stabilization. Furthermore, the differences in foam stabilization between surfactants and surfactants mixtures are also explained briefly.

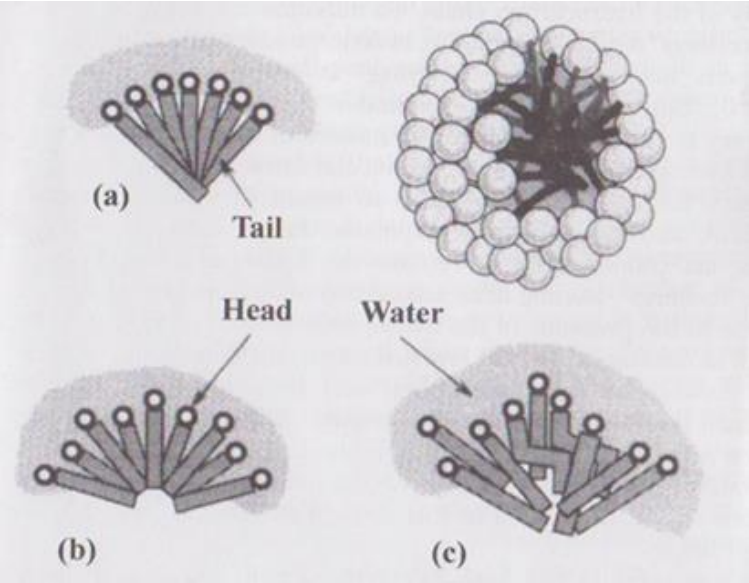

Figure 2: Surfactant molecule components (a) head and (b) tail. Surfactant micelle is at the top right corner (Reprinted from Schramm, 2000)

II.1 Foam Basic Principles and Definitions

II.1.1 Surfactants-Stabilized Foam

The surfactant is an acronym to surface active agents. The surfactants molecules show surface activity by orienting themselves in monolayers and reduce the surface or interfacial tension of the medium in which they are dissolved. The surfactant molecule includes two different parts with different properties: hydrophilic head and a hydrophobic tail, see **figure 2**. At low concentrations, the surfactant molecules exist separately. However, increasing the surfactant's concentration promotes these molecules to gather and form micelles at specific concentration, see **figure 2**. This concentration is called the Critical Micelle Concentration (CMC).

In liquid phase (i.e. water), the water molecules in bulk are attached equally by Van der Waals forces. However, the molecules that are adsorbed at the liquid-gas interface are contracted toward the interior of the liquid by forces that are called the surface tension or interfacial tension between gas and liquid (Porter, 1994).

For the gas to disperse and generate foam bubbles through the liquid phase, there should be a mechanical energy to expand the liquid interface or, in other words, a force to beat the contracting forces between the liquid molecules at the interface. If this energy cannot be maintained, reducing the interfacial tension between the two phases suffices, see **equation 2**.

$$dG = \gamma \, . \, dA \qquad (2)$$

Introducing even smaller amount of surfactant into the liquid phase reduces the amount of energy required for the gas to generate foam bubbles. The surfactant molecules

arrange themselves as a monolayer at the liquid-gas interface to reduce the interfacial tension (i.e. reducing the energy required to create foam bubbles in liquid). If the surface tension or interfacial tension between gas and liquid is γ, and dA is the expansion occurs at the liquid surface (i.e. change in surface area). Then, the energy required to expand the surface against the contracting forces is equal to the increase in surface free energy that accompanies the surface expansion (Schramm and Kutay 2000).

Foam is defined as a gas dispersion in liquid system in which the gas is considered the inner "discontinuous" phase, and the liquid is the external "continuous" phase (Bikerman, 1953). Marsden and Khan (1966) defined the foam as the gas-liquid emulsion that behaves as a viscous fluid in porous media. The foam was also defined as a dispersion of gas in the liquid phase where the gas bubbles are discontinued by lamellae or thin-films (Hirasaki 1989).

Foam bubbles shapes are different. The ideal shape for mobility control is shown in **figure 3**. It shows polyhedral foam bubbles in blue separated by lamellae or thin-films. Each three bubbles are separated by the plateau border. In this system, the surfactant is taking place in the liquid phase in the lamellae regions between the bubbles. As a fact, the foam stabilization mechanisms occur in these regions due to the presence of surfactants.

Pure liquids do not generate foam (Bikerman 1953; Schramm and Kutay 2000). When gas flows through pure liquids, the gas bubbles coalesce and rupture, or buoyancy holds them to the surface to rupture anyway. However, in presence of surfactant, the reduction in surface tension between gas and liquid facilitates the process of foam

generation. Moreover, the adsorption of surfactants molecules at the liquid-gas interface provides the most important stabilization mechanisms that will be explained next.

II.1.2 Thin Film or Lamellae Stability

Once the foam is generated, the liquid drainage from thin-film or foam coarsening occur. Liquid drainage is promoted by two factors: (i) gravity; and (ii) pressure difference (Schramm and Kutay 2000; and Rossen and Kunjappu 2004). Measuring the drainage rate of the liquid from lamellae determines the foam stability and the strength of the surfactant to stabilize the foam (Rossen and Kunjappu, 2004 from Lunkenheimer and Malysa 2003). Moreover, when the pressure in the lamellae is larger than the pressure in the plateau border, see **figure 4**, the liquid drains toward the plateau boarder and consequently the lamellae thins which lead to coalescence or rupture.

For foam stabilized with ionic surfactants, it is assumed that both interfaces of the lamellae hold equally the same charges. **Figure 4** shows positively charged lamella where both interfaces are stabilized with an ionic surfactant. The positively charged interface attracts ions that hold the opposite charges and opposes ions with the same charge forming the so called electric double layer. This equivalent double layer of charges on both interfaces induces electrostatic repulsion keeping the interfaces away from each other and opposing film thinning (Schramm and Wassmuth 1994).

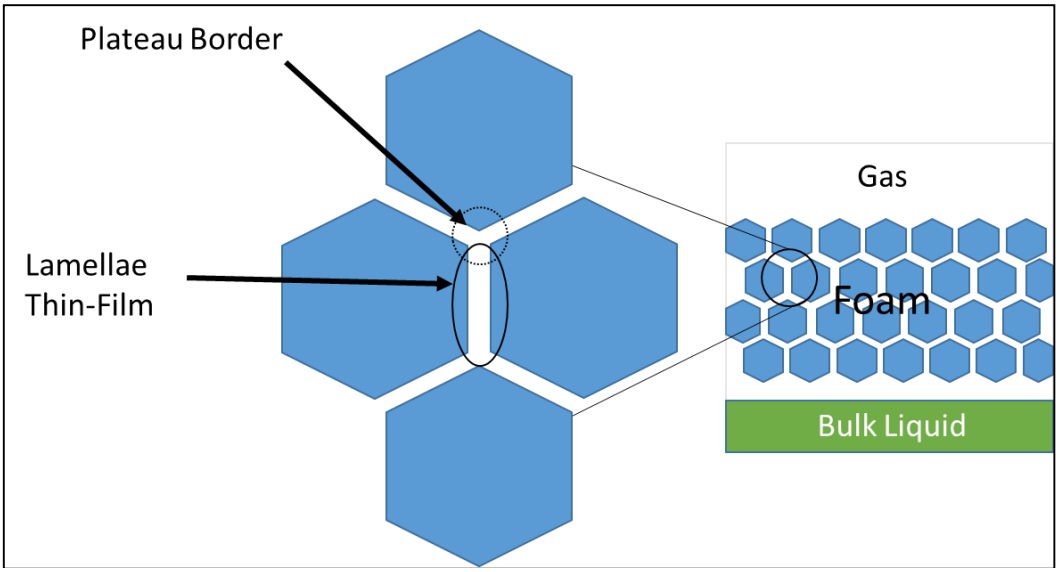

Figure 3: Foam bubble separated by liquid lamellae or thin-films (Modified from Schramm and Kutay 2000).

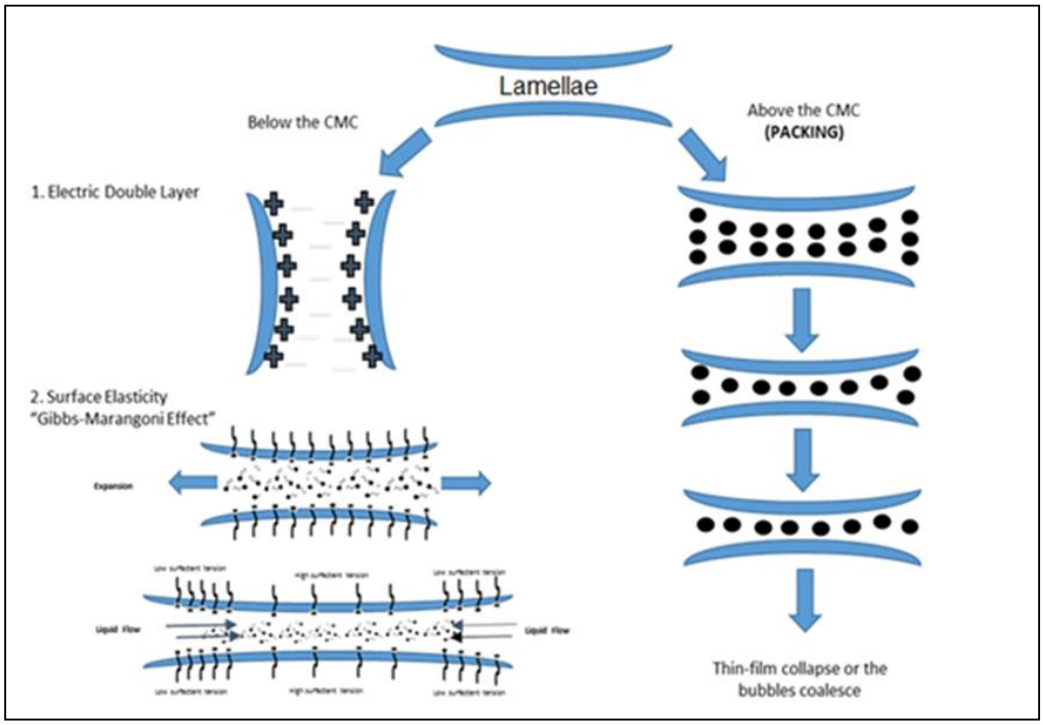

Figure 4: Thin-film stabilizing mechanisms by surfactants (Modified from Schramm and Wassmuth 1994)

The *surface elasticity* of thin-films is another extremely important factor for foam stability at low to moderate surfactant concentrations. Surface elasticity opposes film thinning by enabling the lamella to act against any occurrence of deformation. When a thin-film expands, see **figure 4**, the surface tension distribution at the liquid-gas interface is disturbed. This disturbance causes the center area at the interface to possess low surfactant concentration (e.g. high surface tension), whereas the edges of the interface possess high surfactant concentration (e.g. low surface tension). This surface tension gradient promotes the thin-film surface elasticity and helps to reestablish the balance. The surfactant molecules act to reestablish the equilibrium in two actions:

- Surfactants at the edges of the interface will diffuse from high to low surfactant concentration area (i.e. toward the center of the thin-film), and
- The second action is the diffusion of the surfactant molecules in bulk liquid toward the interfaces where they are needed the most (i.e. at the high surface tension region). The diffusion of the surfactant molecules at the interface will enforce the liquid to return from the plateau border toward the center of lamella to oppose film thinning and reestablishes the balance.

This mechanism along with all actions involved is called the Marangoni effect which is one of the fundamental factors to stabilize the thin-films and the entire foam system. In the absence of this surface tension gradient, the thin-film lacks elasticity which leads to continuous thinning until rupture occurs. Moreover, the optimum efficiency of the Marangoni effect is obtained at specific surfactant concentration at which all actions occur

at the right moment for the thin-film to withstand the surface tension gradient (Schramm and Wassmuth 1994).

Thin-film stabilizing mechanisms that were mentioned above occur at low to moderate surfactant concentrations. **Figure 4** also shows the thin-film stabilizing mechanisms at high surfactant concentration. It shows that the film thinning occurs in a stepwise pattern where every step of the thinning process accompanies the removal of one single layer of the micelles "black dots in **figure 4** above" from the lamella.

At high surfactant concentrations, higher than the CMC, there is one universally acceptable stabilizing mechanism, it is the ordered micellar structure or packing of micelles at which the film thinning exhibits gradual thinning at more than one metastable state (Wasan, Koczo and Nikolov 1994; Manev Sazdanova and Wasan 1984).

Nikolov et al. (1989) conducted an experimental study to provide a physical explanation of the stratification phenomena of the lamella thinning process at high surfactants concentrations. The number and height of the steps were measured and investigated for different surfactants of different carbon chain lengths, with and without electrolytes. They found the following:

- The height of every single drop in thin-film thickness is approximately equal to the size of the micelle.
- The precise measurements of the steps' heights showed that every step is approximately equal to the summation of the micelle size (diameter) and the Debye diameter (the electric double layer around the micelle).

- The number of steps depends on the electrostatic repulsive forces between the micelles that depend directly on the electric double layer or the Debye diameter.

The study concluded that:

- The single drop in the lamella thickness is caused by the removal of one single layer of the micelles that were orderly structured in the lamellae.
- The longer carbon chain length enhances the micellization (e.g. lowers the CMC). This leads to a stronger packing of the ordered micellar structure inside the lamellae. As a result, it increases the number of steps for film thinning which indicates better foam stability.
- Electrolytes cause the Debye diameter of the micelle to decrease which lowers the strength of the packing (i.e. ordered micellar structure) in the lamellae. Therefore, the number of steps of the stratification decreases which indicates faster foam collapse. They also reported that the stratification disappeared at a critical concentration of electrolytes indicating that the foam stability was severely affected by the high electrolytes concentration.

Foam disjoining pressure is also another way to describe the lamella stability. When the disjoining pressure in the lamellae is positive, it represents the dominance of the repulsive forces (high foam stability), and the decrease in disjoining pressure <0 represents the dominance of the attractive forces. For more information, (Kovscek and Radke, 1994) is recommended.

II.2 Foam Assisting EOR Applications

II.2.1 Foam in Porous Media

The static bulk foam properties were described in the previous section. Foam properties in porous media are always explained using the foam properties in bulk even with the differences between the behaviors of foam in bulk and in porous media (Zhang, Freedman, and Zhong 2009). Therefore, both behaviors are indispensable, and the next section is to explain the foam behavior in porous media and for EOR.

Foam as a mobility control agent in gas drive processes in mature oil fields was patented for Bond and Holbrook at 1958 (Bond and Holbrook 1958). However, Fried (1961) was the first to investigate the idea experimentally (Hirasaki, 1989). Fried (1961) reported 44-70% increase in oil recovery by the use of foam for mobility control in waterflooded unconsolidated sandstones. The oil recovery was found to increase as the oil viscosity increased. Fried attributed the results to the ability of foam to divert the injected fluids inside the reservoir and reduce the gas relative permeability.

To describe the foam in porous media, Falls and Hirasaki (1988) divided the types of foam in porous media into two types: continuous gas foam and discontinuous gas foam. Their main conclusion was that the presence of the lamella, everywhere, inside the porous media prevents the continuous gas flow. Moreover, these lamellae must be pushed inside the porous media for the gas to flow.

II.2.2 Foam Generation

In-situ foam generation can be achieved using three methods:

- Gas-liquid co-injection,
- SAG (surfactant alternating gas) injection mode (Farajzadeh et al., 2012), and
- Pre-generated foam by the use of external foam generator (Turta and Singhal, 2002; Haugen et al., 2012). The in-situ foam generation is intended to increase the viscosity in order to enhance the volumetric sweep efficiency (Kovscek and Radke, 1994).

In-situ foam generation mechanisms include:

1. Lamellae leave-behind mechanism,
2. Capillary snap-off mechanism, and
3. Lamellae division mechanism.

The leave-behind mechanism occur when two adjacent pore throats are entered by two gas streams, and it is responsible for weak foam generation (Kovscek and Radke 1994). Moreover, the capillary snap-off generation mechanism depends on water saturation, capillary pressure, pore geometry and wettability (Sanchez and Hazlett, 1992). Many studies observed that snap-off mechanism favors heterogeneous porous media where capillary pressure decreases with increasing permeability (Ransohoff and Radke 1988). Lamellae division occurs after the generation of the lamella in porous media (Falls and Hirasaki. 1988). This mechanism of foam generation depends on the pore geometry, bubble size, pressure gradient and gas velocity (Falls and Hirasaki. 1988). Both Capillary

snap-off and lamella division mechanisms are believed responsible for strong foam generation (Falls and Hirasaki. 1988).

Gauglitz et al. (2002) experimentally investigated N_2 and CO_2 foam generation in different porous media of different permeabilities, surfactants, concentrations, and temperatures. They observed a minimum pressure gradient that must be exceeded to maintain the strong foam generation in porous media. Furthermore, this minimum pressure gradient for strong foam generation with dense CO_2 foam is smaller than that of N_2 foam which could be < 1psi/ft. Moreover, As the permeability increases, the minimum pressure gradient for strong foam generation decreases which is in line with Rossen and Gauglits (1990). This indicates that strong foam generation at lower permeable porous media requires high flow rate, whereas low flow rate is required in high permeable porous media for strong foam generation.

Dicksen, Hirasaki, and Miller (2002) in an experimental study investigated the foam generation in different homogeneous porous media at different permeabilities. For a strong foam generation in homogeneous porous media in transient experiments, the pressure drop must approach or exceed a specific “critical” pressure drop at which the strong foam generation will start to control the mobility. The start of the strong foam generation is usually observed experimentally as a rapid jump in pressure drop across the porous media. Moreover, the rapid jump in the pressure drop indicates the beginning of strong foam generation at which the gas starts to mobilize one or more lamellae formed inside the porous media along with the existence of the snap-off mechanism for foam generation. This critical pressure drop depends on the surfactant composition,

concentration, and shear rate. If this critical pressure drop was not maintained or exceeded, it would result in low mobility control due to the dominant single gas phase flow.

II.2.3 Foam for Mobility Control and Oil Recovery

Huh, and Handy (1989) measured the gas relative permeability to compare the unsteady and steady state methods in the displacement of surfactant solution by N_2 foam in Berea sandstone. N_2 injection induced in-situ foam generation which successfully delayed the gas breakthrough and enhanced the efficiency of the displacement. Both methods resulted in lower gas relative permeability in presence of foam with a better reduction in the steady-state method. They attributed the higher reduction in gas relative permeability in steady state method to the better lamellae stability where the distribution of gas and liquid saturations work in favor of more lamella stabilities.

Tsau and Heller (1992) experimentally evaluated different surfactants or foaming agents with dense CO_2 injection (2500 psi) below the CMC in dolomite cores. For CO_2/Brine flow, increasing the CO_2 fraction increases the mobility and reduces the resistance factor. Moreover, increasing the quality decreases the mobility of CO_2/surfactant solution (Foam) and increases the resistance factor. Resistance factor was at the minimum at qualities range 20 – 33.33%. Furthermore, increasing the flow rate increases the mobility and decreases the resistance factor. For pressure drop responses with different qualities, pressure drop normally fluctuated but at different peaks intervals for different qualities. At low qualities up to 50%, the peaks intervals range between 50 to 100 psi, and the range was extremely smaller (5 to 10 psi) for qualities above 50%.

Lee, Heller, and Hoefer (1991) conducted an experimental study using an anionic surfactant, commercial name and manufacturer were only exposed, and $ScCO_2$ to investigate the mobility reduction of $ScCO_2$ by generating $ScCO_2$ foam and the effect of concentration on mobility and foam stability. It was observed that the foam apparent viscosity increases and mobility decrease as the permeability of rock increases. Moreover, the higher the concentration is the lower the mobility. The authors attributed that to the lamellae stabilization as well as bubbles generation and destruction. Therefore, the higher the concentration of surfactant increased the magnitude of the population of bubbles that induced lower dense CO_2 mobility.

Lawson and Riesberg (1980) performed an experimental investigation to use foam for mobility control instead of polymer in chemical flooding in consolidated sandstone and carbonate cores. They concluded that foam can be utilized as an alternative of polymer for mobility control in chemical flooding processes.

Chen, Margot, and Kovscek (2010), in a simulation study, proposed the use of foam for mobility control in Steam Assisted Gravity Drainage (SAGD). The study concluded that Foam Assisted- SAGD (FA-SAGD) is better than SAGD. The FA-SAGD delayed the steam breakthrough, yielded 5% lower steam production, and 30% more oil recovery than that of SAGD.

Farajzadeh et al. (2010) investigated the use of foam in miscible and immiscible floods using both N_2 and CO_2 gases with AOS surfactant. They conducted core flood experiments with the aid of CT scanner and used SAG injection mode for foam generation. At low pressure and room temperature, N_2 foam resulted in higher pressure drop, higher

recovery, and earlier breakthrough than that of CO_2 foam. The lower pressure drop and the delay in CO_2 breakthrough in miscible CO_2 were attributed to the higher CO_2 dissolution in water. The dispersion of N_2 foam was larger than CO_2 because of the lower amount of CO_2 remaining due to CO_2 water dissolution. At supercritical condition (90 bar and 50°C), $ScCO_2$ injection exhibited gas channeling through the core and had no sharp interface at the flood front. The flood front disappeared in oil zone due to the low foam-oil tolerance. Foam assisting Sc CO_2 flooding resulted in 19% higher oil recovery and higher pressure drop than that of Sc CO_2 flooding without foam. At miscible conditions (137 bar and 50°C), CO_2 foam again had 10% more recovery and higher pressure drop than miscible CO_2 flooding.

Haugen et al. (2012) experimentally investigated the viability of foam in fractured oil wet limestone in comparison with strongly water wet model. Core flood experiments were conducted using pre-generated foam injection and SAG. The pre-generated resulted in higher oil recovery from the oil-wet rock than that of strongly water wet. The study concluded that the results showed successful foam generation in oil-wet rock, water wet rock, and in fractured oil wet cores.

In an experimental study, Li et al. (2012) investigated the use of foam, using SAG injection mode, for wettability alteration, IFT reduction, and control the mobility in alkaline surfactant chemical flooding. The foam was injected after reducing the IFT and changing the wettability in an oil wet 2D sand pack model at 19:1 permeability contrast. They found that foam flood using SAG injection successfully displaced the oil from the high permeability layer, but poor displacement in low permeability layer due to the

dramatic effect of oil on foam stability. As a result, in another run, the blend was mixed with a zwitterionic surfactant (the foam booster lauryl betaine) to enhance the foam-oil tolerance. The addition of the foam booster enabled the foam to produce more oil from the low permeability layer. The alkaline surfactant foam flood recovered 89.4% of the remaining oil after water flooding resulting in 95% total oil recovery.

Turta and Singhal (2002) provided a new survey for over 40 years of foam field applications for different aspects of the oil industry. Here are some examples of the field applications of foam mentioned in the above survey. They reported 12 foam application, among 42 field applications in total, with miscible CO_2 flooding and 6 of the 12 projects were in Texas, USA. The reservoir had low permeability 2-20 md and with an ultimate recovery between 40-50% of OOIP was recovered after WAG application. Using 0.2-0.5wt% of Chaser CD-1045 surfactant, they started with 15 days of surfactant injection cycle and co-injection mode. Co-injection resulted in a loss of injectivity, whereas the use of SAG performed better than co-injection. The best practice was found by performing very fast SAG, with quality ranges between 20-80%, along with continuous WAG. The surfactant injection cycle was reduced to 2-days instead of 15-days. Furthermore, McElmo Creek reservoir in Utah, USA, is a very stratified reservoir of 19-layers at permeability ranges 0.01-1000 md. Co-injection was tested first which resulted in injectivity loss. Consequently, they stopped co-injection and continued with CO_2 injection. 82,000 bbl of CO_2 was injected to restore the injectivity followed by SAG. The reports showed that foam application was beneficial to reduce the GOP by 2-folds and the thief-zone problem was solved by the presence of foam. In a very low permeable reservoir with 5-md, East Mallet

pilot in Texas, USA has been under CO_2 injection for a long time with ultimate recovery 40% OOIP before foam application. Co-injection used first and resulted in the loss of injectivity and converted to SAG. Another pilot for foam field applications, EVGSAU project in the USA is the second most successful foam application because the application was preceded with extensive testing in laboratory. Moreover, this projected lived the longest among all field applications for four years. The problem was premature "early" gas breakthrough from the producer that was noticed to be closer to the injector than in other field applications. The plan was to inject 85% surfactant slug followed by the remaining 15% in a very fast SAG injection. The reported results showed injectivity reduction, 25% increase in reservoir pressure, 12% of the injected fluid was successfully diverted from the thief zone to other zones, GOR decreased by 2-folds and 2-folds increase in oil recovery. Moreover, 10-20 times increase in oil rate was observed in the other producers in the same pattern.

II.3 Mixed Surfactants Systems for Foam

All industries that include interfacial interactions in their chemical processes use mixed surfactants for two reasons: cheaper and might perform better than individual pure surfactants. For our purposes in oil industry, mixed surfactant systems are also applied in EOR applications for reducing the $\sigma_{o/w}$ as well as $\sigma_{g/w}$ in foam application in mobility control.

The main objective of mixing surfactants is to have a mixture that has lower CMC and IFT than that of the individual surfactants (Holland and Rubingh 1992, and Hill 1993).

For foam systems, particularly, studies should be directed toward the measurements of the parameters of the G/W interfaces, whereas the investigations for O/W systems should be directed toward the phase behavior (Hill 1993).

One of the most important factors to understand the interfacial activities is the CMC determination. Knowing the CMC leads to the following:

- To know the onset of the constant monomers concentration. The monomer concentration at any concentration above the CMC is constant;
- To determine the rate at which this surfactant reduce the IFT as the concentration increases below the CMC;
- To identify the maximum ability of this surfactant to lower the IFT. In other words, the lowest IFT value at the surfactant's CMC.
- To measure the adsorption and the area/molecule at the interface. The surface tension vs. logarithmic concentration plot shows a straight line for the concentrations below the CMC. This straight line describes the interfacial activity. The sharper the slope of this straight line is the higher the surface activity, and consequently, the lower the area/molecule at the interface (Hill 1993).

To elucidate the behavior of mixed surfactants systems, **figure 6** shows binary mixed surfactants where one is shown with filled heads and the other with empty heads. **Figure 6** shows the way that the two surfactants form mixed micelles, mixed monolayer at the G/W interface, and mixed bilayer at the solid surface (Holland and Rubingh 1992).

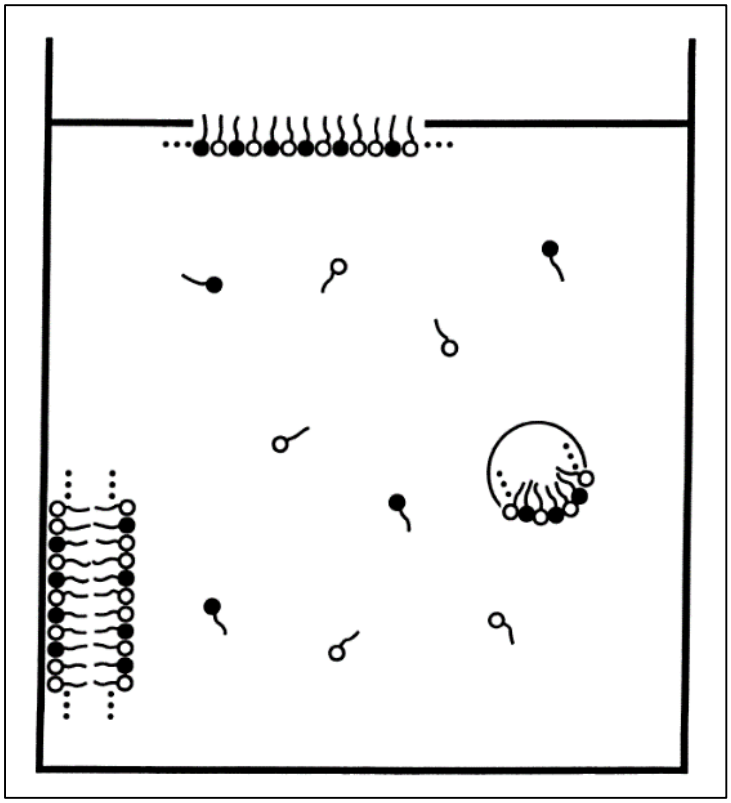

Figure 5*: Binary mixed surfactants system. (Reprinted from Holland and Rubingh 1992)*

II.3.1 Selection of Foam Stabilizers

According to Lai and Dixit (1996), there are plenty of additives that can be used to enhance the foam stability. However, there is no universally accepted technique for selecting the appropriate foam stabilizer or additive for foam. The authors provided a guidelines based on the studies conducted to facilitate the selection process. The following are the main points mentioned:

1. Start with the charge of the surfactant to choose the additive that ensures intuitively the existence of interactions between charges:
    a. For cationic foaming agents use nonionic additives;

b. Amides and amine oxides additives are the best foe enhancing the anionic foaming agents foam stability;

c. For nonionic foaming agents, use anionic or cationic additives;

2. Consider the chemical structure of the foaming agent in the selection of the foam stabilizer: choose the additive that has compatible carbon chain length with the foaming agent.
3. Choose the additive that has the maximum ability to lower the CMC of the foaming agent.
4. Choose the additive with good polarity to ensure the ability to form hydrogen-bonding with water as well as with the foaming agent.

II.3.2 Foam Stability Enhancement by Surfactants Mixtures

Schick and Fowkes (1957) conducted an experimental study to correlate the ability of the nonionic surfactants, as additives, to enhance the foam stability of the anionic surfactants, as detergents. The investigation conducted was to correlate the ability of the nonionic alcohols to lower the CMC and enhance foam stability. They concluded that there is a correlation between lowering the CMC and enhancing foam stability. Moreover, all alcohols were able to reduce the CMC, but the alcohols with straight carbon chains resulted in the maximum CMC reduction and foam stability enhancement. Furthermore, the higher the CMC reduction is the better the foam stability enhancement were observed. Moreover, the antifoaming effect of oleic acid was significantly mitigated in presence of the additives. The study also found that the mixed micelles sizes are larger than that of the

detergent's micelles. They concluded that these results are due to the additives' attachment to the palisade layer of the detergent's micelles not into the interior of the micelles.

Ross and Bramfitt (1957) investigated the effect of nonionic additives on anionic detergents to destabilize or to enhance the stability of foam using conductivity measurements. When mixing nonionic additive with anionic detergent at concentrations above their CMCs, the conductivity may increase or decrease as the concentration of the additive increases. They generalized or upgraded Schick and Fowkes (1957) observations as following: foam stabilizing agents decrease conductivity, whereas the foam destabilizing agents increase the conductivity and consequently, inhibits foaming.

Sharma, Shah and Brigham (1984) investigated the effect of carbon chain length on foam microscopic properties and fluid displacement in porous media. The study used mixtures of the anionic SDS surfactant with nonionic alcohols of different carbon chain lengths. They reported that the lowest surface tension, maximum shear surface viscosity of foaming solutions, lowest mobility in porous media, highest fluid recovery, longest time for gas to breakthrough and smallest bubble sizes were observed when both SDS and the alcohol possessed the same carbon chain lengths.

Oh and Shah (1991) investigated the micellar stability effects in foaming ability of SDS surfactant and mixtures of SDS with alcohols. They measured the *slow* relaxation time of the micelles, as a direct measure of the micellar stability, of SDS and the mixtures of SDS and 1-Hexanol. Moreover, they also correlate the micellar stability with the foam ability. They found that when micellar stability increases, foaming ability decreases, and foam stability increases.

Patist, Axelberd and Shah (1998) investigated the effect of carbon chain length of the alcohols when mixed with SDS. They found that SDS provides the maximum micellar stability at 200 mM concentration. Mixing SDS, at concentrations below 150 mM, with alcohols causes the slow relaxation time or the micellar stability to increase. However, above 150 mM SDS concentrations, mixtures exhibited lower micellar stability except for SDS with C12OH mixtures in which the carbon chain lengths of SDS and the alcohol are equal. They concluded that mixing two surfactants with equal carbon chain length enhances the micellar stability, decreases the foaming ability, but enhances the foam stability.

In the same study, foaming ability investigation were conducted using two methods to compare SDS and SDS-C12OH mixture: shaking for high shear rate and air-blown surfactant solution for low shear rate. They concluded that when the surfactant exhibits high micellar stability, the foamability decreases but the foam stability increases. On the other hand, when micellar stability is lower due to mixing, the foamability increases and the foam stability decreases.

Patist, Devi, and Shah (1999) investigated the effect of mixing SDS anionic surfactant with Cetylpyridinium chloride (CPC) at low concentrations on surface tension, shear surface viscosity, evaporation rate on G/W interface, and foaming ability. It was observed that mixing SDS with CPC decreases the CMC. Moreover, SDS/CPC mixtures at 1:3 and 3:1 molar ratios resulted in minimum surface tension, maximum surface viscosity, minimum evaporation on G/W interface, and minimum foam ability. In contrast with 3:1 molar ratio, 1:3 mixture enhanced foam stability significantly.

Bera, Ojha, and Mandal (2013) investigated the synergistic effect on foamability and foam stability of the anionic SDS, cationic Cetrylmethylammonion bromide surfactant, and their mixtures with alcohol ethylates, nonionic surfactants, of different carbon chain lengths C12-C18. They concluded that the synergistic effect was more obvious with the anionic-cationic mixtures than that of anionic-nonionic mixtures. This result was attributed to the maximum surface adsorption and minimum area/molecule of the cationic surfactant.

Theander and Pugh (2003) conducted synergistic investigation for mixing two nonionic surfactants (C12E6 and C14E6) with fatty soap acid (Sodium Oleate; NaOl). The synergy using intermolecular interactions from which they used to describe the foam properties, i.e. foaming ability and foam stability. This study concluded that correlating the sing intermolecular interaction parameter with foam properties is difficult. They added long discussion about the parameters that should be considered when investigating foaming systems using either surfactants or mixed surfactant systems. The recommended parameters for foam systems investigations are the adsorption and diffusion of the surfactant toward the G/W interface, surfactants composition, structures, micellar stability, and carbon chain lengths compatibility. The same recommendation was mentioned by Hill (1993).

Patist et al. (2000) summarized three decades studies in the Center of Surface Science and Engineering at University of Florida. This summary was specifically written on micellar stability effects at the interfacial properties in mixed surfactants systems.

Some of these studies are summarized above while others are not. This is a chance to summarize the most significant findings of three decades researches:

1. Micellar stability have significant effect on interfacial activities of SDS. It is directly correlated with the slow relaxation time of the micelles. Increasing the micellar stability decreases the foamability but increases the foam stability. At low micellar stability, micelles disintegrates into monomers to enhance the foamability.
2. SDS anionic surfactant exhibits the highest micellar stability at 200 mM concentration. Increasing the concentration below 200 mM increases the slow relaxation time as well as micellar stability and foam stability but decreases foamability. However, increasing the concentrations > 200 mM for SDS, the micellar stability decreases and the foamability increases, whereas the foam stability decreases. Again, the direct correlation of micellar stability with foam stability, and the inverse correlation of micellar stability with foamability can be explained by the integration and disintegration of micelles (i.e. surfactant flux to the newly created interfaces);
3. Mixing SDS with $C_{12}OH$ alcohol increased the micellar stability, provided the minimum surface tension, and maximum shear surface viscosity. This was attributed to the strong ion-dipole interaction of SDS with $C_{12}OH$ alcohol.
4. For hydrocarbon-water systems at specific temperature and pressure, there is an optimum salinity at which ultra-low $\sigma_{o/w}$ can be obtained, and maximum oil recovery.

5. 1:3 and 3:1 molecular ratio of mixed surfactant systems is the optimum ratio due to the tight packing of hexagonal arrangement of the surfactant molecules in the mixed micelles and at the mixed monolayer.
6. Significant enhancement of SDS interfacial activities was noticed when SDS mixed with Tetraalkylammonium salts: the salt increased the micellar stability, decreased surface tension, enhanced foam stability, and minimized the foamability. Moreover, the optimum of all interfacial properties was observed at 5 mM salt concentration. However, micellar stability decreased as the salt concentration increased above 5mM.

Few studies investigated surfactant mixtures for foam applications in mobility control and enhanced oil recovery. Syahputra et al. (2000) found that lignosulfonate alone is a weak foaming agent. However, mixing lignosulphonate with other surfactants enabled better foam generation, better mobility control, and more oil recovery even at lower surfactant concentrations.

Kuhlman, Lau and Falls (2000) studied the foam stability experimentally on Berea sandstone and reservoir rock. The study employed three anionic surfactants of different ranges of ethoxylation and hydrophobic chain lengths, at high temperature, and high salinity. Mixing ethoxylated sulfonate with unethoxylated sulfonate enhanced the foam-oil tolerance.

Llave and Olsen (1994) found the surfactants mixtures in SAG injection mode generates stronger foam with significantly higher pressure drop than that of the individual surfactants, better foam-oil tolerance, and recovered more oil.

Tsau et al. (1999) found that mixing nonionic and anionic surfactants generated more stable foam, lower mobility of CO_2, and less adsorption than that of each surfactant alone.

These results clearly indicate that if synergism exists in surfactants mixtures, they might perform better for foam mobility control which will lead to better sweep efficiency and higher oil recovery.

II.4 Foam Challenges

II.4.1 Foam-Oil Tolerance

Almost all researchers and studies summarized above agree upon the power of crude oil to destabilize foam. Moreover, all agree that it is still under investigation and that foam with crude oil interactions are complex and enigmatic with many unanswered questions. It is a fact that low foam-oil tolerance considerably limits the ability of the foam to control the mobility and represents one of the most formidable challenges for foam utilization in EOR applications. Also, some researchers insisted on enhancing foam-oil tolerance or mitigating the oil destabilization effect (Mannhardt, Novosad, and Schramm 2000).

Vikingstad et al. (2005) investigated the foam-oil interactions by static foam tests for AOS surfactant at a different concentration, salinity, oil-volume, and different oil samples of different molecular weights. In absence of oil, AOS was able to generate foam at concentrations below the CMC, and foam height increased with increasing concentration until it reaches maximum above which the increasing the concentration do

not provide any increase in foam height. Moreover, salts have a significant impact on foam stability. It was observed that AOS was not able to generate foam at low concentrations in presence of salts, but the salinity impact was mitigated by increasing the surfactant concentration. For alkane-oils, lower molecular weight alkanes had a detrimental effect on foam stability, but foam stability was better with higher molecular weight alkane oils. The authors attributed this possible to the power of solubilization of oil in micelles. When oils are solubilized into the interior of the micelles, this influences the foam-oil tolerance negatively. Moreover, spreading and bridging coefficients failed to describe or predict the foam-oil tolerance. Some tests showed good foam oil tolerance with a positive spreading coefficient which indicates low foam-oil tolerance according to the theory. The lamella number method to predict the foam-oil tolerance was found better to explain the oil transport inside the lamellae but failed to predict the foam-oil tolerance, too. Farajzadeh et al. (2012) discussed the detrimental effect of crude oil on foam stability which limits the application of foam in EOR. This paper, in general, covered the available methods, in literature, provided explanations about foam-oil interactions, and presented the ways to describe the foam-oil interactions in modeling as well as in experimental work. Finally, they reviewed the ideas and explanations mentioned in literature on enhancing foam stability in absence and presence of crude oil.

Maini (1986) carried out an experimental study to find out that some crude oils enhance the foam-oil tolerance. However, the foam application in Maini experiments were conducted using heavy crude oils and foam was applied after the steam flood at residual oil saturations.

Wasan, Koczo, and Nikolov (1994) found experimentally that there is a significant relationship between the thin-film stability in presence of crude oil and the pseudoemulsion phase stability inside the thin-film. If the pseudoemulsion film is steady, the foam-oil tolerance is high; otherwise, the foam-oil tolerance is low.

The only proven method to generate stable foam with light crude oil is to use fluorinated surfactants. Vikingstad and Aarra (2009) conducted static and dynamic foam experiments with and without, three different crude oil samples, to investigate the foam generation, propagation, and stability of anionic AOS and zwittreionic (FS-500) perfluorocarbon betaine. They found that both surfactants generated strong foam without oil. However, AOS generated weak foam in presence of oil, while FS-500 generated very stable foam regardless of the type of crude oil. The same conclusion, stable foam with crude oil, was found in many other studies on fluorocarbon surfactants (Mannhardrt, Novosad, and Schramm, 2000).

II.4.2 Foam-with $ScCO_2$

In miscible CO_2 flooding at reservoir conditions, the Sc CO_2 decreases the aqueous solution pH state with much lower pH than neutral (≤ 4) (Fredd et al. 2004). Talley (1988) investigated the effect of pH and salinity change on sulfates class of surfactants. The study reported that sulfates exhibit hydrolysis in acidic solution with pH < 7, Temperature > 50°C, and with oxidization. When sulfates hydrolyze leading to a decrease or complete loss of interfacial activity. Borchardt et al. (1985) also observed loss of ability to stabilize foam when using aged AES surfactant in high temperature. Talley (1988) added that

salinity especially the divalent ions contents exaggerates the effects of low pH on sulfates and concluded that sulfate surfactants have limited applicability under reservoir condition unless pH is kept at 7 or above, and the maximum temperature at which sulfates can work depends on pH and salinity as well as brine composition.

Fluorinated surfactants were also found better than hydrocarbon surfactants with carbon dioxide. Besides their ability to generate stable foam with crude oil (Vikingstad and Aara 2009), they were also found soluble in $ScCO_2$, and able to stabilize water in CO_2 emulsion (Eastoe, Gold, and Seytler 2006),

However, the fluorine chemicals are toxic for humans and environment (Andrianov et al., 2012). The safety and environmental friendliness must be on top of the selection criteria of the chemicals for all industries (Rafati et al., 2012).

Siloxane surfactants is another type showed the same ability to stabilize water in CO_2 emulsions. In a phase behavior study, however, the results indicated that siloxane surfactants need much higher pressure to solubilize with $ScCO_2$ than fluorinated surfactants (Fink and Beckman 2000).

So, during the last 35 years, scientists and researchers were exploring many ideas to determine fluorine-free surfactant that works with $ScCO_2$/water emulsions (Eastoe, Gold, and Seytler 2006).

Borchardt et al. (1985) experimentally investigated the effect of surfactant chemical composition on foam stability using static bulk foam tests with temperature, pressure, salinity, and oil for CO_2 foam. Thermal and chemical stability of foams were the criteria for selecting the surfactants to be used according to the study. The study tested 40

surfactants from different families and types, different temperatures and pressures with CO_2. Sulfates (AES) showed good foaming ability and foam stability at room temperature, but poor at high temperature 75°C. Moreover, AES showed good foaming ability with salinity up to 12-wt% but failed above that. Alcohol Ethoxylates (AE) nonionic surfactant showed the same, good foamability and foam stability at low temperature but failed at high temperature which was attributed to the cloud point temperature. AEGS and AESo surfactants were the best with CO_2 where they exhibited good foaming ability and foam stability. AEGS was the best among the group of surfactants according to their surfactant selection criteria. They concluded that surfactant chemical composition and structure have direct effects of the foaming ability and foam stability. Also, they added that foam bulk tests could be used to investigate the foaming ability and foam stability of surfactants.

Du et al. (2008) investigated the gas-water solubility effect on foam for mobility control at different pressures in Bentheimer sandstone using both N_2 and CO_2 gas at 300 psi with the aid of CT scanner. It was found that CO_2 foam provided lower pressure drop than N_2 foam which is line with Gauglitz et al. (2002) experimental work. Moreover, increasing the back pressure (i.e. experiment pressure) causes the pressure drop across the core in CO_2 foam to decrease with no effect on pressure drop for N_2 foam. Furthermore, the liquid saturation from CT images showed that liquid saturation, after the displacement with CO_2 foam, is higher than that of N_2. Moreover, CT images showed better flood front with N_2 foam than that with CO_2. In addition, the liquid saturation profiles increase as the back pressure increases for CO_2 with no effect on N_2. All of these contrasting results between CO_2 and N_2 foams were attributed to the solubility of CO_2-water compared with

less solubility in N_2-water systems. As explained, CO_2 dissolves in water causing the surfactant solution-water solubility to drop significantly which leads to low CO_2 foam apparent viscosity inside the porous media. However, the N_2-water are naturally insoluble which supports the system for stronger foam generation which induces higher foam apparent viscosity and better mobility reduction.

Xing et al. (2011) investigated several commercially available CO_2-and water-soluble nonionic surfactants in terms of their CO_2 solubility, the ability for in-situ foam generation, and stabilizing CO_2 foam at 1500 psi and 25°C. They found that branched alkyl phenol ethoxylate surfactant is the best. CT images have shown that the dissolution of surfactant in CO_2 caused lower mobility, higher pressure drop, and piston-like displacement than SAG and WAG. Moreover, longer tailed surfactants showed better foamability and foam stability.

Adkins et al. (2010) in "Langmuir" experimentally investigated the high pressure (2500 psi and 50°C) CO_2 foam morphology, viscosity, and stability for 24 nonionic surfactants of different chemical compositions such as single, double-tailed, and branched-tail surfactants. The foam was generated at high pressure 2500 psi by co-injecting CO_2 and surfactant. The branched and double-tailed surfactants generated more stable foam in CO_2/water interface than in air/water. The study attributed the ability of the branched and double tailed surfactants to generate and stabilize the CO_2/water emulsions to the better ability to block the high surface contact area between CO_2 and water. The blockage resulted in higher surface pressure and larger driving force for adsorption to occur, and consequently, further interfacial tension reduction to achieve. Besides the further

reduction in IFT due to the increase in adsorption, branching increases the surface pressure between the foam bubbles, and surfactant efficiency, too. Furthermore, branched and double tailed surfactants also exhibited lower Ostwald ripening and lower drainage rate than single-tailed surfactants which demonstrates the more stable CO_2 foam in branched and double-tailed surfactants. They concluded that the nonionic surfactants favor CO_2 phase and able to generate CO_2 emulsion in water.

In another study at the same year (JCIS journal), Adkins et al. (2010) investigated a different set of nonionic surfactants experimentally to provide more insights and understanding of the differences between interfacial properties of surfactants at Air-Water (G/W) and CO_2-Water (C/W) interfaces. They used surfactants with different hydrophilic head sizes by incorporating different structures of EO and PO groups, and different hydrophobic tail structures such as linear, branched tail, and double tailed. The study was conducted at 2000-psi and 50°C, and conditions were changed according to the CO_2 density investigation requirements. The main discussion, findings, and conclusions are as follows:

- The free energy is the driving force for the surfactant to adsorb at the interface to reduce the surface tension. The free energy is the surface tension at the interface. For example, at G/W interface in absence of any surfactant, the $\sigma_{g/w}$ is 72 mN/m. At C/W interface, the surface tension is 20-30 mN/m. These values of surface tension show that the free energy at G/W interface is higher than that of C/W interface. Therefore, for the surfactant to adsorb at the interface, the driving forces

toward the G/W interface is higher, and the driving for surfactant at C/W interface is low.

- At G/W interface, the high driving forces for adsorption of surfactant at AW interface leads to higher adsorption for a surfactant, and consequently, lower Am and higher pC20 (surfactant efficiency).
- At C/W interface, the low driving force causes low adoption which results in larger Am and low pC20.
- With linear surfactants at G/W interface, they are supposed to be more efficient in stabilizing G/W foam than branched tails and double tails surfactants. This is because of the smaller Am at the interface.
- At the same carbon number of a linear surfactant, the linear tailed surfactants are more efficient than branched or double tailed surfactants at G/W interface. However, at the same carbon length, the branched and double tailed are better than the linear tailed surfactants. These results are in line with a previous work by Varadaraj et al. (1991).
- At C/W interface, the tail solvation in CO_2 causes the absence of the tail-tail interaction (steric repulsion). Therefore, this steric repulsion which is very important for stabilizing G/W foam is not as much as important for C/W emulsion stability. Due to the tail solvation at C/W interface, the contact between CO_2 and water phases is higher than that of G/W.
- Therefore, the tail solvation interaction is inevitable at C/W interfaces. As a result, increasing the tail solvation will increase both the hydrophobicity and adsorption

at the interface which is expected to result in higher surfactant efficiency. Then, tail solvation can be increased by the use of branched and double-tailed surfactants. The use of branched tailed and doubled tailed surfactants were both found more efficient than linear surfactants at C/W interface. Furthermore, the doubled tailed surfactants are more efficient than the branched tailed surfactants at C/W interface.

For more information, Adkins et al. (2010) provided a drawing that shows and explains the way by which different surfactants structures adsorb at C/W interfaces and at G/W interfaces, see **figure 5**.

According to the explanation above, the tail solvation occurs for all surfactant in CO_2 at the C/W interface. This solvation eliminates the steric "repulsive forces" between the tails that normally stabilizes foam. This tail solvation at the C/W interface leads to larger area/molecule for the linear tailed surfactants. On the other hand, the tail solvation for the double and branched tailed surfactants at C/W interface lead to higher adsorption and smaller area/molecule which increase these surfactants' efficiencies. Simply, at the G/W interface, linear tailed surfactants have smaller area/molecule, whereas branched and double-tailed surfactants have larger area/molecule. Therefore, higher efficiency for the linear tailed surfactants, but lower efficiency for the double and branched tailed surfactants at G/W interface.

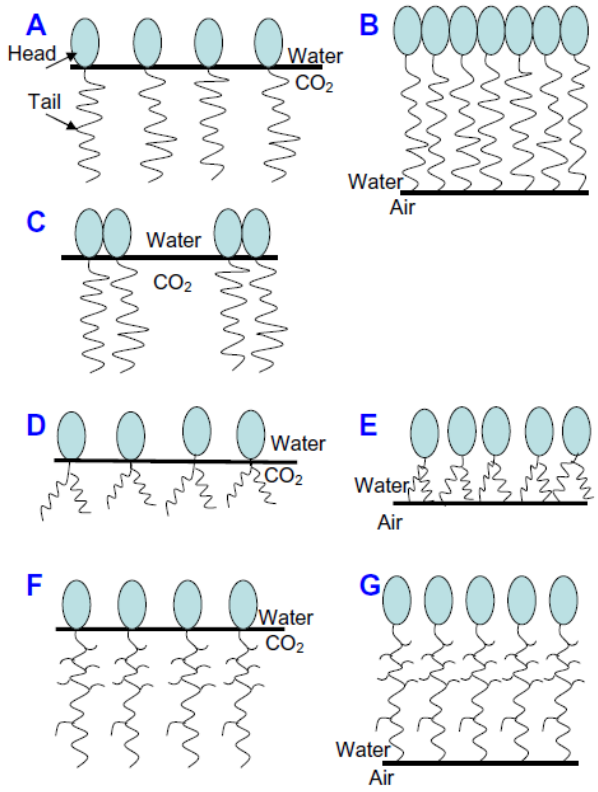

Figure 6: A, B, and C for linear tailed surfactants adsorbed at C/W, G/W, and C/W, respectively. D and E for branched tails surfactants at C/W and G/W. F and G for double-tailed surfactants adsorbed at C/W and G/W (Reprinted from Adkins et al., 2010)

Torino et al. (2010) conducted an experimental study on Tween 80 nonionic surfactant to investigate its ability to generate and stabilize C/W emulsions at high pressure ~3600-psi, 25-60°C temperatures, and 2-10% NaCl concentrations. The main goal is to provide a replacement for the toxic and expensive fluorinated surfactants with non-toxic, cheaper, environmentally benign hydrocarbon surfactants able to stabilize CO_2/water emulsions at supercritical conditions. At 3600-psi and 25-60°C, Tween 80 was found able to generate CO_2 in water emulsion which was observed to have 24-hr. stability. They explained the on the surfactant partitioning between water and $ScCO_2$ phases in

presence of salts and at temperature. Tween 80 is a highly hydrophilic surfactant that partitions into the water at 25-60°C. However, as a nonionic surfactant, increasing the temperature and the addition of electrolytes both causes its hydrophilicity to decrease after which the surfactant becomes in favor toward the CO_2 more than water. In this study, Tween 80 nonionic surfactant was found able to form and stabilize water-CO_2-water double emulsions even at low shear rate. Therefore, the surfactant in salinity and with temperature becomes more hydrophobic and partitions into CO_2 to stabilize the emulsion.

Therefore, the surfactant selection criteria for foam application in mobility control is a challenging step. It was shown that different chemical compositions and structures of surfactants exhibit different foam characteristics in bulk (Borchardt et al. 1985) as well as in porous media (Adkins et al. 2010). The surfactant longevity in acidic solutions is necessary for $ScCO_2$ mobility control using foam. Thus, evaluating the surfactants for acidity tolerance in presence of $ScCO_2$ is crucial before the onset of foam application in such conditions. Moreover, the surfactant ultimate interfacial activity must be maintained for successful interfacial tension reduction and foam stabilization (i.e. thin-film stability).

Schramm and Kutay (2000) suggested a few important considerations that should be included in surfactant selection criteria. The surfactant characteristics for foaming in porous media at reservoir conditions should be soluble in reservoir brine, stable at reservoir temperature, features low adsorption at reservoir rock, partitions weakly in crude oil, maintains high foamability and foam stability, strong mobility reduction ability, and high foam-oil tolerance inside the reservoir. Also, the mobility reduction ability of the surfactant or the foaming agent depends on many factors such as the surfactant chemical

composition and structure, reservoir brine composition, type of gas for foam generation, type of reservoir rock, injection quality, foam texture, flow rate, and reservoir pressure and temperature.

CHAPTER III

MATERIALS, EXPERIMENTAL SETUP AND METHODOLOGY

This chapter includes the materials, apparatus, and experimental setups, procedures, measurements, software, calculations and instruments used throughout this research.

III.1 Materials

Table 1 shows the surfactants and their main properties. The column “name” in **table 1** shows the names of the surfactants that will be used to refer to the surfactants.

Table 1: Surfactants list and main properties

Commercial Name	Name herein,	Type	Carbon Chain Length	Chemical Name	Cloud Point, °C	PEG, %m/m	Thermal Stability, °C	PO/ EO per alcohol, mol/mol	Source
EnordetA771	A771	Anionic	C12-13	AAS	--	--	60	7 PO	Shell Chemicals
EnordetA031	A031	Anionic	C16-17	AAS	--	--	60	3 EO	
EnordetJ771	J771	Anionic	C12-13	AAS	--	--	60	7PO	
EnordetJ071	J071	Anionic	C12-13	AAS	--	--	60	7EO	
EnordetJ13131	J13131	Anionic	C12-13	AAS	--	--	60	13PO	
EnordetO132	O132	Anionic	C12-13	IOS	--	--	200	--	
EnordetO242	O242	Anionic	C20-24	IOS	--	--	200	--	
EnordetO342	O342	Anionic	C19-23	IOS	--	--	200	--	
EnordetO332	O332	Anionic	C15-18	IOS	--	--	200	--	
Neodol25-3	N25-3	Nonionic	C12-15	AE	--	0.5	--	3EO	
Neodol25-7	N25-7	Nonionic	C12-15	AE	46	1	--	7EO	
Neodol91-8	N91-8	Nonionic	C9-11	AE	78	0	--	8EO	
Neodol25-9	N25-9	Nonionic	C12-15	AE	75	1	--	9EO	
Neodol25-12	N25-12	Nonionic	C12-15	AE	80	0	--	12EO	
Neodol45-7	N45-7	Nonionic	C14-15	AE	45	0	--	8EO	
BiotergeAS40	AOS	Anionic	C14-16	AOS			94	--	Stepan
CNF	CNF	Anionic	--	CNF			na	--	Flotek Industries

III.1.1 Sample Preparation

The surfactants solutions were either diluted in DI water or in brine solutions based on the test's requirements. The DI water was always used for dilution (ASTM grade type II from LabChem). For the salinity effect investigations, brine solutions at 1, 2, and 3-wt% NaCl concentrations were used. Moreover, North Burbank Unit (NBU) reservoir brine was prepared synthetically in lab at 18-wt% according to the composition in **table 2**. NBU salinity was used for the surfactants preliminary solubility test. Furthermore, more solubility analysis were conducted at lower salinities, 4, 9, and 12-wt%, by diluting the NBU synthetic brine at the same proportions of the elements shown in **table 2**. After preparing the surfactants solutions, they were stirred for 8-12 hours to ensure complete mixing.

III.1.2 Crude Oil

The crude oil used in this study was the NBU light crude oil. It is 39°API gravity and 3.27 cp at 50°C, and 33.7°API gravity and 8-cp at 23°C.

III.1.3 Gases

For foam generation, surfactant and gas were simultaneously injected in all foam dynamic tests. Both nitrogen (N_2) and carbon dioxide (CO_2) gases, of industrial grades, were used for foam dynamic testing. However, the static tests were always conducted with air.

Table 2: NBU reservoir brine composition.

Component	Molecular Formula	Concentration [wt%]
Sodium Bicarbonate	$NaHCO_2$	0.004
Sodium Sulfate	Na_2SO_4	0.016
Calcium Chloride	$CaCl_2.2H_2O$	5.359
Magnesium Chloride	$MgCl_2.6H_2O$	1.907
Potassium Chloride	KCl	4.313
Sodium Chloride	NaCl	9.107

III.2 Instruments

III.2.1 Density Meter

The density measurements were conducted using Anton Paar DMA 4100-M.

III.2.2 Interfacial Tension Measurements

Dataphysics OCA 20 Pro IFT was used for the surface or interfacial tension measurements using pendant drop method see **figure 7**.

III.2.3 Foam Bubbles Micro-Imaging

The foam bubbles were micro-imaged using a micro-imaging camera with maximum resolution 752X480 pixel. The micro-images were taken at different times during the static (shaking) tests. The bubbles inside the foam columns are smaller at the bottom and increase in size upward. Therefore, the images were carefully captured from

the same position on the tube to ensure that the measurements were applied for the same set of bubbles.

III.2.4 X-Ray Diffraction

XRD was primarily used for quantitative and qualitative identification of the mineralogy in rocks. For more accurate evaluation of the experimental results, the interactions between the injected chemicals and minerals in rock should be well known and defined prior to the test. X-Ray diffraction device provides patterns from which the minerals in rock can be identified. There are standard X-Ray diffraction patterns of the materials. These standard X-Ray diffractions are used with the pattern given to define the rocks' mineralogy.

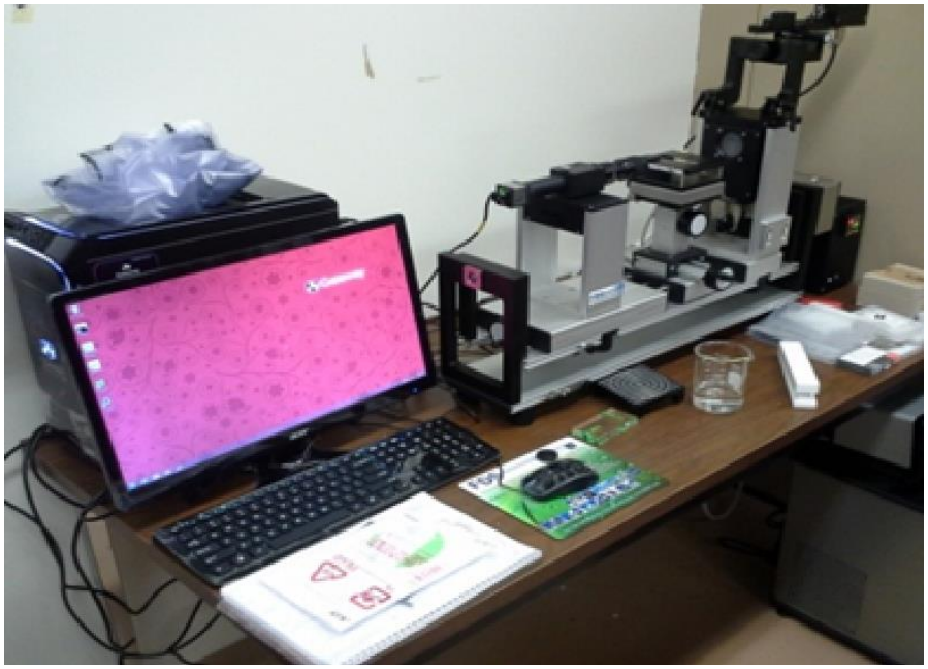

Figure 7: Dataphysics OCA 15 Pro IFT.

III.3 Dynamic Experimental Setups

The dynamic experimental setups were used to measure the viscosity, mobility, and to perform core flooding experiments. The system is equipped with back pressure regulator to enable testing at higher pressures. Moreover, the whole system is installed inside a temperature air-bath to perform the experiments at higher temperatures. Furthermore, the setup includes three ISCO pumps connected to four accumulators from which the fluids such as water, surfactant, gas, and oil, were injected to the porous media. These accumulators are also placed inside the temperature bath so that the injected fluids are also at the test's temperature.

Two porous media were used for the dynamic foam experiments. **Figure 8** shows the experimental setup for the high permeability glass-beads pack. Also, Bentheimer sandstone was also used as the lower permeability porous media, see **figure 9**.

The glass beads pack is an in-house made porous media. It consists of three parts: 120-180 μm glass-beads, ¼" OD X 0.18" ID stainless steel tube, and two 6-micrometer filters (*Swagelok* brand) that are connected to both ends of the tube. The tube is filled with the glass-beads and the glass-beads are contained inside the tube by the filters. **Table 3** shows the main properties of the glass-beads porous media. The glass-beads pack is shown in **figure10**.

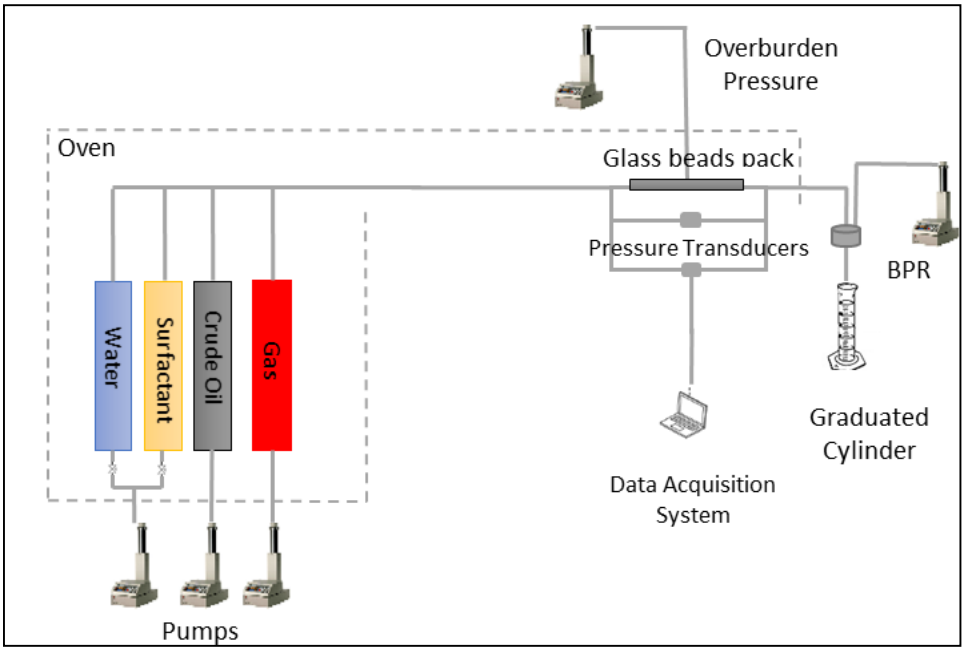

Figure 8: Mobility reduction evaluation experimental setup for glass-beads pack (Modified from Almobarky, Al-Yousef and Schechter (2017))

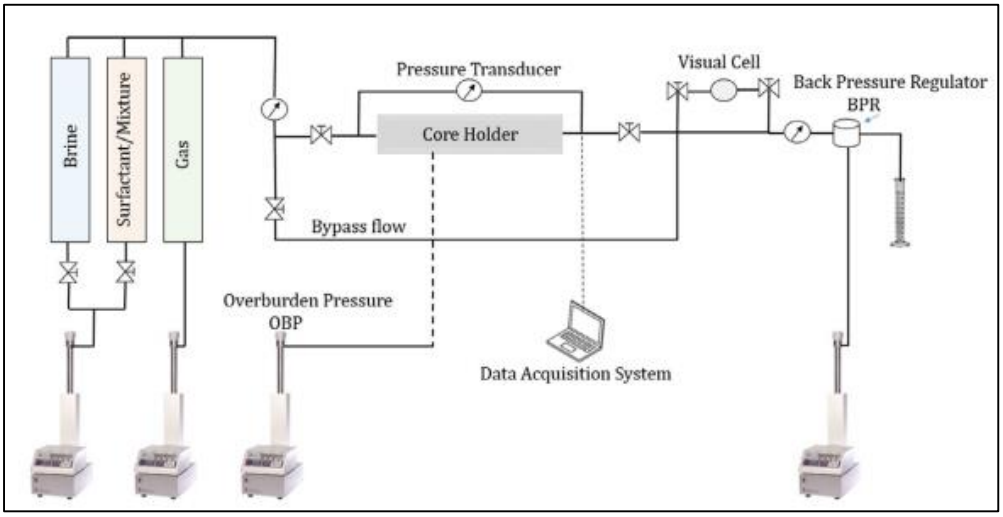

Figure 9: Mobility reduction evaluation and core flooding experimental setup for cores (Reprinted from AlYousef, Almobarky, and Schechter (2017))

Table 3: Glass beads porous media properties

Glass Beads Size	120-180 μm
Length	13 in
Diameter	0.18 in
Pore Volume	1.625 ml
Porosity	30%
Permeability	17.1-Darcy

Figure 10: The glass-beads pack porous media

III.4 Experimental Procedure

This section covers the surfactants solutions preparations, static foam tests, and dynamic experimental procedures.

The surfactants were diluted in DI water first at 1-wt% concentration. Then, they were usually stirred in a closed vials for 8 to 12 hours to ensure complete mixing. Then, the 1-wt% surfactant solutions were used to prepare the lower concentrations as required. Finally, samples were again stirred for 8 to 12-hrs to ensure complete mixing before sampling and testing.

III.4.1 Static Bulk Foam Tests

Static bulk foam test refer to the shaking tests or the foam column decay monitoring with time, average bubbles sizes from micro-images, and the interfacial properties measurements.

The interfacial properties measurements include $\sigma_{g/w}$, $\sigma_{o/w}$, $\sigma_{g/o}$, and CMC determination. Using these properties, the surface density (Γ) and area per molecule (A) at the air-water interface can be calculated or interpreted using the $\sigma_{g/w}$ vs. Log(concentrations) plot.

Foam column decay method or shaking test is a fast and convenient experiment that is widely used in literature for surfactants screening. In this study, the shaking tests were conducted to measure the foamability and foam stability according to the procedure below.

Simply, after placing 3 ml of the surfactant solution in a 9 ml Pyrex glass capped tube, the sample is shaken gently for foam generation. After the foam has been generated, the foam column decay was monitored by taking photos at different times. The sample was also used to capture micro-images from which the average bubble sizes were measured.

The foam columns lengths and the average bubble sizes were measured from the photos and micro-images using ImageJ software. Below is a list of the definitions and principles about the parameters and measurements conducted through the static tests.

1. The initial foam height was used as an indication of the foamability of the surfactant. Lunkenheimer and Maysa (2003) and Rosen and Kunjappu (2004)

defined the foamability as the ability of the surfactant to produce foam which depends on how much this surfactant can reduce the surface tension.

2. The foam half-life is the time at which the foam column loses half of the initial foam height. It is a measure of the foam stability. Also, the foam life can be represented on a plot of the normalized foam height vs. time as a measure of the foam stability, too. The normalized foam height is the ratio of the foam column length at any time to the initial foam height. The time at which a complete decay of the foam column might take hours or days for strong foam, whereas transient foams last in less than a minute (Rosen and Kunjappu 2004).
3. The average bubble sizes were obtained from the micro-images of the bubbles using ImajeJ software. The criteria employed was that the smaller the bubbles with time indicates the higher foam stability or the slower the liquid drainage rate from the thin-film. Both are indicators of good foam stability.
4. The CMC was determined from the plot of the surface tension measurements at different concentrations vs. Log (concentration).
5. The foam-oil tolerance is a measure of the foam stability in presence of crude oil. This test was also conducted by shaking the surfactant solutions after adding 10-wt% crude oil on top of the surfactant solution. The same parameters were obtained: initial foam height for foamability in presence of oil, and foam half-life for foam-oil tolerance.
6. Foam-oil tolerance can be represented qualitatively by calculating the entering- (E), spreading- (S), and bridging-coefficients (B) using **equations 3** through **5**.

These coefficients are widely used theories to interpret the foam-oil tolerance using the procedures listed below. In general, the positive value of any coefficient indicates the lower foam stability with oil. These coefficients are used as follows:

- If $E < 0$, then the oil droplet will not enter the gas-water interface and the foam-oil tolerance is good;
- If $E > 0$, then S should be calculated for more precise prediction.
- If E and S both > 0, then the oil droplet will enter and spread over the gas-liquid interface and will destabilize the foam.
- If $E > 0$, but $S < 0$, then B should be calculated for accurate prediction.
- If $E>0$, $S < 0$, and $B > 0$, then the oil droplet will displace the water from the thin-film, build a bridge between the interfaces inside the thin-film, and lead to foam collapse in presence of oil; otherwise, stable foam with oil is expected.

$$E=\sigma_{g/w} + \sigma_{o/w} - \sigma_{o/g} \quad (3)$$

$$S=\sigma_{g/w} - (\sigma_{o/w} + \sigma_{o/g}) \quad (4)$$

$$B=\sigma^2_{g/w} + \sigma^2_{o/w} - \sigma^2_{o/g} \quad (5)$$

7. Schramm and Novosad (1990) developed the lamellae number (L) theory by which the stability of the thin-film in presence of crude oil can be predicted. The L number can be calculated using **equation 6**. Basically, the foam is stable with crude oil if $L<1$ because oil emulsification into the lamellae is not expected to occur, and this foam is classified as of type A. The foam is of type B when $1<L<7$ where oil emulsification occurs but probably in favor of the foam stability. Type

C foam is when L>7 where oil is emulsified heavily into the thin-film causing the oil to penetrate the liquid-gas interface which results in lamellae-rupture (Vikingstad et al. 2005).

$$L = 0.15\ \frac{\sigma_{a/w}}{\sigma_{o/w}} \tag{6}$$

III.4.2 Mobility Reduction Evaluation

The main objective of the foam generation inside the reservoir is to assist the injected fluids by enhancing the sweep efficiency (Kovscek and Radke 1994). Enhancing the sweep efficiency occurs due to the high foam viscosity (Andrianov et al. 2012). The viscosity of foam refers to the amount of resistance that foam flow provides inside the porous media (Heller, Lien, and Kuntamukkula 1985).

The foam was always generated by surfactant and gas simultaneous injection through the porous media either in glass beads pack or Bernheimer sandstone at specific injection qualities. The strong foam was recognized as a rapid increase in pressure drop across the porous media (Dicksen, Hirasaki, and Miller 2002). In each test, the foam flow continued until the steady state pressure drop was maintained. The pressure drop data across the porous media were collected using pressure transducers and used to calculate the foam effective viscosity using **equations 7** through **9**.

$$\lambda = \frac{k}{\mu} = \frac{q\ l}{A\ \Delta P} \tag{7}$$

Where,

λ: Mobility

k: Permeability

μ: Viscosity

q: Flow rate

l: Length of the media

A: Cross-sectional area of the media

ΔP: Pressure drop across the porous media

$$\lambda_r = \frac{\lambda}{k} \tag{8}$$

Where,

λ_r: Relative mobility

λ: foam mobility from **equation 7**;

k: Absolute permeability of the porous medium;

$$\mu_{eff} = \frac{1}{\lambda_r} \tag{9}$$

Where,

μ_{eff}: Foam effective viscosity [cp]

λ_r: Relative mobility, from **equation 8**;

The mobility reduction factor (MRF) is the ability of the foam to reduce the mobility of gas related to the mobility in baseline experiment. MRF can be calculated using the following **equation 10**:

$$MRF = \frac{\mu_{foam\ apparent}}{\mu_{baseline}} = \frac{\Delta P_{foam}}{\Delta P_{baseline}} \tag{10}$$

These foam measurements including foam effective viscosity, and MRF are investigated in high/low permeability porous media, at high/low flow "*shear"* rate, in DI and saline water, using N_2 and CO_2 gases.

The experimental protocol for foam mobility reduction evaluation is as follows:

1. Prepare the brine and surfactant solution at the required salinities and concentrations. For mobility measurements in glass beads pack, go to step # 4; otherwise proceed to step 2.
2. The core must be dried in an oven overnight.
3. It is recommended to wrap the core with lead foil. Then, insert it into the rubber cylinder, and mount it into the core holder to apply the Over Burden Pressure (OBP).
4. Vacuum the core (porous media) from air using a vacuum pump.
5. Saturate the core with a known amount (or known volume) of the required brine. The consumed amount (or volume) of the brine minus the dead volume is the pore volume of the porous media. After that, knowing the bulk volume of the porous media, porosity can be also calculated at this step.
6. Inject 5 to 6 pore volumes of brine to ensure complete saturation of the core.
7. Set the test pressure using the OBP, and the temperature inside the temperature bath.
8. When the entire system is at stable pressure and temperature, measure the core's absolute permeability by taking three data points of the flow rate and the pressure drop across the porous media using Darcy law.
9. Inject 1 pore volume of the surfactant solution. This step is applied to mitigate the effect of the surfactant adsorption on rock surfaces.
10. Start the surfactant-gas co-injection at the required flow rate and injection quality.
11. Collect the pressure drop data across the core for the analysis.

III.4.3 Core Flooding Experiments:

The only significant difference between the mobility reduction evaluation and core flooding experiment is the presence of crude oil in the core flooding experiment. The main objectives of this experiment are

1. To examine the ability of the materials under investigation to enhance the oil recovery under reservoir conditions through the oil recovery measurements;
2. To examine the ability of the surfactant solution to generate foam even in presence of crude oil and to enhance the oil recovery; and
3. To examine the oil destabilization effect through the pressure drop data while performing the surfactant/gas co-injection after water flooding at the residual oil saturation;

The protocol for core flooding experiment is as follows:

1. Prepare the brine and surfactant solution at the required salinities and concentrations. For mobility measurements in glass beads pack, go to step # 4; otherwise proceed to step 2.
2. The core must be dried in an oven overnight.
3. It is recommended to wrap the core with lead foil. Then, insert it into the rubber cylinder, and mount it into the core holder to apply the Over Burden Pressure (OBP).
4. Vacuum the core (porous media) from air using a vacuum pump.
5. Saturate the core with a known amount (or known volume) of the required brine. The consumed amount (or volume) of the brine minus the dead volume is the pore

volume of the porous media. After that, knowing the bulk volume of the porous media, porosity can be also calculated at this step.

6. Inject 5 to 6 pore volumes of brine to ensure complete saturation of the core.
7. Set the test pressure using the OBP, and the temperature inside the temperature bath.
8. When the entire system is at stable pressure and temperature, measure the core's absolute permeability by taking three data points of the flow rate and the pressure drop across the porous media using Darcy law.
9. Inject crude oil at specific flow rate until no more water production. The irreducible water saturation (S_{wi}) and the Original Oil In Place (OOIP) can be calculated at the end of this step.
10. Apply water flooding by injecting water until no more oil production can be observed as a result of water injection. The residual oil saturation (S_{or}) can be calculated using the amount of oil produced (displaced). This step was conducted by injecting around 5 pore volumes over 24-hr.
11. Inject 1 PV of the surfactant solution to mitigate the surfactant adsorption.
12. Start the pressure drop data acquisition system and the surfactant-gas co-injection. Collect the effluent for the oil production measurements.

III.5 Methodology

The primary objective of the proposed design for this experimental work is to enhance the oil recovery using foam as a mobility control agent in either surfactant

flooding or miscible CO_2 injection. Moreover, this study examines the mixtures of commercially available surfactants to enhance the foam stability either in absence or presence of crude oil and with salinity in comparison with the individual surfactants.

Figure 11 shows the stages of the experimental work, tests, and measurements of each stage.

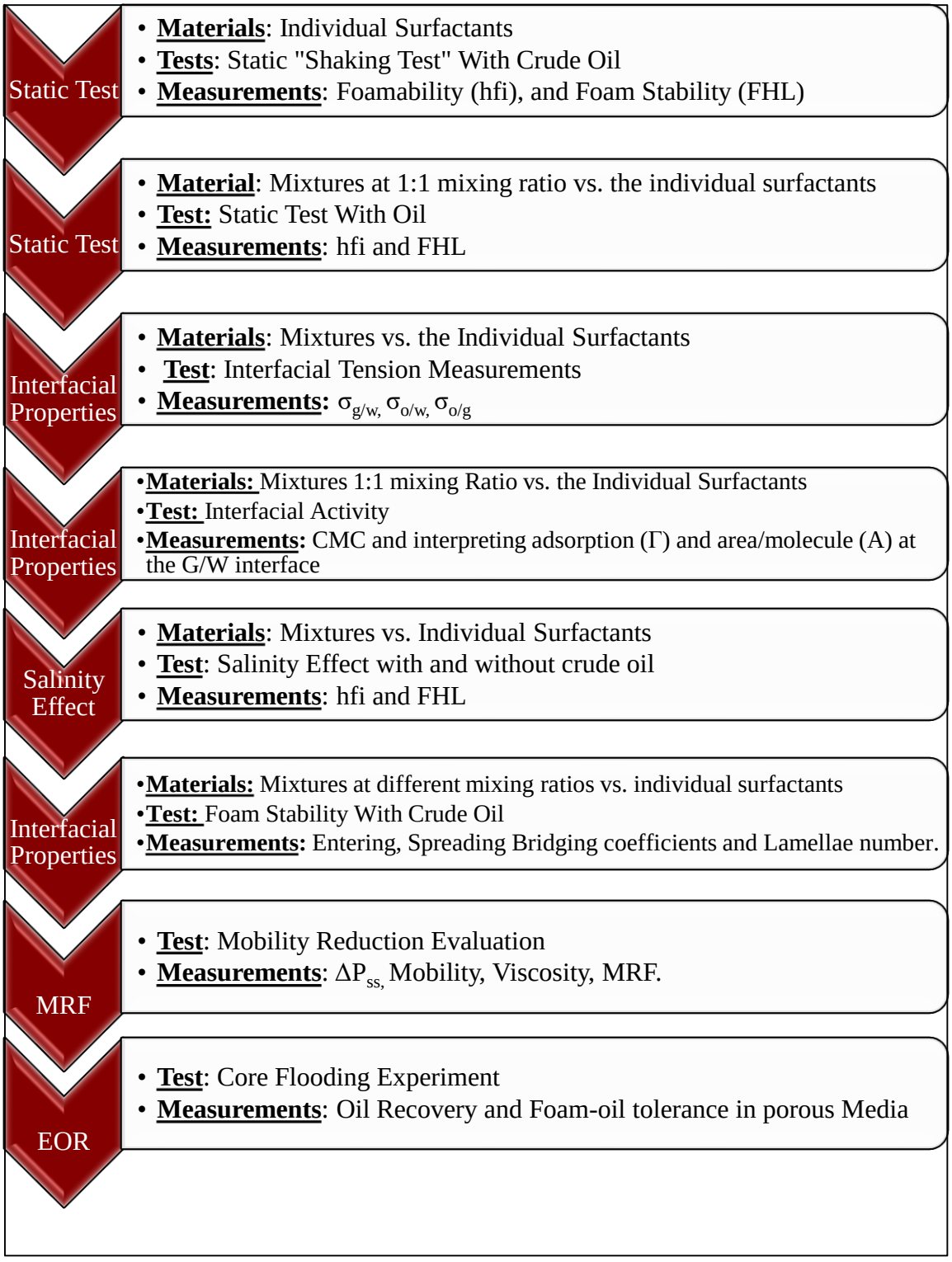

Figure 11: Research Methodology

CHAPTER IV
PRELIMINARY WORK RESULTS AND DISCUSSION

This chapter is to introduce the results of the preliminary experimental work conducted in this study. The main purpose of this experimental work was to obtain a comprehensive understanding of the ability of the surfactants to generate foam "*foamability"* and to stabilize foam "*foam stability*". Also, this work was to provide a guidance to understand the behavior of these surfactants when mixed together to provide better foaming properties than that of the individual surfactants.

IV.1 Individual Surfactants

In this test, the surfactants were visually inspected in terms of their solubility in water and brine solutions. Then, foamability and foam stability were measured by performing shaking tests for individual surfactants in presence of crude oil. Salinities includes NBU salinity, and dilutions of NBU salinity to 4, 9, and 12-wt%.

IV.1.1 Solubility in Brine Solutions

Results in **table 4** show the soluble and insoluble surfactants in water and in brine solutions. The surfactants solutions were prepared at 0.5-wt% concentrations. In DI water, all surfactants were completely soluble with 100% transparent solutions except N25-3 and O132.

Table 4: Surfactants and solubility of surfactants

Surfactant	Type	Chemical Name	Solubility				
			Salinity, wt%				
			DI water	4	9	12	18
EnordetA771	Anionic	AAS	√	√	√	√	√
EnordetA031	Anionic	AAS	√	X	X	X	X
EnordetJ771	Anionic	AAS	√	√	√	√	√
EnordetJ13131	Anionic	AAS	√	X	X	X	X
EnordetJ071	Anionic	AAS	√	√	√	√	√
EnordetO132	Anionic	IOS	X	X	X	X	X
EnordetO242	Anionic	IOS	√	X	X	X	X
EnordetO342	Anionic	IOS	√	X	X	X	X
EnordetO332	Anionic	IOS	√	X	X	X	X
Neodol25-3	Nonionic	AE	X	X	X	X	X
Neodol25-7	Nonionic	AE	√	√	√	√	X
Neodol91-8	Nonionic	AE	√	√	√	√	X
Neodol25-9	Nonionic	AE	√	√	√	√	X
Neodol25-12	Nonionic	AE	√	√	√	√	√
Neodol45-7	Nonionic	AE	√	√	√	√	X

N25-3 is an alcohol ethoxylate nonionic surfactant has 3 EO groups. Its poor solubility in DI water at 25°C indicates that its cloud point temperature is below the room temperature. The cloud point temperature is a crucial factor to consider when using nonionic surfactants at high temperatures. The solubility of the nonionic surfactants in water decreases as the temperature increases approaching their cloud point. Moreover, the surfactant precipitates after losing the water solubility at or above the cloud point temperature.

O132 is an anionic surfactant belongs to the IOS family. It precipitated in DI water at room temperature. This is because of the high hydrophobicity induced by the longest

carbon chain length among the IOS surfactants in **table 4**. The main conclusions can be drawn from these results in **table 4** are:

- J771, J071, and A771 showed the best water-solubility showing that they are the most hydrophilic surfactants among the anionic surfactants.
- N25-12 nonionic surfactant was the only one showed 100% transparent solution in brine up to NBU salinity.
- Increasing the EO number either for the anionic or nonionic provides better water-solubility. The best example is N25-12 with 12 EO groups in comparison with other nonionic surfactants N25-9 with 9 EO.
- The water solubility of the IOS anionic surfactants (O123, O242, O342, and O332) decreases according to the carbon chain length. The longer the hydrophobic tail is the higher the hydrophobicity and the lower the water-solubility.

IV.1.2 Shaking Tests With Crude Oil

According to Schick and Fowkes, and Ross and Bramfitt (1957), they concluded that the attachment of the alcohol on the palisade layer of the micelles of a foaming agent enhances the foam stability in absence and in presence of crude oil. The surfactants provided for this study are very well-known of their foaming properties in absence of oil. Therefore, it would be difficult to compare their foamability and foam stability in absence of oil by conducting shaking test. Also, due to the importance of the foam-oil stability, shaking tests were conducted first at the most severe environment for foam stability (i.e. in presence of crude oil). The test was conducted according to the following:

- Samples Volumes: 3-ml in 9-ml Pyrex test tube.
- Surfactant Concentration: 0.05-wt% in DI water.
- Oil concentration: 10-wt%
- Salinity: DI water, 1-wt% NaCl, and NBU salinity.

The objectives:

- Foamability in presence of crude oil by measuring the initial foam height (hfi);
- Foam stability in presence of oil by measuring the foam half-life (FHL);
- Foam stability in presence oil in saline water;

Table 5: Surfactants foamability and foam stability in presence of oil in DI water at 0.05-wt% surfactant concentration

Surfactants	hfi [cm]	FHL [min]	FHL [hr]
J071	3.114	90	1.500
N25-12	0.78	180	3.000
N25-9	0.598	64	1.067
N91-8	1.108	1	0.000
N45-7	0.456	--	0.000
N25-7	0.453	--	0.000
AOS	4.878	450	7.5
J771	2.589	100	1.667
A771	1.027	700	11.667
A031	1.926	550	9.167
O242	3.108	1400	23.333
O342	1.021	85	1.417
O332	4.935	120	2.000
J13131	1.926	50	0.833
AF	2.7	1	0.000

IV.1.2.1 Results in DI Water

Table 5 shows the initial foam heights (hfi) and foam half-lives (FHL) from shaking tests in presence of oil. This test was conducted in DI water for individual surfactants only. **Figure 12** shows the results from **table 5** in descending order, strongest to weakest.

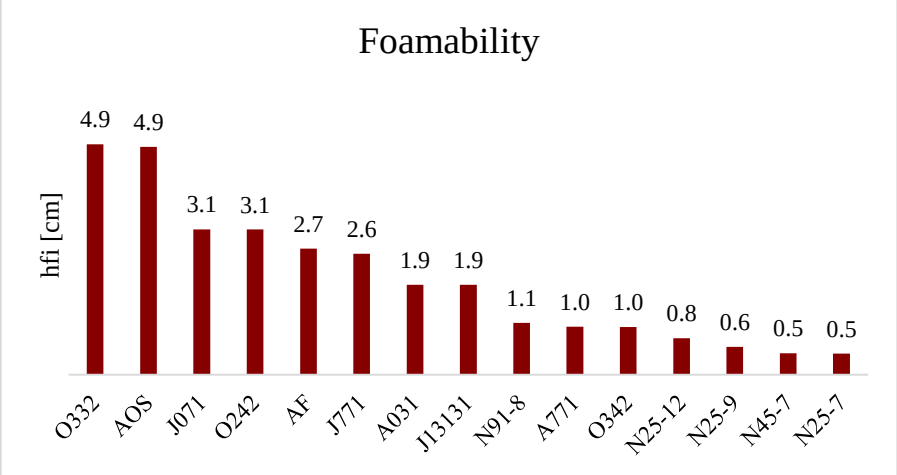

Figure 12: Initial foam heights of the individual surfactants in presence of crude oil.

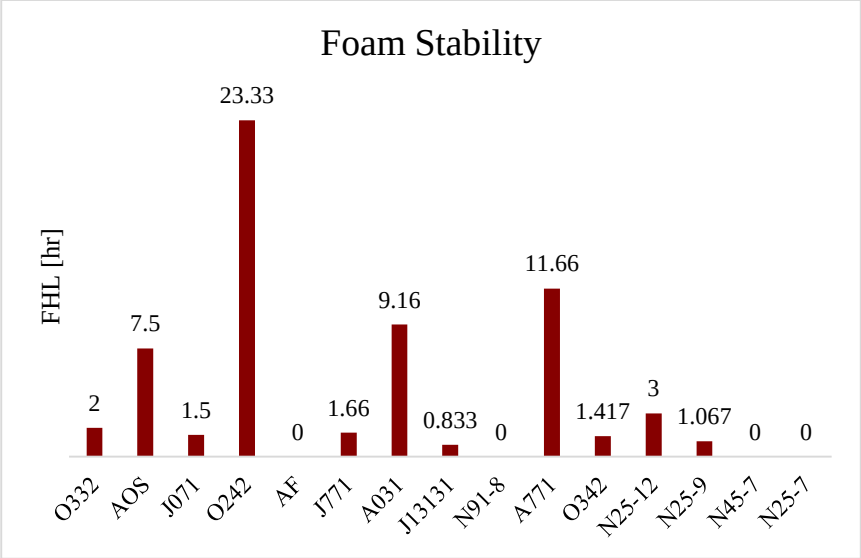

Figure 13: Foam half-life for the individual surfactants in presence of oil in DI water.

Surfactants from O332 to O342, in **figure 12**, are anionic surfactants except N91-8. The remaining surfactants, from N25-12 to N25-7, are nonionic surfactants. It is obvious that the anionic surfactants have extremely better foaming ability in presence of crude oil than the nonionic surfactants. Overall, the best foaming agents according to this test are: O332 to J13131 in **figure 12**.

Figure 13, in the same order of **figure 12**, shows the foam half-lives which refers to the foam stability in presence of oil. The good foaming ability in **figure 12** does not necessarily correspond to good foam-oil tolerance. For instance, the best foaming agents in foamability, in **figure 12,** are O332, AOS, and J071. However, these surfactants in terms of foam-oil tolerance, **figure 13**, are moderate to weak. Another more obvious evidence of this test is the anionic AF surfactant. It was able to generate 2.7-cm initial foam height but failed to stabilize the foam in presence of oil for more than a minute. Moreover, **figure**

13 shows that we have three anionic surfactants with significant foam-oil tolerance: O242, A031, and A771 with foam half-life 23-hr, 10-hr, and 12-hr, respectively. In fact, O242 was the only surfactant showed good foamability and best foam-oil tolerance in DI water.

IV.1.2.2 Results in NBU Brine

At NBU salinity (18-wt%), none of the surfactants were able to generate foam in presence of oil but J071 anionic surfactant. This surfactant is an alcohol alkoxy sulfate. Sulfates. The high ethoxylation EO number in this surfactant also maintained its high solubility in NBU salinity. The results about J071 anionic surfactant were in line with Borchardt et al. (1985) where the powerful foamability of the alcohol ether sulfate was observed at salinities up to 12-wt%.

IV.1.2.3 Results in 1-wt% NaCl Salinity

Table 6 shows the foamability (hfi) and foam stability (FHL) for the best surfactants selected according to the previous test results. The foamability and foam stability in DI water and in 1-wt% NaCl salinity are shown in **Figures 14** and **15**, respectively.

Table 6: The best individual surfactants foamability and foam stability in presence of oil in 1-wt% NaCl salinity

Surfactants	Concentration [wt%]	DI water		1-wt% NaCl	
		hfi [cm]	FH [hr]	hfi [cm]	FH [hr]
J071	0.05	3.114	1.5	1.451	0.58
AOS	0.05	5.733	8	3.518	7.5
A031	0.05	1.926	9.17	0.629	1.17
A771	0.05	1.07	11.67	0	0
O242	0.05	3.108	23.33	0.504	0.67
O342	0.05	1.021	1.42	0.794	0.42
O332	0.05	4.935	2	1.102	1.58

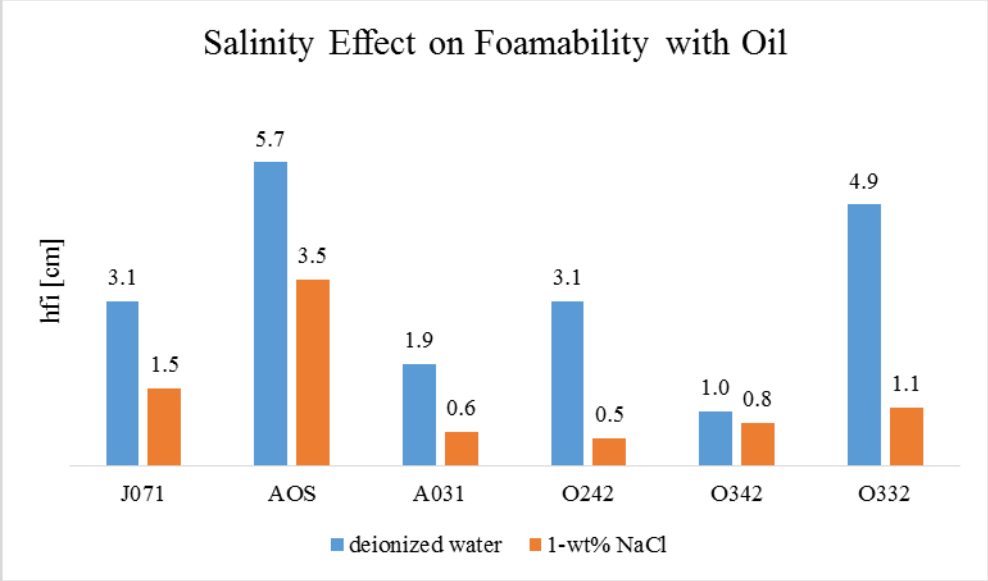

Figure 14: Individual surfactants at 0.05-wt% foamability in presence of oil in deionized water and 1-wt% NaCl salinity

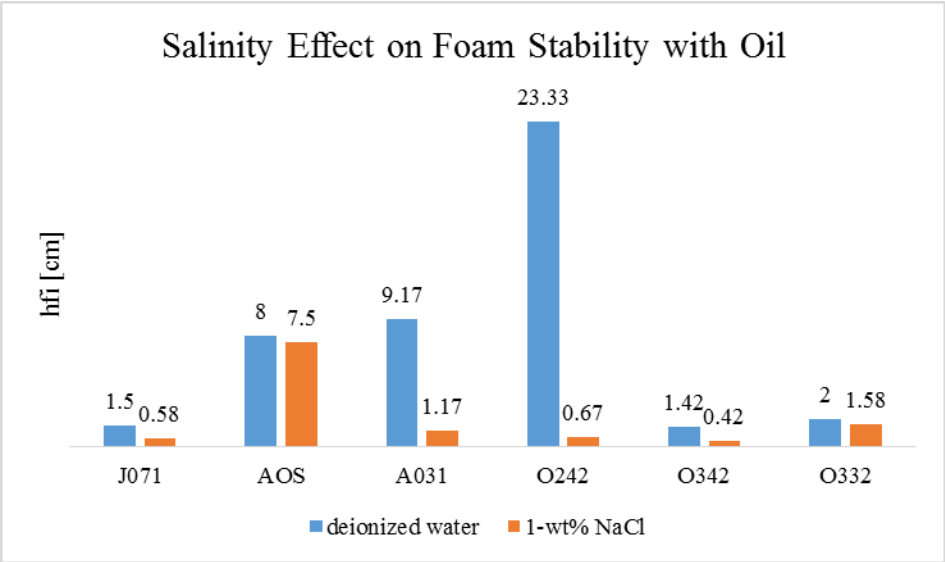

Figure 15: Individual surfactants at 0.05-wt% foam stability in presence of oil in deionized water and in 1-wt% NaCl salinity

Figures 14 and **15** show the dramatic effect of the addition of 1-wt% sodium chloride on the foamability and foam stability of these surfactants in presence of oil. This affect can be attributed to the ability of the surfactant to reduce the $\sigma_{o/w}$ in saline water. Such feature can be considered in surfactant flooding but not for foam applications for mobility control. Moreover, the best foam-oil tolerant surfactants in DI water were A031 and O242. The foamability and foam stability of both A031 and O242 were severely affected in saline water.

Therefore, some foaming agents (J071, O332, and AOS) were able to generate large foam volumes but with moderate to poor foam stability in presence of oil. Also, there are two surfactants exhibited powerful foam-oil tolerance in DI water, O242 and A031. However, the addition of 1-wt% NaCl salinity induced a severe drop in their foaming properties.

The best foaming agents (J071, O332, and AOS) were targeted to enhance their foam-oil tolerance by mixing them with the best foam-oil stabilizers (O242 and A031). Moreover, for comprehensive experimental work, these three foaming agents were mixed with all other surfactants. Results are shown in the next few sections.

IV.2 Surfactants Mixtures

IV.2.1 J071 Mixtures

Table 7 shows the foamability and foam stability for J071 anionic surfactant and its mixtures with the other surfactants at 1:1 mixing ratio, 0.05-wt% concentrations in DI water with oil.

Table 7: Foamability and foam stability of J071 vs. mixtures at 0.05-wt%, 1:1 mixing ratio in DI water in presence of oil

Surfactant	Mixing Ratio	hfi [cm]	FHL [hr]
J071	-	3.114	1.50
J071/O242	1:1	6.249	8.33
J071/A031	1:1	6.169	5
J071/O332	1:1	5.102	4.17
J071/J771	1:1	4.334	0.92
J071/O342	1:1	3.963	3.33
J071/AOS	1:1	1.993	4.17
J071/A771	1:1	3.638	0.67
J071/J13131	1:1	2.942	1.42
J071/N91-8	1:1	2.105	2.17
J071/N25-7	1:1	1.693	3.5
J071/N45-7	1:1	1.596	4.5
J071/N25-12	1:1	1.468	7.83
J071/N25-9	1:1	1.294	9

Figure 16 and **17** shows the foamability and foam stability in presence of oil for J071 in comparison with J071 mixtures with the other surfactants at 0.05-wt% and 1:L1 mixing ratio. The mixtures exhibited no effect on the foamability. However, it is very obvious that some mixtures showed better foam-oil tolerance "stability" than J071 alone. Interestingly, two of these surfactants are the ones exhibited the best foam stability in presence of crude oil previously in DI water (i.e. O242 and A031).

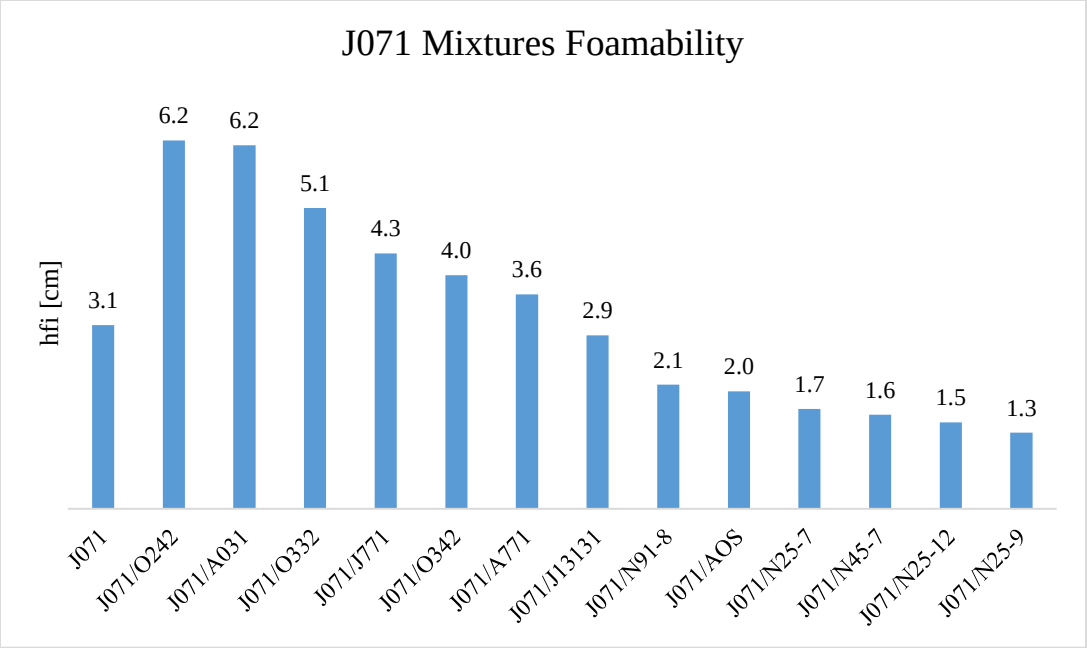

Figure 16: Foamability of J071 vs. mixtures at 0.05-wt%, 1:1 mixing ratio in DI water in presence of oil

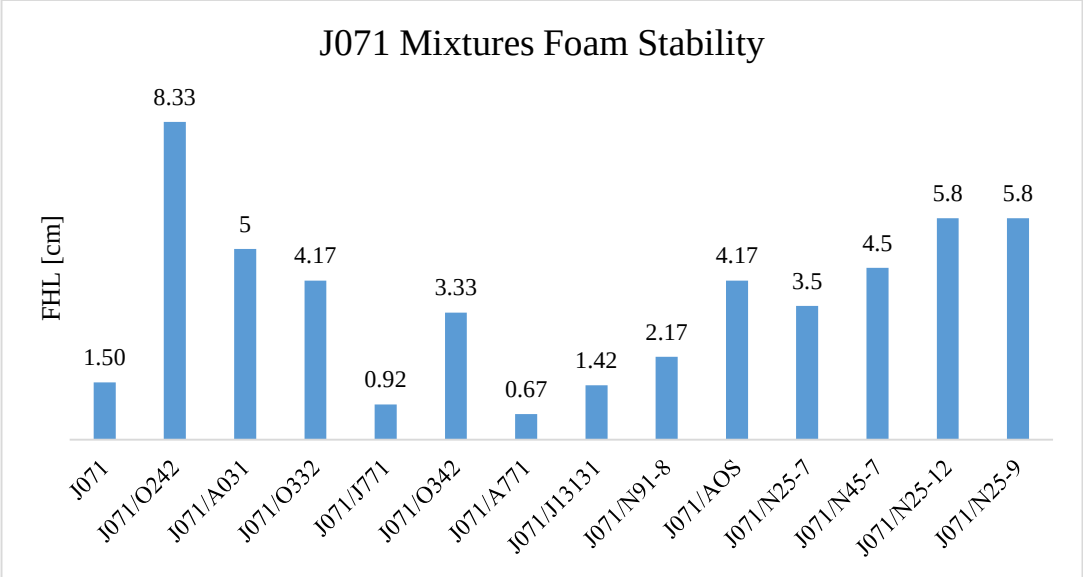

Figure 17: Foam stability of J071 vs. mixtures at 0.05-wt%, 1:1 mixing ratio in DI water in presence of oil

For J071 mixtures with the nonionic surfactants in **figure 17**, they also show significant enhancement in foam-oil tolerance even better than that of J071 blends with the anionic surfactants. However, these blends did not provide reasonable or good foamability as it is clear in **figure 16**. Such enhancement in foam stability is not considered because of the low ability to generate foam in presence of oil. If foamability is lost, then the high foam stability of a very short column is obsolete.

IV.2.2 AOS Mixtures

Table 8, **figure 18**, and **figure 19** show the initial foam heights and foam half-lives for AOS surfactant and its mixtures with the other surfactants. Mixtures were prepared at 1:1 mixing ratio, 0.05-wt% concentration, in presence of oil in DI water.

Table 8: Foamability and foam stability of AOS vs. mixtures at 0.05-wt%, 1:1 mixing ratio in DI water in presence of oil

Surfactants	hfi [cm]	FHL [hr]
AOS	4.878	7.5
AOS/O332	5.378	11.67
AOS/O242	4.333	6.00
AOS/A031	3.691	6.00
AOS/O342	2.548	3.33
AOS/J771	2.066	3.33
AOS/N25-7	1.74	3.33
AOS/J13131	1.616	2.50
AOS/N91-8	1.462	2.00
AOS/A771	1.444	1.67
AOS/N45-7	1.262	1.33
AOS/N25-9	1.208	1.33
AOS/N25-12	1.142	0.67

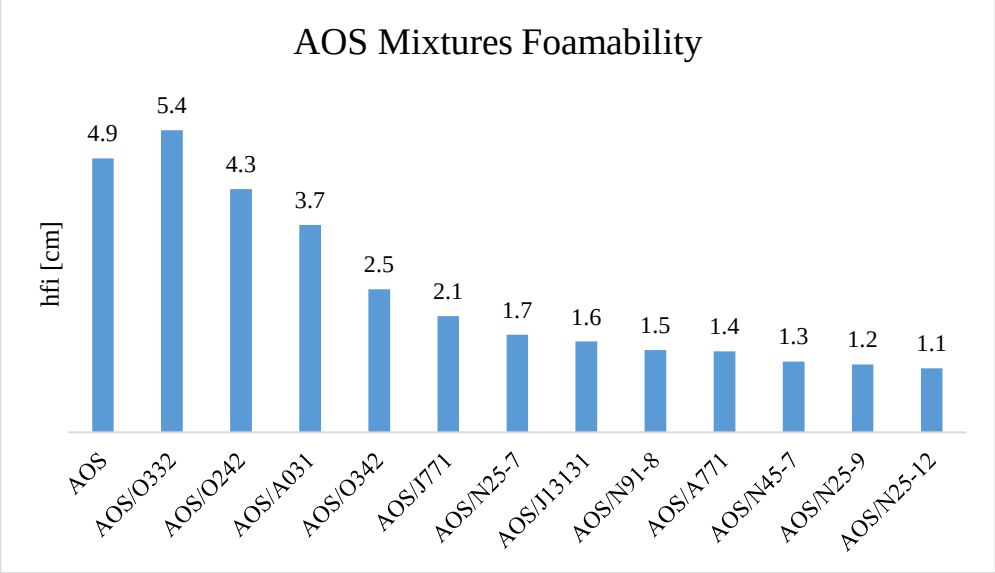

Figure 18: Foamability of AOS vs. 1:1 mixtures with AOS at 0.05-wt% in descending order in presence of oil in DI water

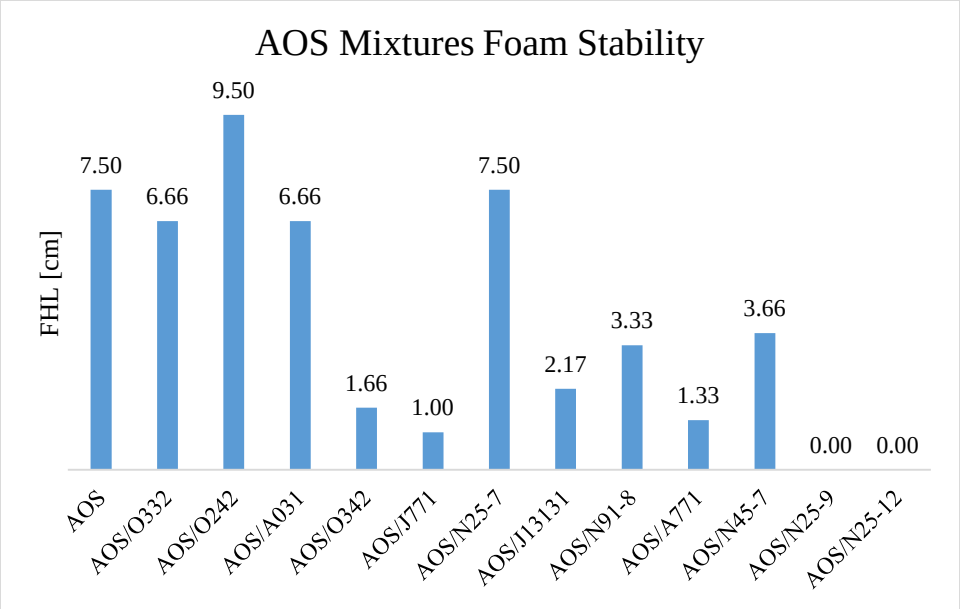

Figure 19: Foam stability of AOS vs. 1:1 mixtures with AOS at 0.05-wt% in descending order in presence of oil in DI water

Again, the main observation can be drawn from the behavior of AOS vs. AOS mixtures is that blending with anionic surfactants provide better synergy over nonionic surfactants in terms of foamability, see AOS/O242, AOS/O332, AOS/O342, and AOS/A031 in **figure 18**. For foam stability, **figure 19** shows that AOS/O242 was the only mixture exhibited better stability than AOS itself. Again, O242 was one the of best foam oil stabilizers in DI water. Moreover, AOS/N25-7 also exhibited good stability, but its foamability is low as shown in **figure 18**.

IV.2.3 O332 Mixtures

Table 9, **figure 20**, and **figure 21** show the results for O332 vs. O332 mixtures with the other surfactants, at 1:1 mixing ratio, 0.05-wt% concentration, in presence of oil, and in DI water. As a remainder, O242 and A031 were the best in terms of foam-oil tolerance in DI water. Repeatedly, O332/O242 and O332/A031 showed good foamability when mixed with O332 in **figure 20**, and better foam stability than O332 in **figure 21** in presence of oil.

Table 9: Foamability and foam stability of O332 vs. mixtures at 0.05-wt%, 1:1 mixing ratio in DI water in presence of oil

Surfactant	hfi[cm]	FHL [hr]
O332	4.935	2
O332/N25-9	6.771	1
O332/N25-7	6.629	2
O332/N25-12	6.466	2.33
O332/AOS	5.378	6
O332/J071	5.102	4.17
O332/AF	4.525	3.33
O332/A031	4.369	13.83
O332/O242	4.356	13.83
O332/A771	3.686	1.5
O332/J13131	3.432	0.5
O332/N25-9	2.397	1
O332/N45-7	1.247	4.45

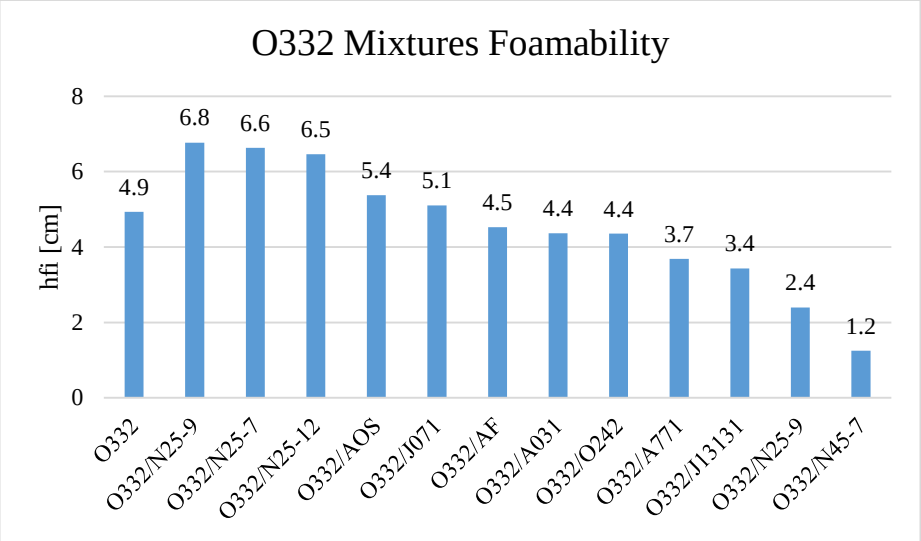

Figure 20: Foamability of O332 vs. mixtures at 0.05-wt%, 1:1 mixing ratio in DI water in presence of oil

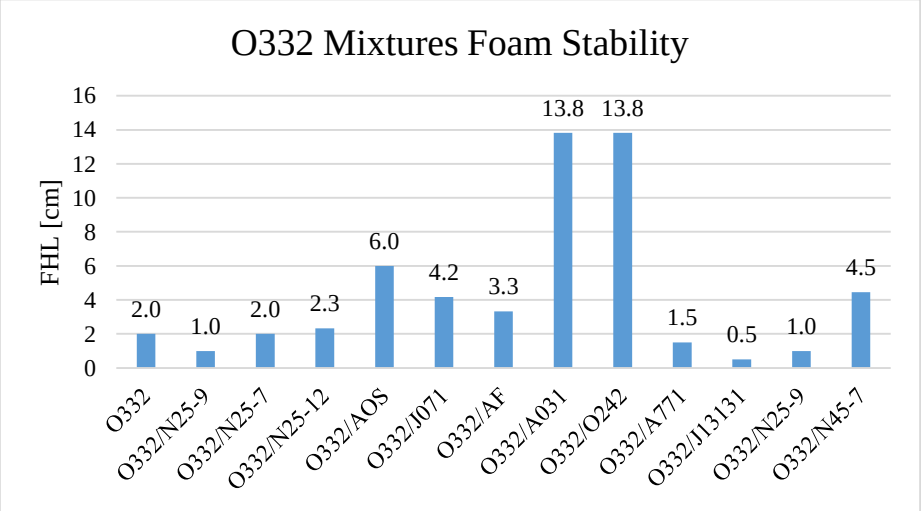

Figure 21: Foams stability and foam stability of O332 vs. mixtures at 0.05-wt%, 1:1 mixing ratio in DI water in presence of oil

IV.3 Concluding Remarks

Surfactants in this study were tested in terms of their foamability and foam stability in presence of crude oil in DI water, NBU salinity, and in 1-wt% NaCl.

In DI water, it was found that anionic surfactants in this study are better foaming agents in presence of crude oil. Overall, anionic surfactants exhibited better ability than nonionic surfactants to generate and stabilize foam in presence of oil in DI water. This is attributed to the abilities of the nonionic surfactants to reduce the $\sigma_{o/w}$.

In NBU salinity, 18-wt%, J071 anionic sulfates was the only showed ability to generate foam at such high salinity in presence of oil. However, it showed poor foam stability, and the salinity exaggerated the oil destabilization effect.

The best three foaming agents in terms of foamability were J071, AOS, and O332. All of these surfactant showed medium to poor foam stability.

Moreover, it was also found that there are three anionic surfactants that have strong foam-oil tolerance: O242, A031, and A771 with variable foamabilities in DI water. However, they exhibited severe drop in foamability and foam stability in presence of oil with salinity. Mixing these surfactants in presence of oil with the best foaming agents in terms of foamability resulted in better foam stability in presence of oil in DI water.

A surfactant with strong ability to reduce the $\sigma_{o/w}$ is not a good foaming agent. Moreover, it might be impossible to find a surfactant that can reduce the $\sigma_{o/w}$ at high reservoir salinity to enhance the oil recovery without compromising the foam stability in presence of oil. Therefore, Farzaneh and Soharbi (2013) proposed the idea of mixing two surfactants where one reduces the $\sigma_{o/w}$ and the other shows good foamability. Such mixture, according to results in this preliminary experiments would work.

In light of the failure of the best surfactants in terms of foam oil tolerance in saline water (O242 and A031) and Farzaneh and Soharbi (2013) suggestion:

- J071 mixtures at 1:1 mixing ratio with O242, A031, and O332 showed better foam oil tolerance than J071 as a good foaming agent.
- AOS by itself is a very good commercially available foaming agent with and without oil. Mixing AOS with other surfactants must result in a good synergism; otherwise, this surfactant alone, in literature, is a well-known foaming agent for mobility control in EOR. There are several mixtures showed better stability with oil than AOS alone, but none of these were able to overcome the AOS foamability.
- For O332, two mixtures were able to enhance the foam stability for O332: O332/O242 and O332/A031 with almost the same foamability.

Therefore, J071 mixtures with the anionic surfactants, O242 and A031, and with the nonionic surfactants will be dealt with separately in the next chapter.

CHAPTER V
EXPERIMENTAL RESULTS AND DISCUSSION*

The preliminary work in previous chapter provided the blends showed better foaming properties in comparison with the individual surfactants that showed the best foamability. This chapter is to show the results of more comprehensive experimental investigation for these blends for one foaming agent, the anionic J071 surfactant. The study includes results from shaking tests, interfacial tension measurements, bubble sizes determination, and dynamic tests that include mobility reduction evaluation and core flooding experiments for oil recovery investigation. All experiments here were conducted using the individual surfactant (J071) and its mixtures for comparison purposes.

V.1 J071-IOS Mixtures

This section is to show the results for J071 in comparison with J071 mixtures with IOS surfactants, see **table 1**. The IOS surfactants are O242, O342, and O332. IOS surfactant O132 is not included due to the insolubility in DI water.

*Reprinted with permission from "A Comparison Between Two Anionic Surfactants for Mobility Control of Super Critical CO_2 in Foam-Assisted Miscible EOR" by Almobarky, M. A., AlYousef, Z., and Schechter, D., 2017, Conference proceedings of the 2017 Carbon Management Technology Conference, Houston TX, July 2017, http://carbonmanagement.org/cmtc/2017", *Society of Petroleum Engineers*, https://doi.org/10.7122/486486-MS, CMTC-486486-MS.

V.1.1 Shaking Tests

Results in **figure 22** show a summary of foam half-lives of the individual surfactants and mixtures at 0.05-wt% in DI water and in 1-wt% NaCl. The best among the individual surfactants was O242 in DI water. However, it was affected severely with the addition of 1-wt% NaCl due to the high hydrophobicity induced by the long carbon chain length. Mixing J071 and O242 synergized in saline water and provided better foam stability than both J071 and O242. However, no synergism was observed with mixing J071 with O342 or O332.

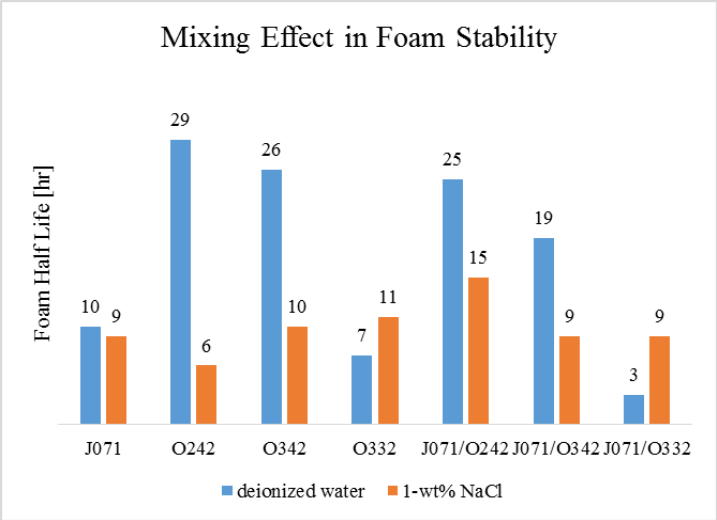

Figure 22: Foam-half lives for individual surfactants and mixtures at 1:1 mixing ratio at 0.05-wt% in DI water and at 1-wt% NaCl.

Figures 23 and **24** show the normalized foam heights in DI water for the individual surfactants and mixtures, respectively. For the individual surfactants, O242 foam showed

the best stability, and J071/O242 at 1:1 mixing ratio also showed the best stability among the other mixtures.

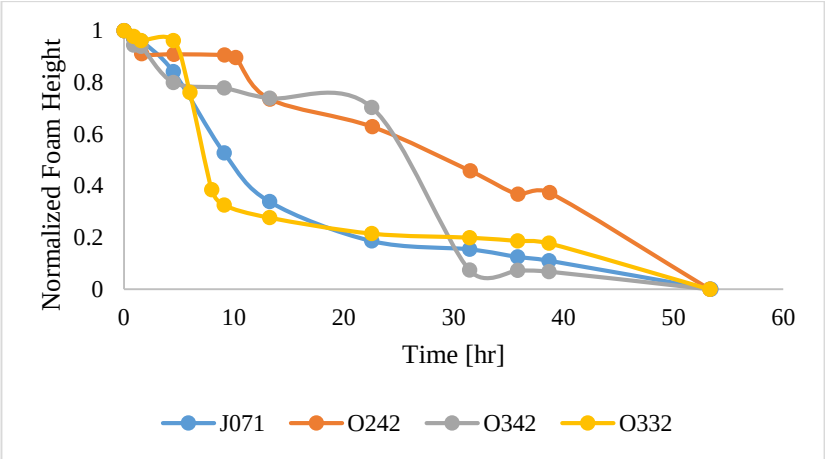

Figure 23: Foam columns decay for individual surfactants in DI water at 0.05-wt%

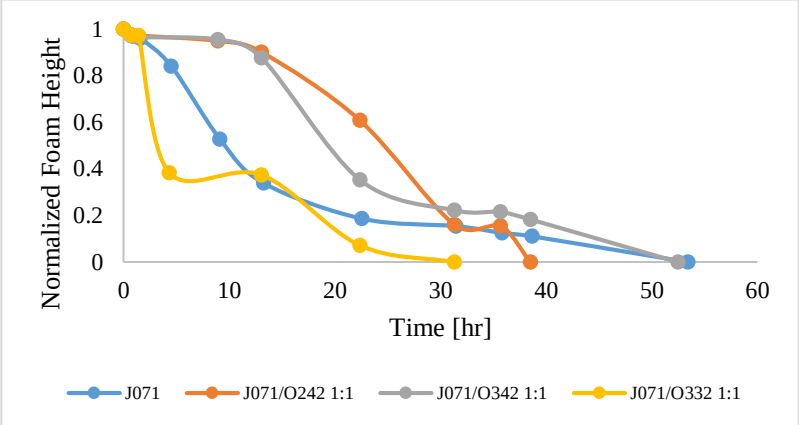

Figure 24: Foam columns decay in DI water for J071 in comparison with the mixtures at 1:1 mixing ratio

V.1.2 Shaking Tests With Oil

Figure 25 shows the foam half-lives for J071 in comparison with J071-IOS mixtures, in presence of oil in DI and in 1-wt% saline water. All mixtures showed better

foam-oil tolerance than J071 in DI water. However, in salinity, J071/O242 mixture was the only one observed with better foam stability than J071. **Figure 26** below shows the initial foam columns for J071, O242, and J071/O242 at 1:1 mixing ratio in DI water and saline water. It is clear that O242 lost the ability to generate foam in 1-wt% NaCl due to the ability to reduce $\sigma_{o/w}$. However, mixing J071 with O242 generated larger foam volume in saline water and exhibited better foam-oil tolerance than both individual surfactants.

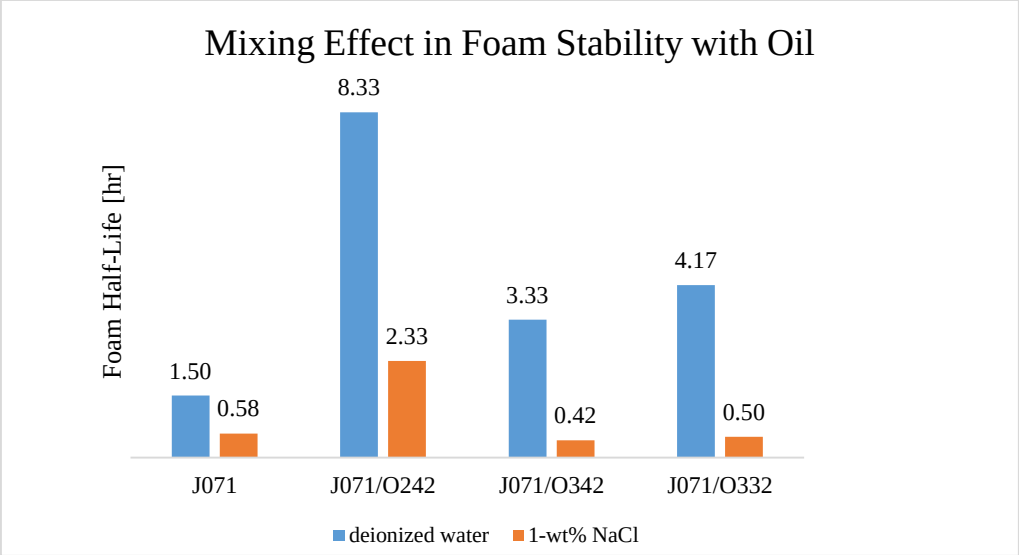

Figure 25: Foam half lives in presence of oil.

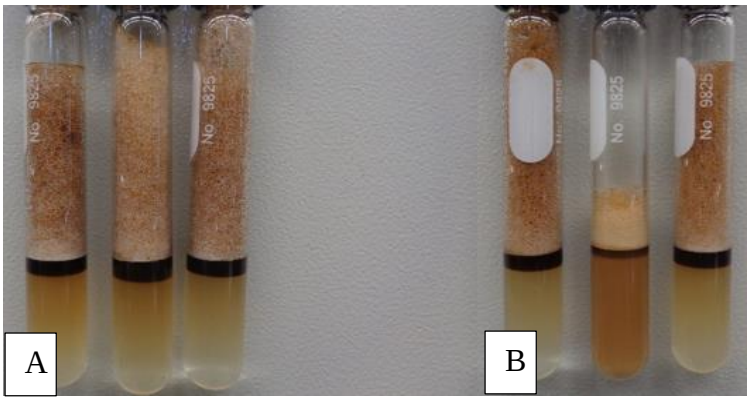

Figure 26: A) J071, O242, J071/O242 1:1 mixing ratio in DI water, and B) J071, O242, and J071/O242 1:1 in 1-wt% NaCl salinity

V.1.3 Interfacial Properties

Figures 27 and **28** show the surface tension values at different concentrations for J071 and the other IOS surfactants. CMC values, surface densities (Γ) and area/molecule (A) at the G/W interface for all surfactants are listed in **Table 10**.

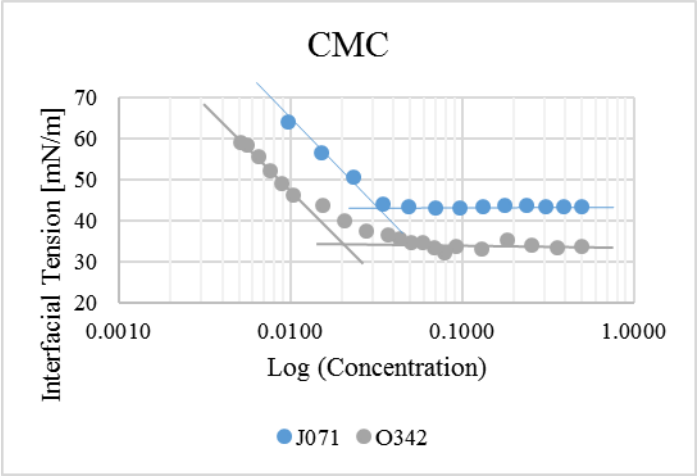

Figure 27: CMC for J071 and O342

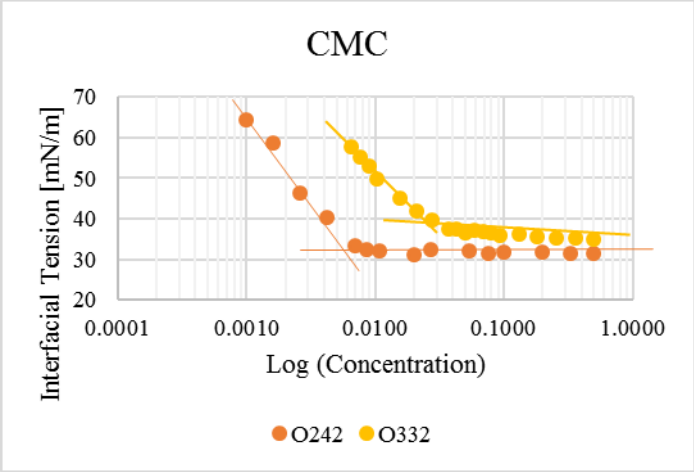

Figure 28: CMC for O242 and O332

Table 10: Interfacial properties

Surfactant	CMC [wt%]	Γ [mol/cm^2]	A [Å^2/mol]
J071	0.036	6.00E-10	27.66
O242	0.005	9.56E-10	17.37
O342	0.02	7.63E-10	21.75
O332	0.027	5.90E-10	28.15

From **table 10**, the high foaming ability and high foam stability of O242 can be attributed to the highest surface density (Γ) (i.e. the highest adsorption at the air-liquid interface) which normally leads to the minimum area/ molecule at the interface (A). In fact, this behavior can be inferred from the sharper slope of the straight line of the concentrations below the CMC for O242 in **figure 28**. The sharper the slope indicates the higher adsorption and the smaller area/molecule at the G/W interface. This combination of interfacial properties according to Rosen and Kunjappu (2004) indicates tight packing

of the monolayer of the surfactants at the interface which normally results in higher foam stability.

Figure 29 shows the $\sigma_{g/w}$ and foam stability for the individual surfactants and the mixtures. J071/O242 (1:1) mixture has the lowest $\sigma_{g/w}$ and the maximum foam stability in comparison with J071 and other mixtures. When J071 was mixed with O242, the higher adsorption and smaller area/molecule of O242 perhaps provided the same properties for J071/O242 in comparison with J071 and other mixtures. The same reasoning was used in (Bera, Ojha, and Mandal 2013)

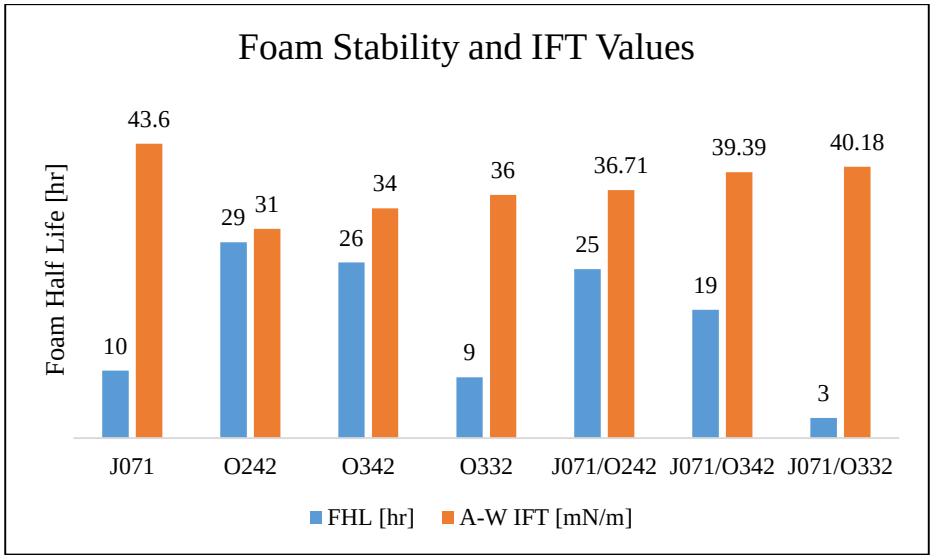

Figure 29: Foam half-lives and $\sigma_{g/w}$

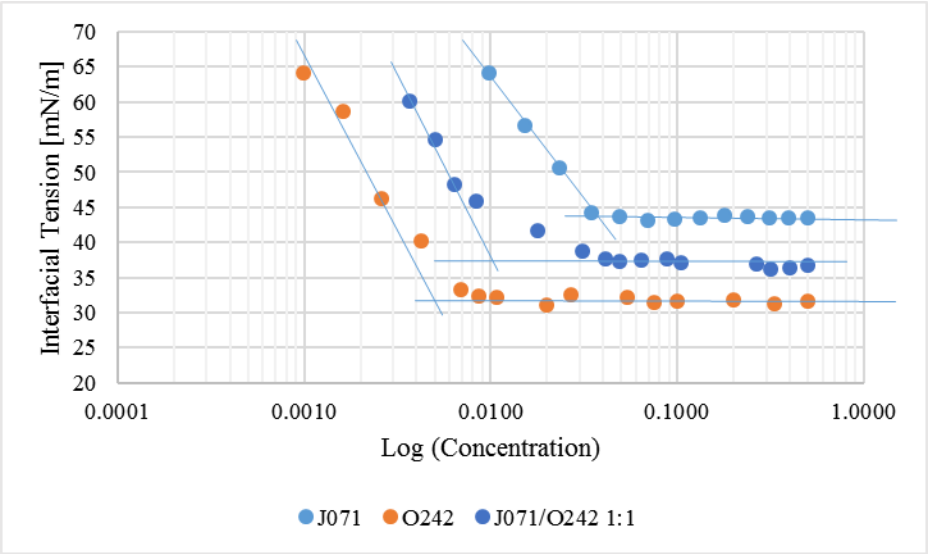

Figure 30: CMC for J071, O242, and J071/O242 1:1

Moreover, the best enhancement in foam stability by mixing anionic and nonionic surfactants was correlated with the maximum reduction in CMC (Schick and Fowkes 1957). As observed, O242 has the lowest CMC due to the high hydrophobicity, and consequently, it is expected to provide the maximum reduction in J071 surfactant CMC. **Figure 30** shows that J071/O242 at 1:1 mixing ratio in DI water gives 0.01-wt% CMC in comparison with 0.036-wt% for J071, but still higher than the CMC of O242 which was 0.005-wt%.

V.1.4 Effect of Surfactant Concentration

At 0.05-wt% in absence of oil, the foam stabilities of J071, O242, and J071/O242 1:1 dropped from 10, 29, and 26-hr in DI water to 9, 6, and 10-hr in 1-wt% NaCl,

respectively. In presence of oil, the foam stabilities dropped from 1.5, 23, 8-hr in DI water to 0.5-hr for the individual surfactants and 2-hr for the mixture.

Figure 31 shows the results at 0.05-wt% in comparison with higher concentration, 0.5-wt%, for J071, O242, and their mixture at 1:1 mixing ratio in DI and saline water. The foam stabilities in DI water decreased when increasing the concentration. However, in 1-wt% salinity, increasing the concentration increased the foam stabilities.

The drop in foam stability in DI water with increasing the concertation can be attributed to the decrease in surface elasticity (i.e. Marangoni effect). Surface elasticity depends inversely on the surfactant concentration (Schramm and Kutay 2000). Moreover, increasing the concentration of a very long carbon chain length surfactant may further decrease the elasticity of the thin-film because of the cohesion of long hydrophobic tails at the interface. However, the study will proceed with the high concertation because of the oil effect and the adsorption at rock surfaces inside the porous media.

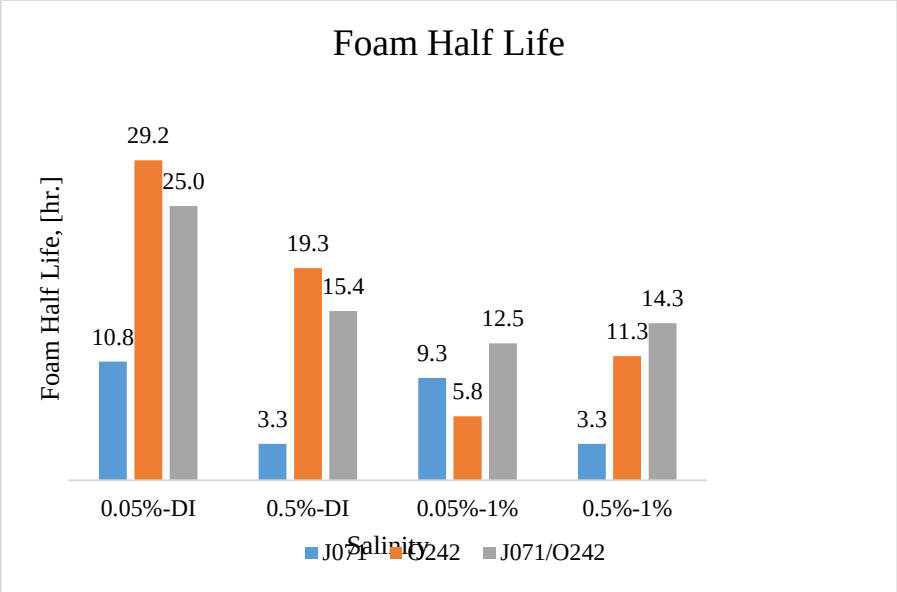

Figure 31: Effect of concentration on foam stability from 0.05 to 0.5-wt%

V.1.5 Effect of Mixing Ratio

This effect was investigated to optimize the mixture's solubility and foam stability with salinity. Patist et al. (1999) showed that 1:3 and 3:1 molar ratios in mixed surfactants systems has many benefits for the interfacial activity especially in foaming systems. Shah (1971) attributed the better foam stabilities at 1:3 and 3:1 molar ratios to the tightest hexagonal packing of the micelles in the lamellae.

Figure 32 shows samples for J071, O242, and the mixture at 1:1 mixing ratio at 0.5-wt% in DI water, 1, 2, and 3-wt% NaCl. As shown, O242 showed less solubility in brine solutions as salinity increases and precipitated at 3-wt% NaCl. However, the mixture at 1:1 ratio showed better solubility with less haziness than O242. **Figure 33** shows more mixing ratios for J071/O242 at 2:1, 4:1, and 1:2. Increasing J071 concentrations (i.e. 2:1 and 4:1) enhanced the solubility in brine solutions. On the other hand, increasing O242

concentration in mixture (i.e. 1:2 mixing ratio) caused less solubility in brine solutions as salinity increases.

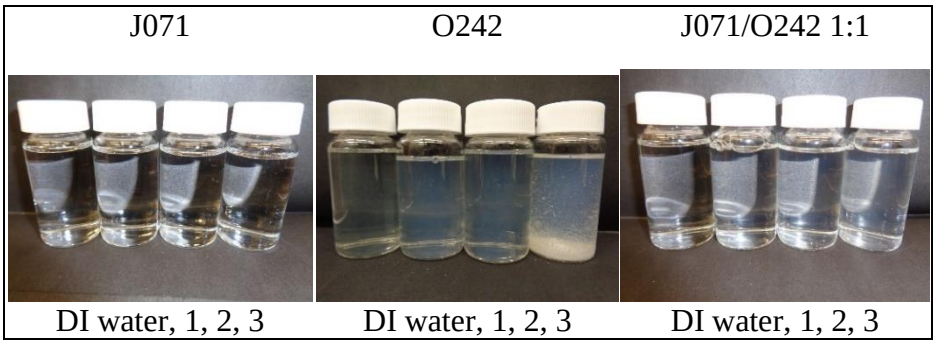

Figure 32: Effect of Salinity in water-solubility

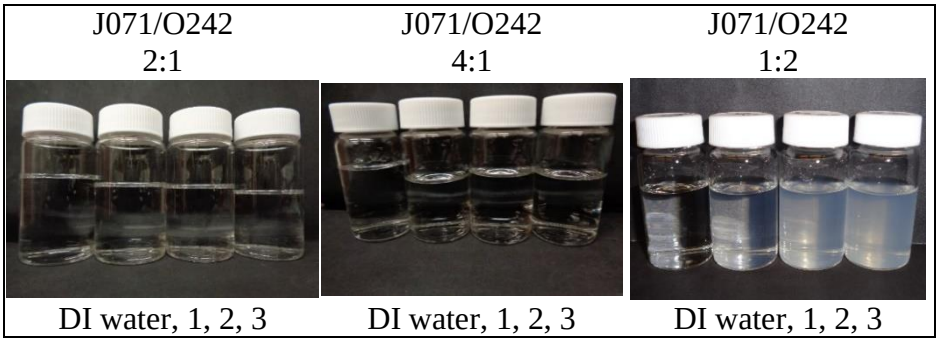

Figure 33: Effect of Salinity in water-solubility at different mixing ratios

The mixing ratio 1:2 in DI water was found very effective in terms of foam stability in absence and presence of crude oil, results are not shown. For the ultimate synergism in interfacial activity in mixed surfactants systems, it was recommended to use a high concertation of the surfactant that has lower CMC according to Rosen (2004). However, this 1:2 mixing ratio at 0.5-wt% total surfactant concentration exhibited lower foamability

and foam stability in saline water due to the low solubility in brine solutions, see **figure 33.** Therefore, the mixing ratio effect will continue with 2:1 and 4:1 ratios only.

Figure 34 shows the foam stabilities for all mixing ratios in comparison with J071 and O242 in all salinities from DI water to 3-wt% NaCl. All samples were prepared at 0.5-wt% concentrations. It is clear that changing the mixing ratio did not change the conclusion that J071/O242 mixture was better than J071either in DI water or in 1-wt% NaCl.

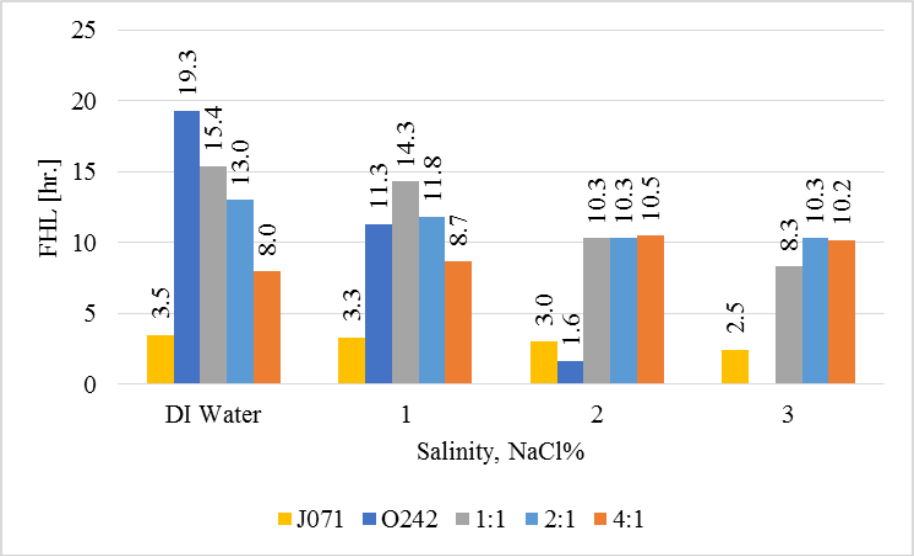

Figure 34: Foam half-lives for J071, O242 and J071/O242 at 1:1, 2:1 and 4:1 at 0.5-wt% in DI water, 1, 2, and 3-wt% NaCl

However, in **figure 34**, for 1:1 mixing ratio, the foam stability decreases as the salinity increases. For 2:1, the foam stability decreases and plateaued from 2 to 3-wt% NaCl. For 4:1 mixing ratio, the foam stability was increasing as the salinity increases. This

behavior can be explained by the effect of salinity on the size of the electric double layer around the micelle and the reflection of such effect on the ordered micellar structure of the micelles inside the lamellae.

According to Nikolov et al. (1989), the addition of electrolyte causes the electric double layer diameter around the micelle to decrease causing less repulsive forces between the micelles. The lower repulsive forces disrupted the ordered micellar structure and accelerated the thin-film thinning process that resulted in lower foam stability (Nikolov et al. 1989). This normally occurs as the salinity increases in 1:1 and 2:1 mixing ratios. However, 4:1 mixing ratio was abnormally increasing in foam stability as salinity increases.

In light of the results in **figure 34** above and Nikolov et al. (1989) conclusions:

- 1:1 mixture of DI water gave 15.4-hr FHL. The addition of more hydrophilic surfactant in DI water (1:1 to 2:1 to 4:1) decreased the foam stability because of the higher repulsive forces between the micelles. In this case, increasing the repulsive forces caused large distances between the micelles which induces weaker packing (i.e. ordered micellar structure) in the lamellae region, see **figure 35**.
- From DI water to 1-wt% NaCl, the repulsive forces decreased between the micelles. Consequently, both 1:1 and 2:1 mixing ratios exhibited lower foam stability. However, 4:1 mixing ratio exhibited higher foam stability from DI water to 1-wt% NaCl. This is because the drop in the repulsive forces is increasing the strength of the micelles packing in the lamellae without compromising the foam stability. As salinity increases, the strength of the packing in 4:1 mixing ratio is

increasing, whereas the packing is becoming weaker for both 2:1 and 1:1. This is shown graphically in **figure 35**.

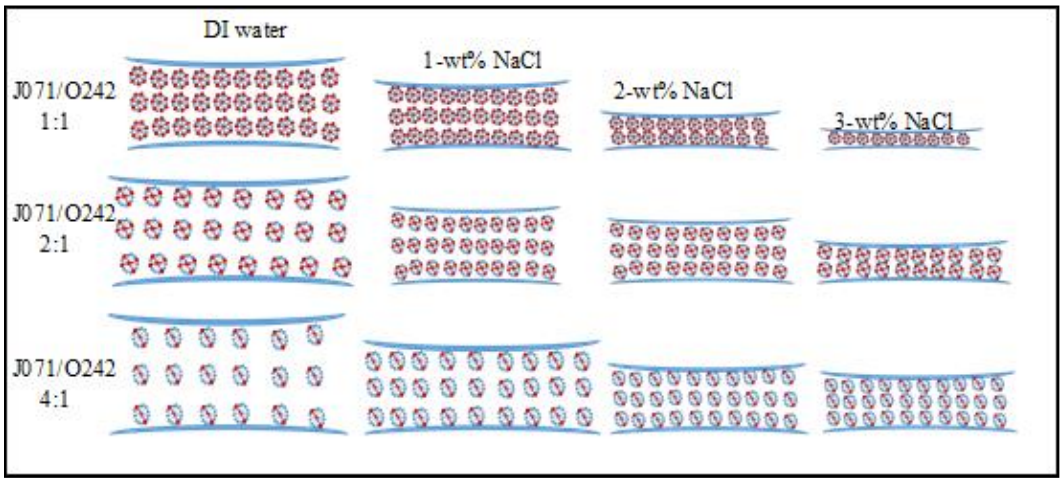

Figure 35: Mixing ratio effect on foam stability

V.1.6 Effect of Oil

The $\sigma_{o/w}$ and $\sigma_{g/w}$ values at 0.5-wt% are listed in **tables 11** and **12**. Moreover, entering (E), spreading (S), and bridging-coefficients (B) were calculated and tabulated in **tables 13** through **15**.

Table 11: $\sigma_{o/w}$ measurements, 0.5-wt% concentration, at 25°C temperature

Surfactant	DI water	1-wt% NaCl	2-wt% NaCl	3-wt% NaCl
J071	3.48	0.62	0.5	0.458
O242	0.26	--	--	--
J071/O242 1:1	0.51	0.11	0.17	0.14
J071/O242 2:1	2.83	0.66	0.59	0.32
J071/O242 4:1	3.97	0.54	0.41	0.35

Table 12: $\sigma_{g/w}$ measurements, 0.5-wt% concentration, at 25°C temperature

Surfactant	DI water	1-wt% NaCl	2-wt% NaCl	3-wt% NaCl
J071	43.6	39.55	38.59	36.51
O242	30.78	29.11	29.29	--
J071/O242 1:1	35.71	30.19	30.91	30.99
J071/O242 2:1	37.07	32.81	31.62	30.73
J071/O242 4:1	38.18	32.53	31.82	30.65

Table 13: J071 vs. J071/O242 2:1 entering coefficients at 0.5-wt% surfactant concentration at room temperature

Surfactant	DI water	1-wt% NaCl	2-wt% NaCl	3-wt% NaCl
J071	15.58	8.67	7.585	5.468
O242	**-0.46**	--	--	--
J071/O242 1:1	4.72	**-1.2**	**-0.42**	**-0.37**
J071/O242 2:1	8.4	1.965	0.71	**-0.455**
J071/O242 4:1	10.65	1.57	0.73	**-0.498**

Table 14: J071 vs. J071/O242 2:1 spreading coefficient at 0.5-wt% surfactant concentration at room temperature

Surfactant	DI water	1-wt% NaCl	2-wt% NaCl	3-wt% NaCl
J071	8.62	7.43	6.595	4.552
O242	**-0.98**	--	--	--
J071/O242 1:1	3.7	**-1.42**	**-0.76**	**-0.65**
J071/O242 2:1	2.74	0.655	**-0.47**	**-1.085**
J071/O242 4:1	2.71	0.49	**-0.09**	**-1.202**

Table 15: J071 vs. J071/O242 2:1 bridging coefficient at 0.5-wt% surfactant concentration at room temperature

Surfactant	DI water	1-wt% NaCl	2-wt% NaCl	3-wt% NaCl
J071	920.82	572.34	497.18	340.94
O242	**-44.77**	--	--	--
J071/O242 1:1	283.21	**-80.80**	**-36.79**	**-31.85**
J071/O242 2:1	389.94	84.68	7.92	**-47.82**
J071/O242 4:1	481.22	66.24	20.43	**-52.70**

For **tables 13**, **14**, and **15** for entering, spreading, and bridging-coefficients, the surfactant is stable with oil if these coefficients are negative values. Accordingly, the best in terms of foam-oil tolerance are O242 in DI water, J071/O242 1:1 mixture at all salinities but not in DI water, and both 2:1 and 4:1 at 2 and 3-wt% NaCl salinities.

Table 16: J071 vs. J071/O242 2:1 lamellae number at 0.5-wt% surfactant concentration at room temperature

Surfactant	DI water	1-wt% NaCl	2-wt% NaCl	3-wt% NaCl
J071	1.88	9.57	11.69	11.96
O242	17.76	--	--	--
J071/O242 1:1	10.50	41.17	27.27	33.20
J071/O242 2:1	1.96	7.51	8.04	14.63
J071/O242 4:1	1.44	9.04	11.64	13.06

The lamellae numbers are shown in **table 16**. J071 is semi-stable at DI water and unstable at all salinities. Moreover, since L>7, O242 is unstable. For the mixtures, the lamellae numbers interpretations show that 1:1 mixing ratio is unstable at all conditions. However, 2:1 and 4:1 mixtures are semi-stable in DI water, and unstable in saline waters.

The foam columns in presence of oil for J071/O242 1:1, 2:1, and 4:1 are in the following figures. **Figure 36** shows 1:1 mixing ratio after 0-hr, 1-hr, and 6-hrs. Each three samples in each image represent DI, w-wt% NaCl, and 2-wt% NaCl left to right. Mixing ratio 1:1 showed high foam stability with oil in saline solutions.

Mixing ratios 2:1 and 4:1 are also showing good foam-oil tolerance in salinity samples, see **figure 37** and **38**. Foam in mixing ratio 4:1 collapsed before the 6-hr shot was taken.

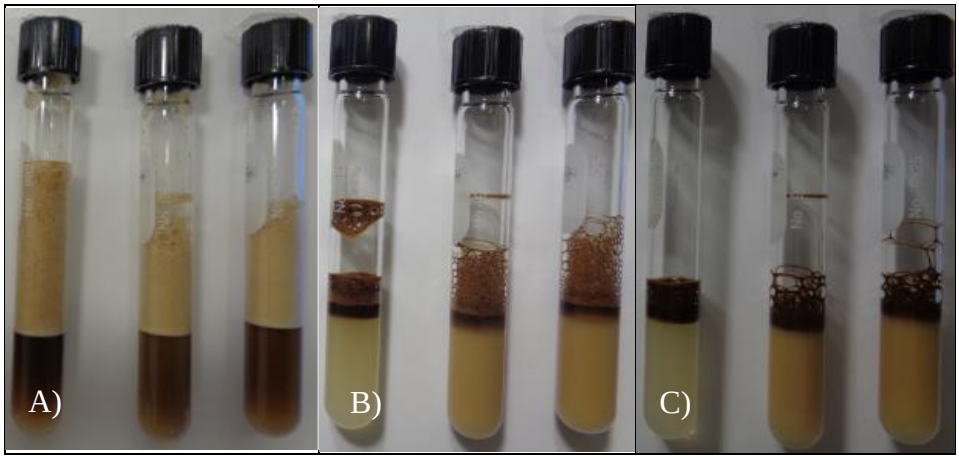

Figure 36: Foam columns in presence of oil for J071/O242 at 1:1 mixing ratio at 0.5-wt% in DI water, 1, and 2-wt%. a) At 0-hr; B) At 1-hr; and C) At 6-hr.

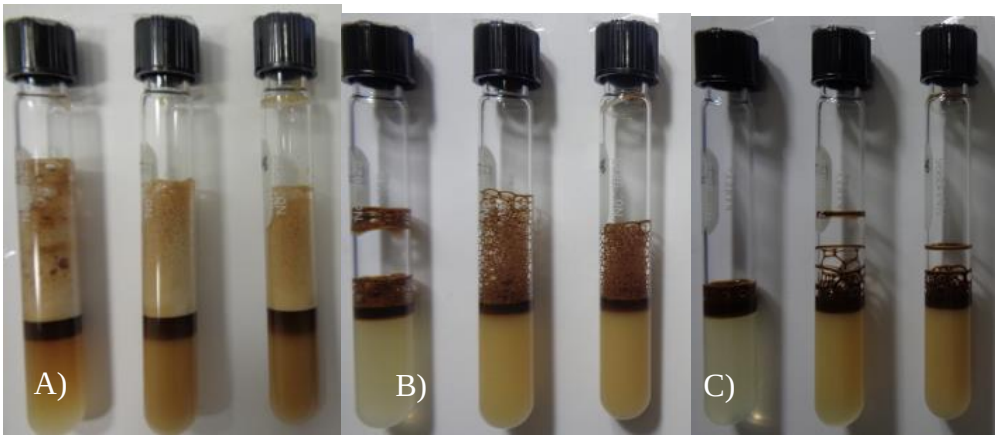

Figure 37: Foam columns in presence of oil for J071/O242 at 2:1 mixing ratio at 0.5-wt% in DI water, 1, and 2-wt%. a) At 0-hr; B) At 1-hr; and C) At 6-hr.

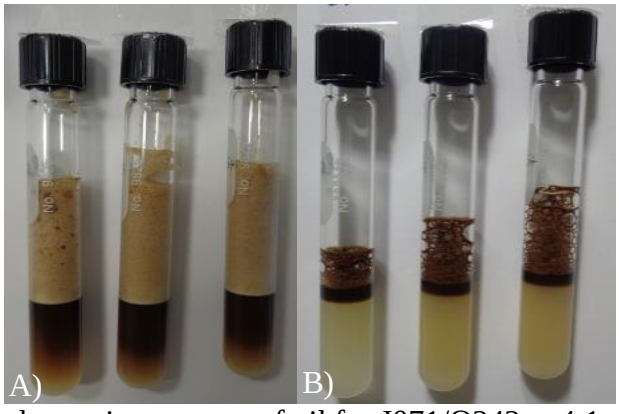

Figure 38: Foam columns in presence of oil for J071/O242 at 4:1 mixing ratio at 0.5-wt% in DI water, 1, and 2-wt%. a) At 0-hr; B) At 1-hr; and no foam column was observed at 6-hr.

In general, shaking tests observations with oil were in agreement with the entering, spreading, and bridging coefficients interpretations. However, the lamellae numbers interpretations were in a disagreement with the shaking tests observations.

V.1.7 Micro-Imaging and Bubble Sizes

Figure 39 through **41** show J071 foam bubbles in comparison with all mixing ratios in DI water, 1, and 3-wt% NaCl, respectively. All mixing ratios at all salinities are showing smaller foam bubbles than J071 bubbles after 1-hr.

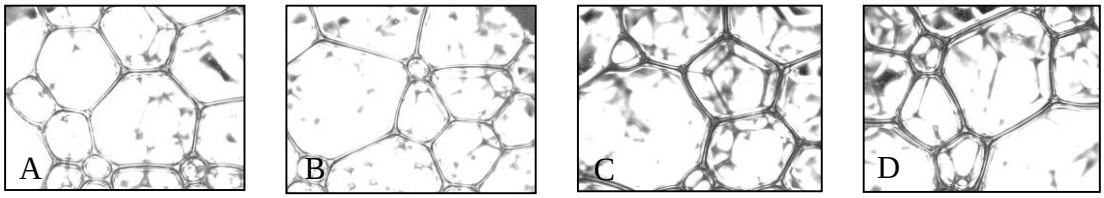

Figure 39: Micro-images after 1-hr. at 0.5-wt% surfactant concentration In DI water, A) J071; B)J071/O242 1:1; C) J071/O242 2:1; and D) J071/O242 4:1

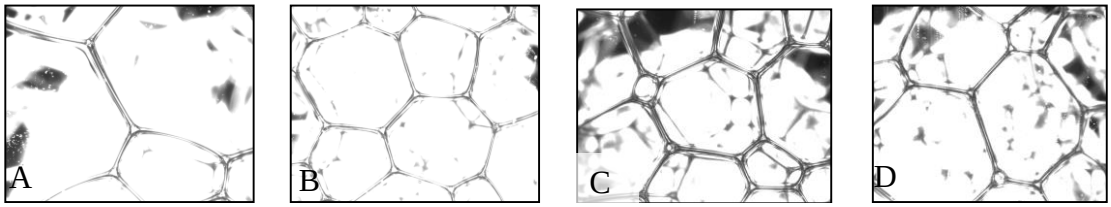

Figure 40: Micro-images after 1-hr. at 0.5-wt% surfactant concentration in 1-wt% NaCl salinity, A) J071; B)J071/O242 1:1; C) J071/O242 2:1; and D) J071/O242 4:1

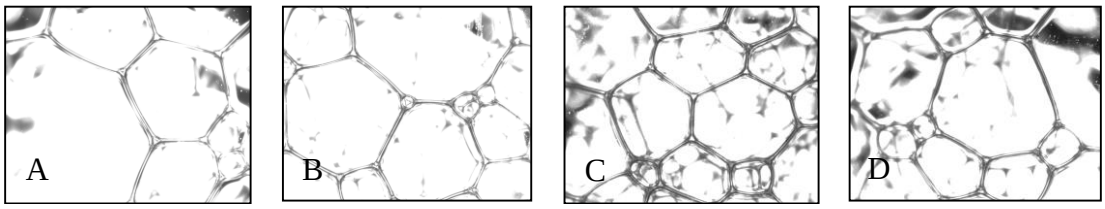

Figure 41: Micro-images after 1-hr. at 0.5-wt% surfactant concentration in 3-wt% NaCl salinity, A) J071; B)J071/O242 1:1; C) J071/O242 2:1; and D) J071/O242 4:1

Moreover, the average bubble sizes are shown in **figures 42** through **45** after 1-hr period of time in DI water, 1, 2, and 3-wt% NaCl, respectively. As salinity increases, the bubble sizes of the mixtures are smaller than J071 with time. The smaller bubble sizes with time refer to less effect of destabilization mechanisms such as lower rate of liquid drainage from the lamellae.

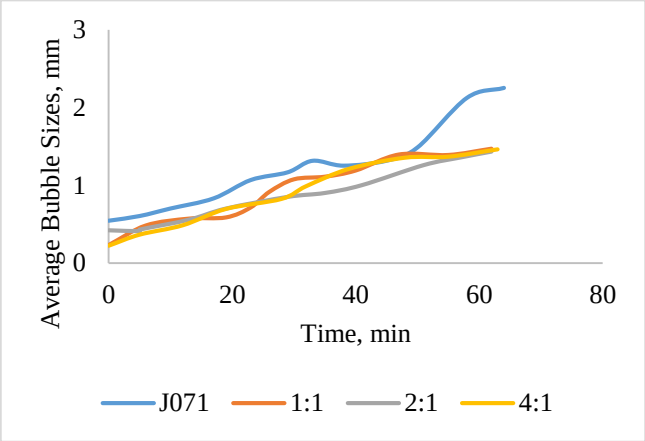

Figure 42 Average bubble sizes with time for J071 vs. all mixing ratios in DI water

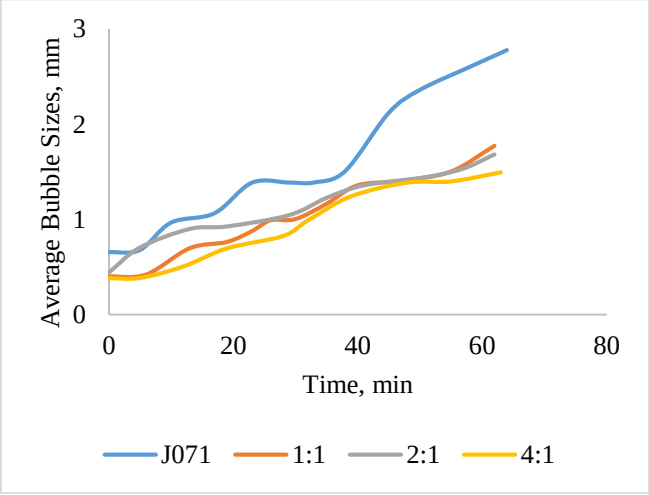

Figure 43: Average bubble sizes with time for J071 vs. all mixing ratios in 1-wt% NaCl

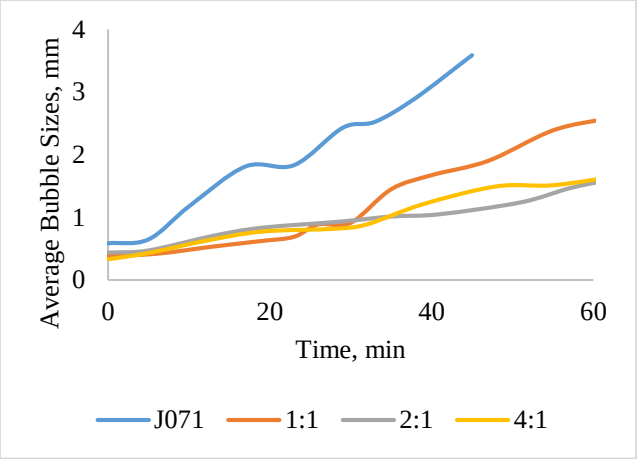

Figure 44: Average bubble sizes with time for J071 vs. all mixing ratios in 2-wt% NaCl

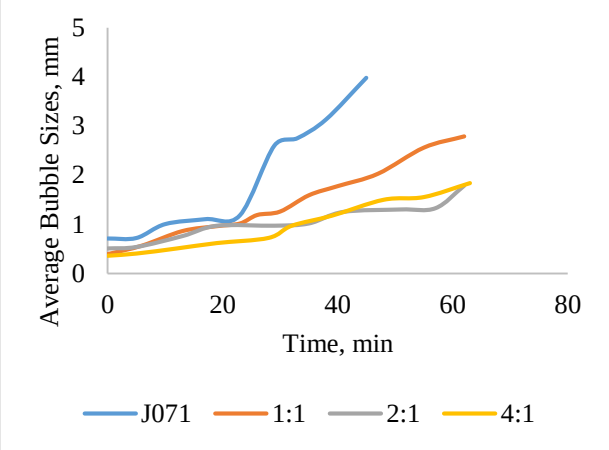

Figure 45: Average bubble sizes with time for J071 vs. all mixing ratios in 3-wt% NaCl

V.1.8 Foam Dynamic Tests

This section is to show the mobility reduction evaluation of J071 in comparison with J071/O242 at 2:1 mixing ratio. The experimental conditions are shown in **table 17**. **Table 18** also shows the results of all experiments conducted in this section.

Foam placement was achieved by surfactant and N_2 simultaneous injection. Moreover, one baseline experiment was conducted using N_2 injection without surfactant.

Table 17: Experimental Conditions for J071 vs. J071/O242 mixtures

Run #	Surfactant	Concentration [wt%]	Salinity NaCl [wt%]	Porous Media	k [Darcy]	φ [%]	P [psi]	T [°C]	Q [ml/min]	Injection Quality [%]	Velocity [ft/D]	Shear rate [1/sec]
1	J071	0.5	DI water	Glass beads	17.1	30	850	50	0.5	70	--	454.74
2	J071/O242 (2:1)	0.5	DI water	Glass beads	17.1	30	850	50	0.5	70	--	454.74
3	J071	0.5	1	Sandstone	1.62	21.84	850	50	0.117	90	5	9.15
4	J071	0.5	1	Sandstone	1.63	20.22	850	50	0.109	70	5	8.84
5	J071/O242 (2:1)	0.5	1	Sandstone	1.62	21.84	850	50	0.117	90	5	9.15
6	J071/O242 (2:1)	0.5	1	Sandstone	1.62	20.22	850	50	0.107	70	5	8.87
7	--	--	1	Sandstone	1.62	21.84	850	50	0.117	90	5	9.15

Table 18: Results for J071 vs. J071/O242 2:1 mobility evaluation

Run #	Surfactant	Porous media	Shear rate [1/sec]	k [Darcy]	Injection Quality [%]	ΔP_{ss} [psi]	Mobility [md/cp]	μ_{eff} [cp]	MRF
1	J071	Glass beads	454.74	17.1	70	481	72	334	1200
2	J071/O242 2:1	Glass beads	454.74	17.1	70	325	76	225	813
3	J071	Sandstone	9.15	1.62	90	5.27	33	50	13
4	J071	Sandstone	8.84	1.63	70	2.24	72	23	5.6
5	J071/O242 2:1	Sandstone	9.15	1.62	90	27	6.4	254	67.5
6	J071/O242 2:1	Sandstone	8.87	1.62	70	30	5.3	304	75
7	--	Sandstone	9.15	1.62	--	0.4	431	3.8	--

V.1.8.1 Results

Figure 46 shows the pressure drop profiles vs. pore volumes injected for both J071 and the mixture, runs 1 and 2 in **tables 17** and **18**. These runs were conducted in glass beads pack at high shear rate ~455 sec^{-1}. The pressure drop profiles show the foam was successfully generated inside the glass beads pack. In disagreement with the results in the previous static foam tests, J071 foam had higher pressure drop (i.e. higher flow resistance) than that of the mixture. However, in the first 12 pore volumes injected, **figure 47**, the mixture outweighed J071 but J071 proved stronger after the 12 pore volumes to the end of the run.

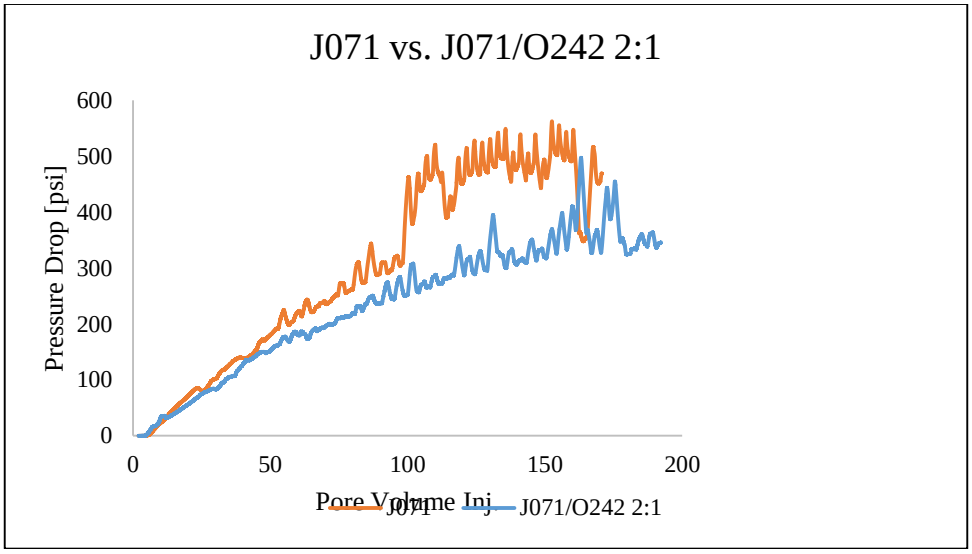

Figure 46: Run 1 J0171 vs. run 2 J071/O242 at 2:1 mixing ratio, high shear rate in the Glass Beads Pack

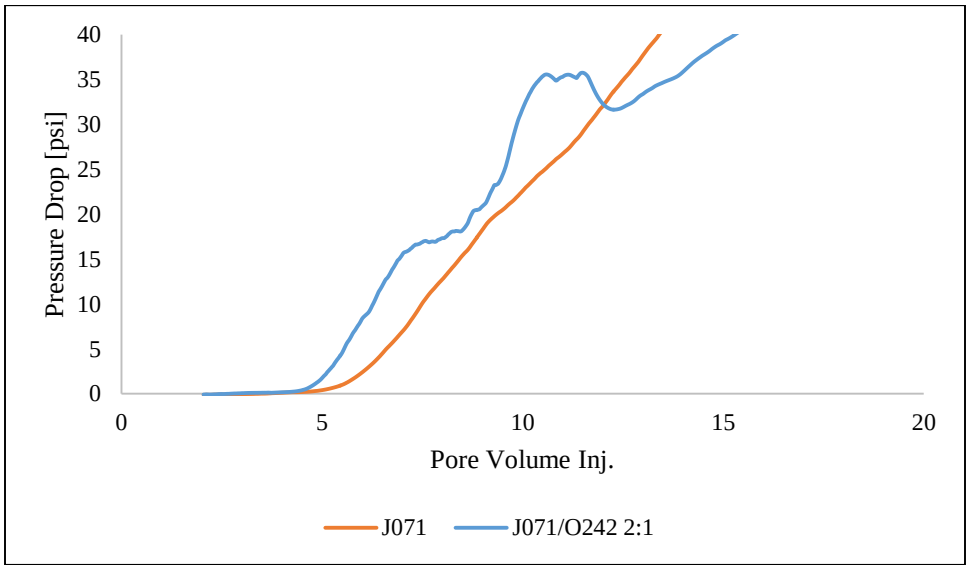

Figure 47: The first 20 pore volumes of Run 1 and run 2

Figure 48 and **49** show J071 vs. the mixture at 90% and 70% injection quality at low shear rate ~9-sec^{-1} in sandstone. At low shear rate, the mixture provided higher pressure drop (i.e. higher flow resistance) than J071 at both injection qualities. These results are in agreement with the static tests results, but in disagreement with the previous high shear rate dynamic tests.

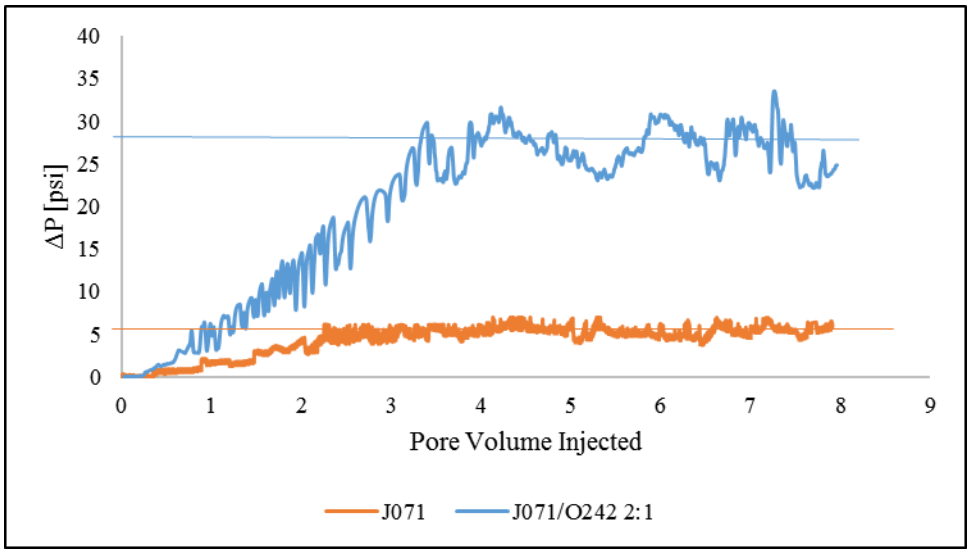

Figure 48: Run 3 vs. run 5 at 90% injection quality

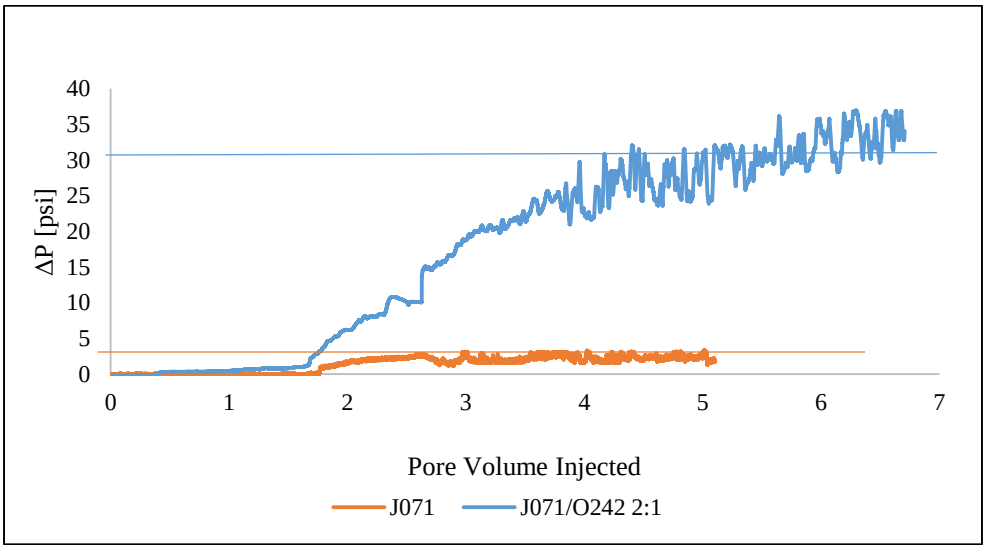

Figure 49: Run 4 vs. run 6 at 70% injection quality

V.1.8.2 Discussion

The pressure profiles in both porous media showed the rapid pressure increase in pressure drop. This is a sign of successful strong in-situ foam generation indicating that both J071 and the mixture are good foaming agents.

The flow resistance due to the foam generation was higher in the high permeability glass beads pack. This is eventually because foam favors the high permeable porous media in which the foam generation is easier (Rossen and Gauglitz 2002).

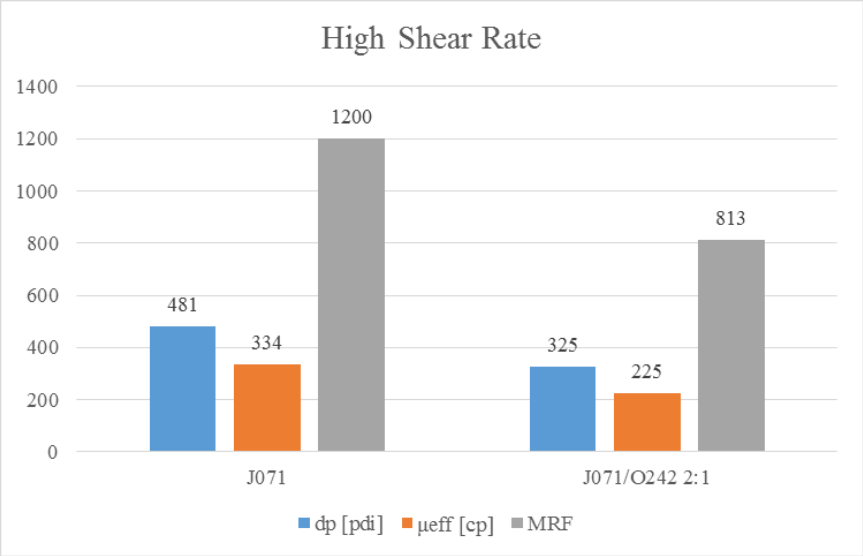

Figure 50: Glass beads pack results for J071 vs. J071/O242 2:1, run 1 vs. run 2

In high permeability glass beads pack at high shear rate, J071/N_2 simultaneous injection generated higher steady state pressure drop, higher foam viscosity and higher mobility reduction than that of the mixture**,** see **figure 50**. However, the ability of the

mixture to lower the $\sigma_{g/w}$ (37.3 mN/m) less than that of J071 (43.6 mN/m) promoted earlier strong foam generation with the mixture during the first 12 pore volumes, see **figure 47**.

On the contrary, in sandstone at low shear rate, the mixture provided higher flow resistance with higher pressure drop than that of J071. These contradictory behaviors of J071 and the mixture at high and low shear rates from what has been observed during the static tests can be explained by the effect of micellar stability on the foamability and foam stability.

Patist et al. (2000) and (2001) found a correlation between the micellar stability with the foamability and foam stability. Their studies were conducted with SDS anionic surfactant, nonionic surfactants, and mixtures of SDS with alcohols. It was found that increasing the micellar stability of SDS anionic surfactant leads to decrease the foamability and increase the foam stability.

J071 anionic surfactant, in the static tests, showed impressive foamability at all conditions even at high salinity such as NBU salinity. Such high foamability perhaps indicates the high monomeric activity of this surfactant (i.e. low micellar stability). When the micellar stability is low, the micelles break up into monomers at high shear rate and stabilize the newly created interfaces during the foam generation. As a result, the foam viscosity during the foam generation is too high. On the other hand, with the mixture when the micelles are very stable, the high shear rate will not disintegrate the micelles into monomers, and the newly created interfaces during foam generation will collapse due to the depletion of monomers. At the low shear rate, the higher micellar stability of the

mixture was helpful to generate stronger foam because J071 micelles were not able to disintegrate into monomers.

Figure 51 shows the results for J071 and the mixture at low shear rate in sandstone. At the low shear rate, the mixture's steady state pressure drop, foam viscosity, and MRF were better than that of J071.

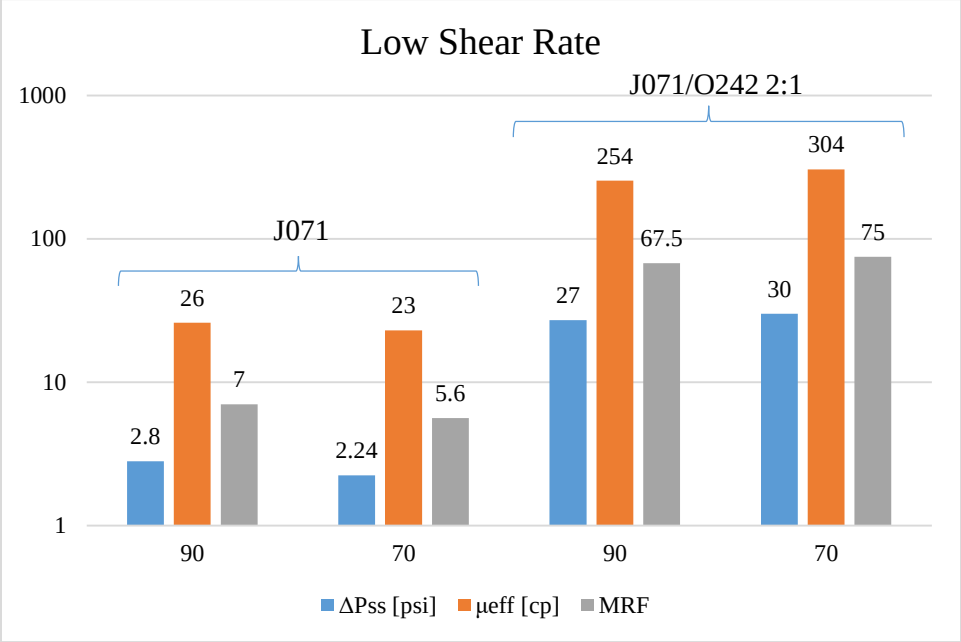

Figure 51: Runs 3, 4, 5 and 6 for J071 and J071/O242 at 70-90% injection qualities

Therefore, the low micellar stability enabled J071 surfactant to generate stronger foam than the mixture at high shear rate only. However, the higher micellar stability of the mixture promoted the generation of a stronger foam in sandstone at low shear rate.

V.1.9 Core flooding Experiments

To evaluate and compare J071 and the mixture in terms of oil recovery, two core flooding experiments were conducted at the same conditions. The surfactants concentrations were 0.5-wt% prepared at 1-wt% NaCl salinity. The core floods were conducted in Bentheimer sandstone. Each core flood included three injection stages: water flooding, surfactant pre-flush and surfactant/N_2 (i.e. foam) flooding. The recovery stages were conducted at constant flow rate equivalent to 5 ft/day velocity in porous media. The surfactant/N_2 simultaneous injection or foam flooding was conducted at 90% injection quality and at 5 ft/day velocity. The results of the core floods of J071 and J071/O242 at 2:1 mixing ratio are shown in **figures 52** and **53**, respectively.

Figure 52 shows that the water flooding produced 37.7% of the OOIP. In fact, the ultimate oil recovery from water flooding was approached after injecting 1 pore volume approximately. However, the water injection continued for 5 pore volumes in total to ensure that no additional oil can be produced by water injection. After that, almost 1.5 pore volumes of J071 surfactant solution were injected to mitigate the surfactant adsorption at the rock surfaces. As shown in **figure 52**, no additional oil recovery was observed during the surfactant pre-flush. After that, 5 to 6 pore volumes of foam (J071/N_2 simultaneous injection) were injected at 5 ft/day by which an additional 2.5% oil recovery was observed. The total oil recovery for this core flood was 40.17% OOIP.

Figure 53 shows the results of the core flood experiment using J071/O242 (2:1) mixture. The water flooding produced 37.69% of the OOIP. Moreover, no additional oil recovery was observed during the injection of 1.5 pore volumes of the mixture pre-flush.

Then, 5.7 pore volumes of the mixture and N_2 co-injection (foam flooding) produced an additional 7.5% of OOIP compared with 2.5% with J071 foam. This core flood resulted in 45.2% total oil recovery compared with 40.17% total oil recovery using J071 foam. These results confirmed that the mixture's foam flooding was able to extract more oil than J071 alone.

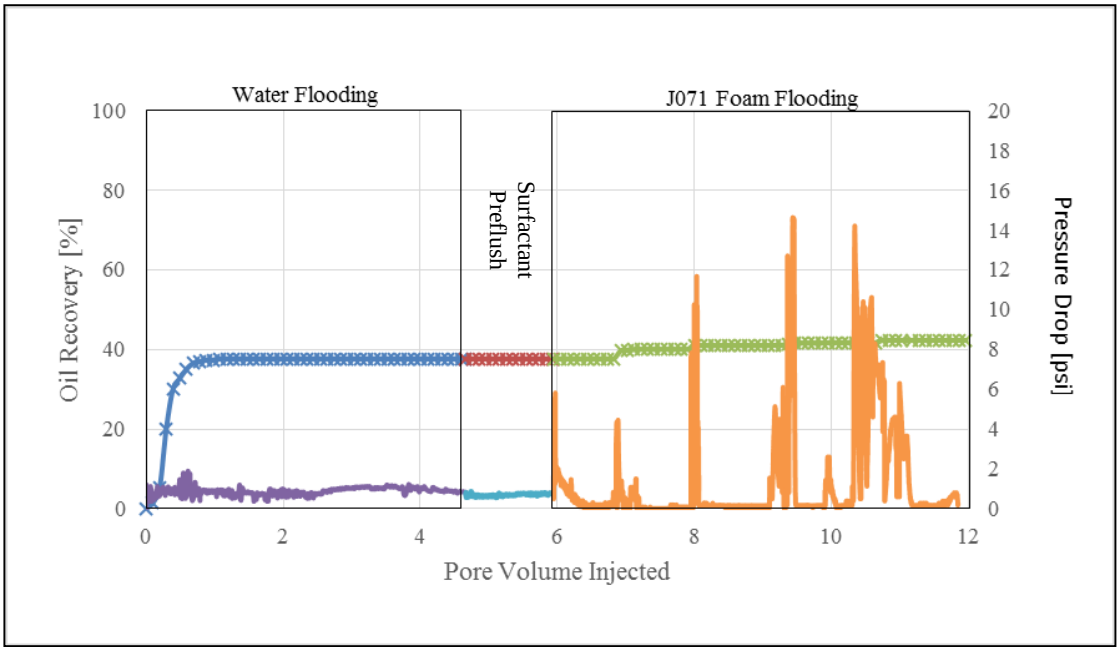

Figure 52: J071 core flooding experiment

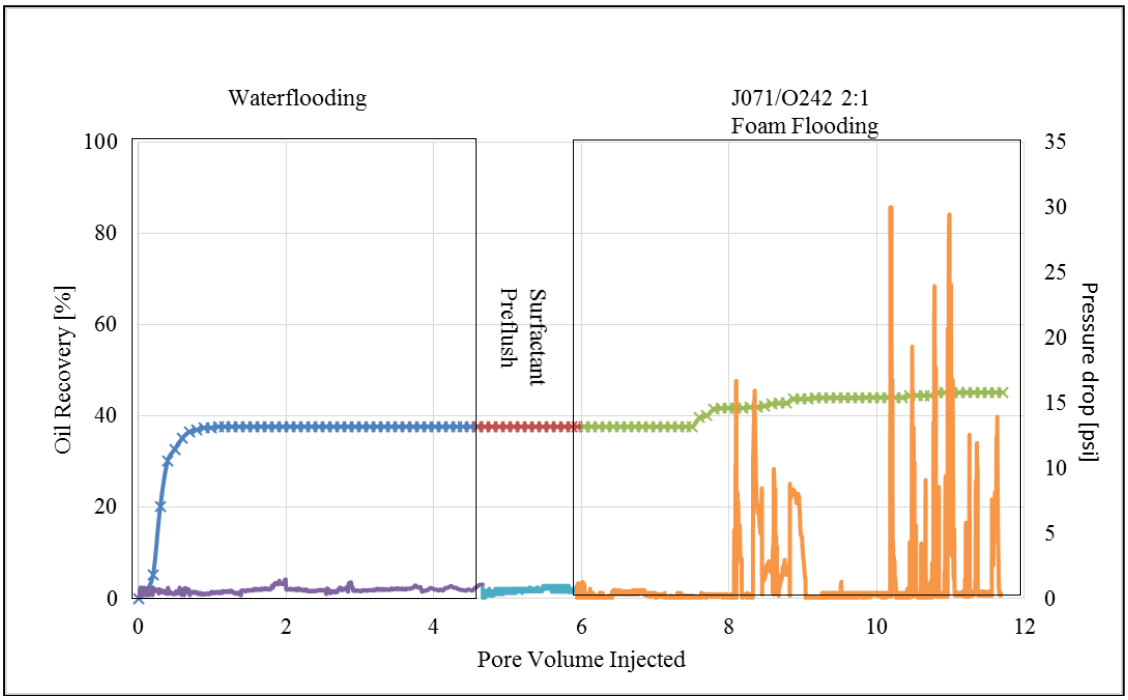

Figure 53: J071/O242 core flooding experiment

V.2 J071-A031 Mixtures

This section introduces the results of mixing J071 anionic surfactant with another anionic surfactant A031. The same procedure was used with the previous mixture, J071/O242, was used for J071 mixture with A031. The investigations included testing and comparing the foamability, foam stability, mobility, and oil recovery.

Previously, the preliminary work results in the last chapter defined A031 anionic surfactant as one of the best surfactants in terms of foam-oil tolerance in DI water with NBU crude oil. Moreover, mixing J071 with A031 at 1:1 mixing ratio in DI water enhanced the foam-oil tolerance in DI water without losing J071 anionic foamability. Furthermore, the salinity had dramatic effect on A031 foam-oil tolerance and foamability. This section is to proceed with J071/A031 mixtures considering J071 as the foaming agent and A031 as the foam stabilizing agent.

V.2.1 Static Foam Tests With Oil

Figure 54 shows the results from shaking tests in presence of oil for J071, A031 and 1:1 mixture at 0.05-wt% in DI and 1-wt% NaCl salinity. The same observations of J071/O242 mixtures were observed with J071/A031 mixture. The foam-oil tolerance of the mixture in DI water is better than J071 only, whereas A031 is the best. The addition of 1-wt% NaCl salinity caused a severe drop in A031 foam-oil tolerance, whereas the mixture is showing better foaming properties than both J071 and A031.

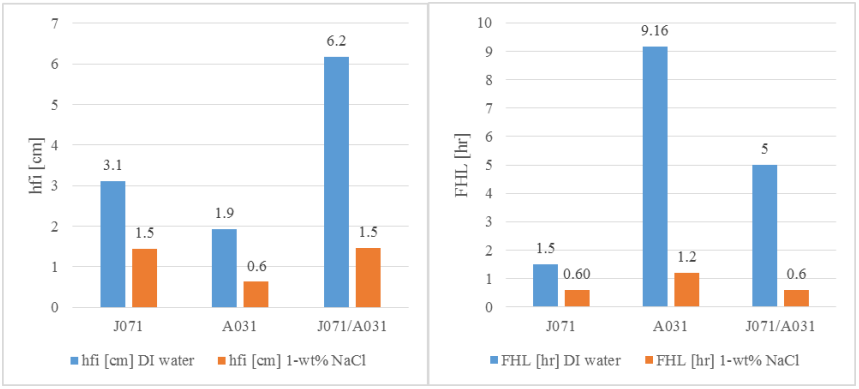

Figure 54: Foamability (left) and foam stability (right) for J071, A031, and J071/A031 at 1:1 mixing ration, in presence of oil, at 0.05-wt%, in DI and saline water

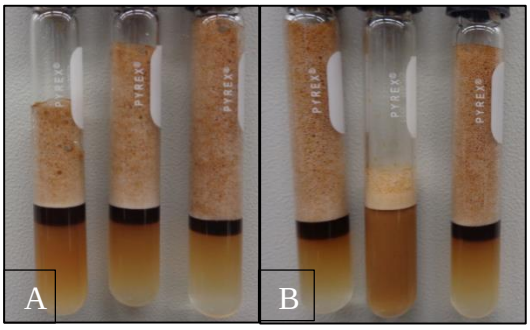

Figure 55: Shaking test with oil initial images A) J071, A031, mixture at 1:1 mixing ratio in DI water and B) J071, A031, mixture at 1:1 mixing ratio in saline water

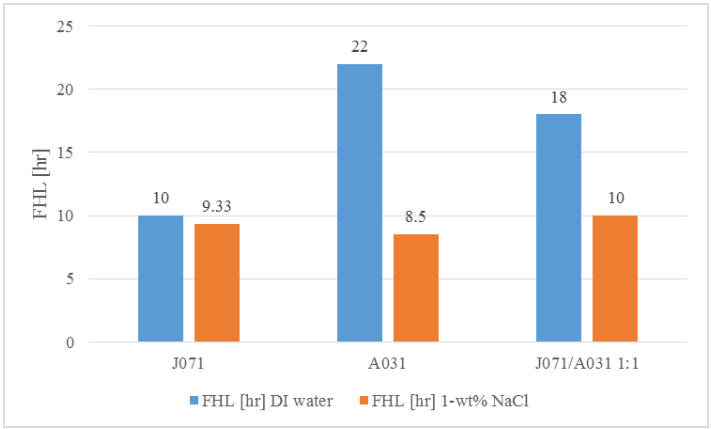

Figure 56: Foam half-lives for the individual surfactants and mixture at 1:1 mixing ratio in DI and saline water in absence of oil at 0.05-wt%

Figure 55 is showing the foam columns for all samples (J071, A031, and 1:1 mixture) in DI water (A) and at 1-wt% NaCl (B). The turbidity in liquid below the foam column of A031 sample at 1-wt% NaCl salinity indicates that A031 has the ability to reduce the $\sigma_{o/w}$ which affected its foaming properties severely in saline water.

V.2.2 Static Tests Without Oil

In absence of oil, **figure 56** shows A031 as the best in DI water, and the mixture is the best in brine at 1-wt% NaCl.

V.2.3 Interfacial Properties

Figure 57 shows the IFT measurements at different concentrations for the individual surfactants and for J071/A031 at 1:1, 2:1 and 4:1 mixing ratios in DI water. The CMC values are listed in **table 19**.

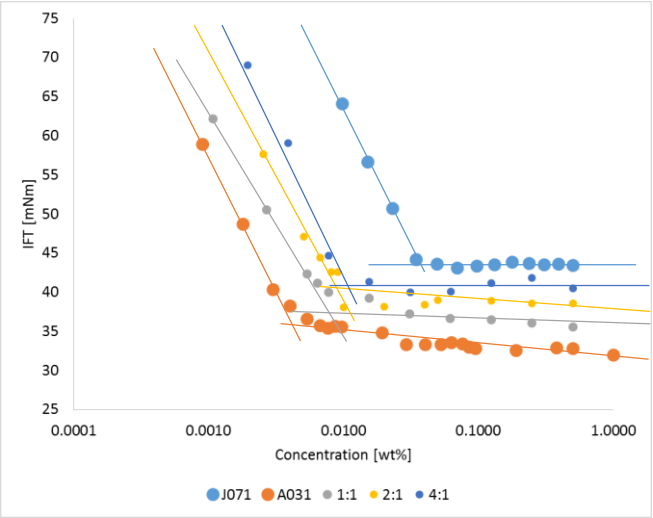

Figure 57: CMC for the individual surfactants and the mixtures at all mixing ratios in DI

Table 19: CMC values for J071, A031, and their mixtures at different mixing ratios

Surfactant	CMC [wt%]
J071	0.036
A031	0.0051
J071/A031 1:1	0.007
J071/A031 2:1	0.009
J071/A031 4:1	0.01

No large differences between the CMC values of the different mixing ratios of J071 with A031 in DI water, **table 19**. However, the mixtures have lower CMC values than J071. Mixing ratio 1:1 resulted in a reduction of J071 CMC from 0.036-wt% to 0.007-wt%. Moreover, **figure 57** also shows the significant reduction in $\sigma_{g/w}$ when mixing J071 with A031 in comparison with J071. Therefore, these mixtures are expected to have better foaming efficiency than J071 according to Rossen and Kunjappu (2004).

V.2.4 Effect of Mixing Ratio

At first, solubility were tested in brine solutions at 1, 2, and 3-wt%. **Figure 58** shows the sample images (left to right) for A031, J071/A031 at 1:1, 2:1, and 4:1 mixing ratios. Each image includes 4 samples (left to right): DI, 1, 2, and 3-wt% NaCl. As shown, A031 is turbid in saline water (i.e. low solubility in brine) where the turbidity increases as the salinity increases. These images show that mixing J071 with A031 increases the solubility of A031 in saline water.

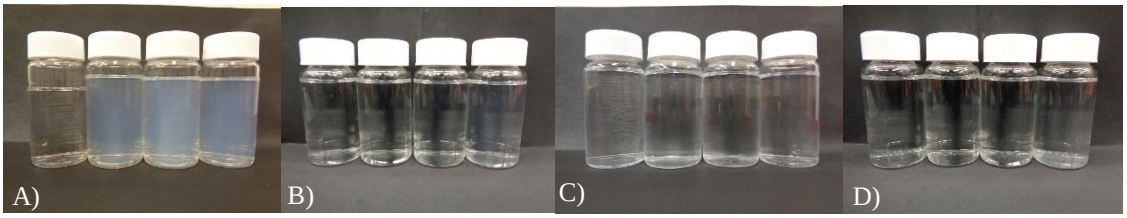

Figure 58: Samples images for A) A031, B) J071/A031 1:1; C) J071/A031 2:1; D) J071/A031 4:1. Each images (left to right) DI water, 1, 2, and 3-wt% NaCl

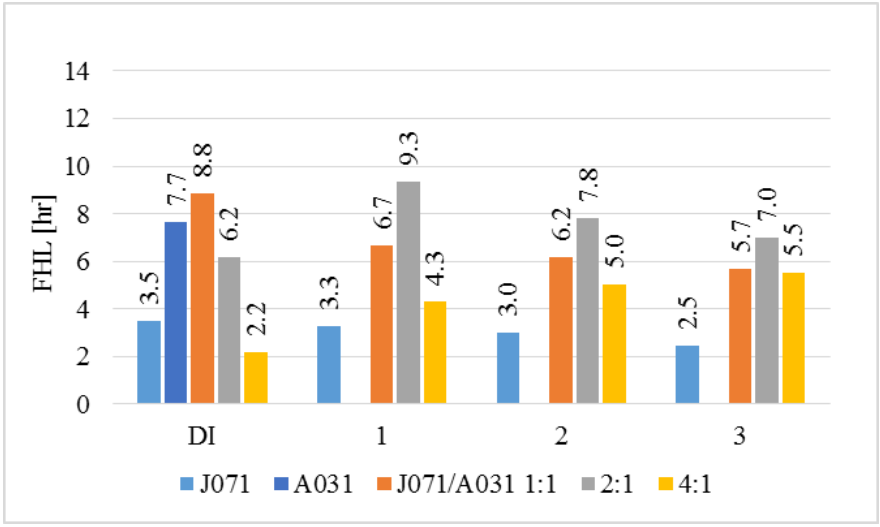

Figure 59: Foam half-lives for all surfactants at 0.5-wt% in DI and all NaCl salinities

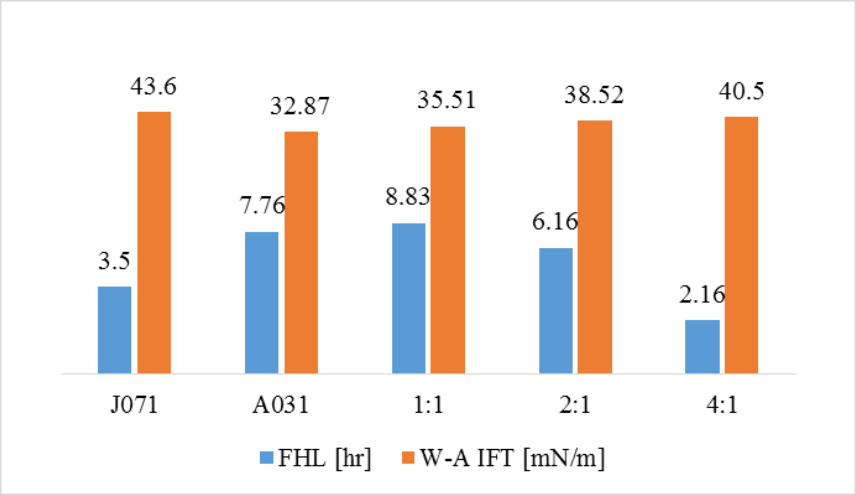

Figure 60: FHL and $\sigma_{g/w}$ for J071, A031, and their mixtures at 0.5-wt% in DI water

Next, the foam stability were investigated for J071/A031 mixtures at different mixing ratios in comparison with the individual surfactants. **Figure 59** shows the foam half-lives for J071, A031, and J071/A031 at 1:1, 2:1, and 4:1 mixing ratios. Interestingly, the same observations, for the foam stability, of J071/O242 were almost repeated and observed with J071/A031 mixtures. In DI water, increasing the hydrophilic surfactant concentration (J071) decreased the foam stability. Moreover, the mixtures at all mixing ratios in all solutions showed better foam stability than J071.

For 1:1 mixing ratio, increasing the salinity decreased the foam stability. However, for 2:1 mixing ratio, the foam stability increased from DI to 1-wt% NaCl, and then it decreases as the salinity increased to 2 and 3-wt% NaCl. Interestingly, the 4:1 mixing ratio foam stability was increasing as the salinity increased.

The $\sigma_{g/w}$ measurements with the foam stability in DI water at 0.5-wt% concentrations are shown in **figure 60**. This is again the same behavior that was observed

with J071/O242 mixture. As J071 concentration increases in the mixture, the $\sigma_{g/w}$ increases and the foam stability decreases.

In saline water, **figure 61** shows that the $\sigma_{g/w}$ measurements and the foam stability at 3-wt% NaCl for J071 and J071/A031 mixtures. This indicates that the $\sigma_{g/w}$ cannot be used to explain the foam stabilization mechanisms in saline water. As shown, A031 was not tested at this salinity because of the high turbidity of the solution. Other foam stabilization mechanisms include the ordered micellar structure in the lamellae and the electric double layer effect (Nikolov et al. 1989). It was explained previously under the effect of mixing ratio on foam stability for J071/O242 mixtures.

The solubility of the foam stabilizing additives occur by the attachment to the palisade layer of the micelle of the anionic detergent. This attachment was concluded to be the reason behind the enhancement in foam stability in absence and presence of oil (Schick and Fowkes 1957).

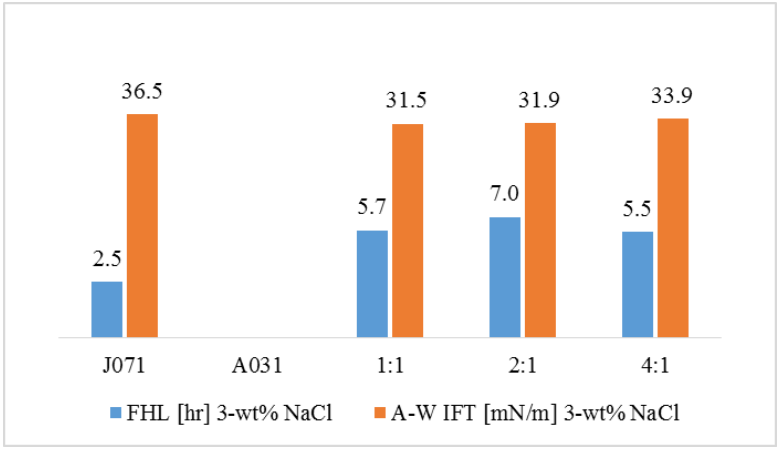

Figure 61: Foam half-life and $\sigma_{g/w}$ for J071, A031, and their mixtures at 0.5-wt% in 3-wt% NaCl

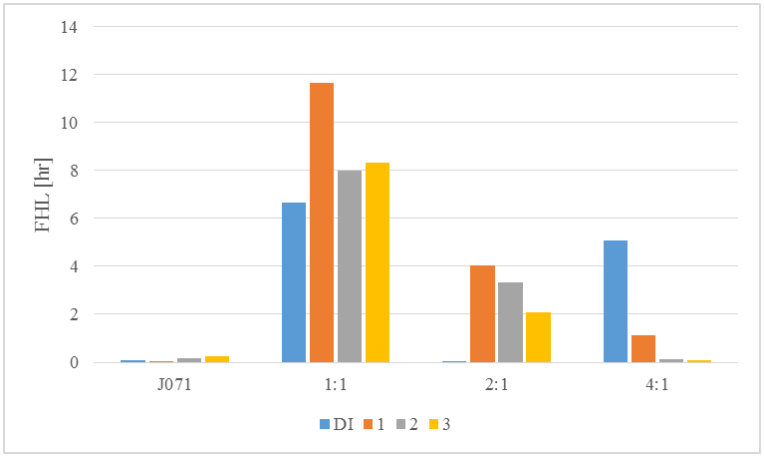

Figure 62: Foam half-lives for J071 in comparison with all mixtures at all salinities at 0.5-wt%

V.2.5 Effect of Oil

Foam-oil tolerance or foam stability with oil of J071 and the mixtures J071/A031 in DI and at all salinities at 0.5-wt% are shown in **figure 62**. Besides the dramatic effect of oil on J071 foam, J071/A031 1:1 was the best among the mixtures. The 2:1 mixing ratio showed better foam stability in saline water than that of DI water in presence of oil. For 4:1 mixing ratio, the foam-oil tolerance was high in DI water, but low in saline waters. Therefore, mixing J071 with A031 also enhanced the foam stability in presence of oil.

For qualitative description of the foam-oil tolerance, the following tables are showing the $\sigma_{o/w}$, $\sigma_{g/w}$, entering coefficient, spreading coefficient, bridging coefficient, and lamellae number. The calculations done based on $\sigma_{g/o}$ 31.5 mN/m with the NBU oil.

Table 20: $\sigma_{o/w}$ measurements, 0.5-wt% concentration, at 25°C temperature

Surfactant	DI water	1-wt% NaCl	2-wt% NaCl	3-wt% NaCl
J071	3.48	0.62	0.5	0.458
A031	0.5	--	--	--
J071/A031 1:1	3.16	0.23	0.38	0.123
J071/A031 2:1	3.22	0.655	0.59	0.38
J071/A031 4:1	3.56	0.79	0.67	0.42

Table 21: $\sigma_{g/w}$ measurements, 0.5-wt% concentration, at 25°C temperature

Surfactant	DI water	1-wt% NaCl	2-wt% NaCl	3-wt% NaCl
J071	43.6	39.55	38.59	36.51
A031	30.78	29.11	29.29	--
J071/A031 1:1	35.51	31.19	31.17	31.53
J071/A031 2:1	38.52	32.20	32.55	32.23
J071/A031 4:1	40.50	35.51	36.04	34.00

Table 22 for the entering coefficient shows that A031 in DI water and 1:1 mixture in 1-wt% NaCl are expected to exhibit good foam-oil tolerance as the entering coefficient was negative for these two samples. The remaining sample of 1:1 at high salinities are expected to have good foam-oil tolerance inside the porous media because the spreading coefficient is negative in **table 23**. The bridging coefficient, **table 24**, confirmed the results for A031 and 1:1 mixing ratio in 1 and 2-wt% NaCl only.

Table 22: J071 vs. J071/A031 2:1 entering coefficients at 0.5-wt% surfactant concentration at room temperature

Surfactant	DI water	1-wt% NaCl	2-wt% NaCl	3-wt% NaCl
J071	15.58	8.67	7.585	5.468
A031	**-0.22**	--	--	--
J071/A031 1:1	7.17	**-0.08**	0.05	0.15
J071/A031 2:1	11.24	1.36	1.64	1.11
J071/A031 4:1	12.56	4.80	5.21	2.92

Table 23: J071 vs. J071/A031 2:1 spreading coefficients (0.5-wt%) surfactant concentration at room temperature

Surfactant	DI water	1-wt% NaCl	2-wt% NaCl	3-wt% NaCl
J071	8.62	7.43	6.595	4.552
A031	**-1.22**	--	--	--
J071/A031 1:1	0.85	**-0.54**	**-0.71**	**-0.10**
J071/A031 2:1	4.80	0.05	0.46	0.35
J071/A031 4:1	5.44	3.22	3.87	2.08

Table 24: J071 vs. J071/A031 2:1 bridging coefficients at 0.5-wt% surfactant concentration at room temperature

Surfactant	DI water	1-wt% NaCl	2-wt% NaCl	3-wt% NaCl
J071	920.82	572.34	497.18	340.94
A031	**-44.59**			
J071/A031 1:1	278.70	**-19.38**	**-20.54**	**1.70**
J071/A031 2:1	579.95	45.02	67.60	46.67
J071/A031 4:1	660.67	269.33	307.08	163.93

Table 25: J071 vs. J071/A031 2:1 lamellae number at 0.5-wt% surfactant concentration at room temperature

Surfactant	DI water	1-wt% NaCl	2-wt% NaCl	3-wt% NaCl
J071	1.88	9.57	11.69	11.96
A031	9.23			
J071/A031 1:1	4.59	20.34	12.30	38.45
J071/A031 2:1	1.84	7.37	8.28	12.72
J071/A031 4:1	1.71	6.74	8.07	12.14

According to the lamellae number theory, the results in **table 25** indicate that A031, J071, and all the mixing ratios in saline water are unstable in presence of oil. However, the mixtures in DI water only are expected to be of type B foam (i.e. semi-stable). These results are in disagreement with the coefficients interpretations in **tables 22, 23** and **24** as well as the static tests observations with oil.

V.2.6 Micro-Images and Bubble Sizes

At 3-wt% NaCl salinity, **figures 63** shows the micro-images for J071 bubbles in comparison with all mixtures after 1-hr. **Figure 64** shows the average bubble sizes vs. time for J071 and all the mixtures in 3-wt% NaCl salinity. These figures indicate clearly that all the mixtures at 1:1, 2:1 and 4:1 have smaller bubbles than J071 after 1-hr. Therefore, the mixtures are better than J071 foam in opposing the foam coarsening mechanisms such as liquid drainage and gas diffusion between the bubbles even at high salinity.

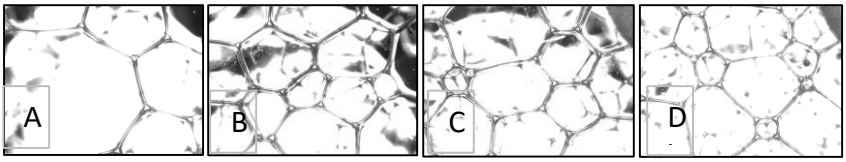

Figure 63: Micro-images after 1-hr. at 0.5-wt% surfactant concentration in 3-wt% NaCl saline water, A) J071; B) J071/A031 1:1; C) J071/A031 2:1; and D) J071/A031 4:1.

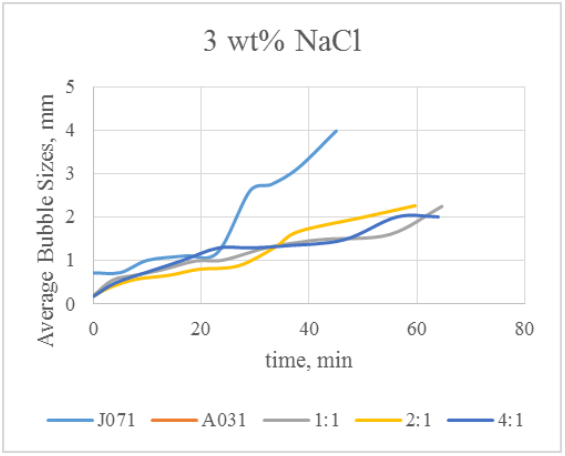

Figure 64: Average bubble sizes at 0.5-wt% in 3-wt% NaCl

V.2.7 Foam Dynamic Tests

As explained previously, this section is all about the results of the foam dynamic testing to compare the surfactant and the mixture in terms of mobility reduction inside the reservoir at reservoir conditions. Both J071 and the mixture J071/A031 at 2:1 mixing ratio were used to measure the foam effective viscosity and mobility reduction in comparison with N_2 gas injection as the baseline experiment. The foam generation was applied by surfactant-N_2 simultaneous injection at specific injection quality and constant flow rates. The parameters investigated are shown in **table 26** below. This mixture was compared with J071 in sandstone at low shear rate only, see **table 27** for results.

Table 26: Experimental conditions for J071 vs. J071/A031 mixtures

Run #	Surfac-tant	C [wt%]	Mixing Ratio	Salinity NaCl [wt%]	Porous Media	K [Darcy]	φ[%]	P [psi]	T [°C]	Q [ml/min]	Injection Quality [%]	Velocity [ft/D]	Shear rate [1/sec]
1	J071	0.5	--	DI water	Glass beads	1.62	21.84	850	50	0.117	90	5	9.15
2	J071/A031	0.5	2:1	DI water	Glass beads	1.61	21.52	850	50	0.117	90	5	9.15
3	--	--	--	DI water	Glass beads	1.62	21.84	850	50	0.117	90	5	9.15

Table 27: Mobility evaluation for J071 vs. J071/A031 2:1

Run #	Surfactant	Porous media	Shear rate [1/sec]	Permeability [Darcy]	Injection Quality [%]	ΔP_{ss} [psi]	Mobility [md/cp]	μ_{eff} [cp]	MRF
1	J071	Sandstone	9.15	1.62	90	5.27	33	50	13
2	J071/A031 2:1	Sandstone	9.15	1.61	90	33.35	5.17	311	67.5
3	--	Sandstone	9.15	1.62	--	0.4	431	3.8	83

To mitigate the effect of surfactant adsorption on rock, 1 to 1.5 pore volumes of surfactant solution were injected into the porous media followed by 5 pore volumes of surfactant-gas simultaneous injection for 24-hr for mobility evaluation.

The Pressure profiles for J071 vs. the mixture at 2:1 mixing ratio are shown in **figure 65**. It was observed clearly that the strong foam generation was successful generated inside the porous media for both surfactants. Moreover, the mixture provided 67 times reduction in mobility inside the porous media compared with nitrogen injection at the same conditions. Furthermore, the mixture provided 10 times lower mobility than J071 alone. This is attributed to the higher effective viscosity of the mixture's foam, 311-cp compared with 26-cp of J071 foam.

The results here are in line with the previous static tests where the mixtures of J071/A031 provided better foaming properties than J071 alone.

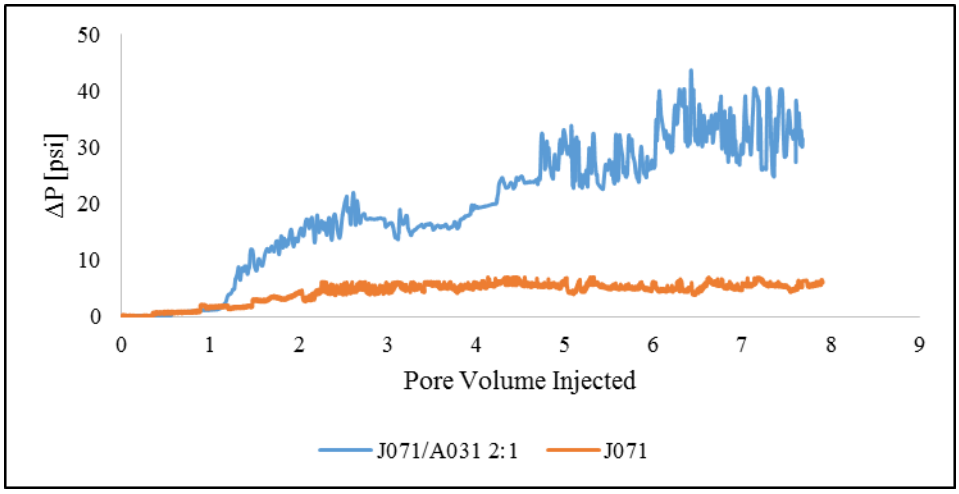

Figure 65: Pressure profiles for J071 foam vs. J071/A031 at 2:1 mixing ratio in Bentheimer sandstone

V.2.8 Core Flooding Experiments

This section is to provide the results of the core flooding experiments for J071/A031 at 2:1 mixing ratio vs. J071 to compare their abilities to recover oil. Both surfactants were prepared at 0.5-wt% surfactant concentration at 1-wt% NaCl brine solutions.

As mentioned previously, J071 foam core flooding resulted in 37.7% oil recovery by water flooding. Moreover, no additional oil recovery during the injecting of 1.5 pore volumes of J071 as the surfactant pre-flush. Also, 2.5% additional oil recovery by 5 pore volumes of J071/N_2 co-injection at 90% injection quality and 40.17% total oil recovery, see **figure 66**.

Figure 67 shows the results of the core flood experiment using J071/A031 (2:1) as a foaming agent. The water flooding resulted in 38.19% oil recovery and no additional oil recovery was observed during the injection of 1.5 pore volumes of J071/A031 (2:1) pre-flush as shown in **figure 67**. Moreover, the injection of 5.55 pore volumes of J071/A031 (2:1) mixture with N_2 gas at 90% injection quality resulted in 7.48% additional oil recovery compared with 2.5% only using J071 foam flooding. The total oil recovery by the mixture was 46.16% compared with 40.17% total oil recovery in J071 foam core flooding experiment.

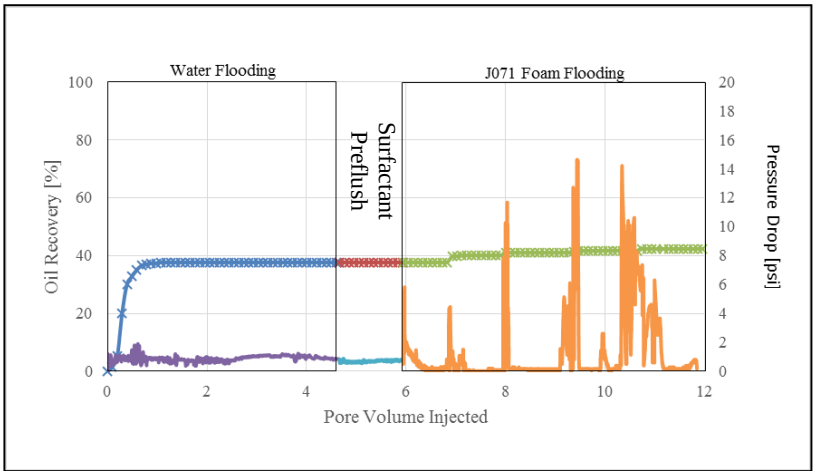

Figure 66: J071 core flooding experiment

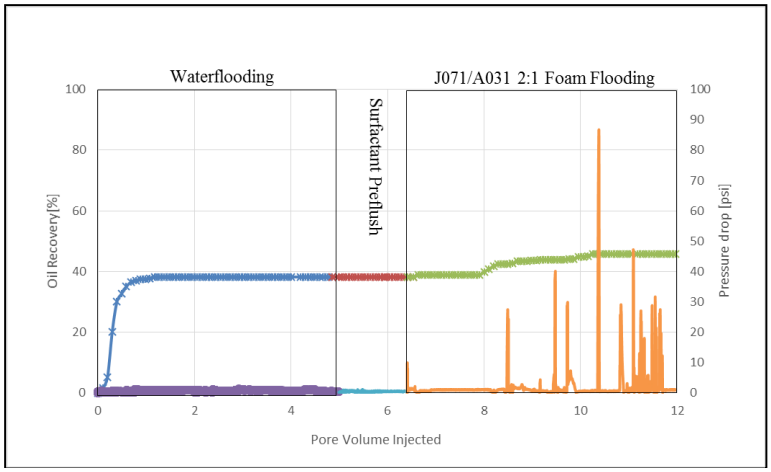

Figure 67: J071/A031 at 2:1 mixing ratio core flood experiment

V.3 J071-Nonionic Surfactants Mixtures

The previous mixtures were found to enhance the foam stability in presence of oil during the preliminary experimental work. The investigation was extended to include the effect of mixing to enhance the foam stability in absence of oil and with NaCl salinity. This section is to show the results for mixtures of the anionic J071 surfactant with the nonionic surfactants. Some of the results that were shown in chapter 4 were used here for comparison purposes. The experimental results are introduced in the same procedure that was used with the previous mixtures.

V.3.1 Introduction

The surfactants under investigation are listed in **table 28** along with their main properties and differences according to the supplied information by the manufacturer. The nonionic surfactants are different in Ethylene Oxide (EO) group number (i.e. ethoxylation) and perhaps in their chemical structures.

Table 28: Surfactants and their main properties at 25°C

Surfactant	Type	Chemical Type	Carbon Chain Length	Cloud Point, °C	PEG, [%m/m]	Thermal Stability[°C]	PO/ EO per alcohol, [mol/mol]	HLB No.	CMC [wt%]
J071	Anionic	AAS	C12-13	--	--	60	7EO		0.036
N25-12	Nonionic	AE	C12-15	80	0	--	12EO	14.4	0.007
N25-9	Nonionic	AE	C12-15	75	1	--	9EO	13.2	0.0015
N25-7	Nonionic	AE	C12-15	46	1	--	7EO	12.2	0.0016
N25-3	Nonionic	AE	C12-15	--	0.5	--	3EO	7.5	--
N91-8	Nonionic	AE	C9-11	78	0	--	8EO	13.7	0.038
N45-7	Nonionic	AE	C14-15	45	0	--	~8EO	11.7	0.00066

The nonionic surfactants are well known for their high sensitivity toward temperatures and insensitivity toward salinity. The cloud point temperature is the temperature at which the nonionic surfactant solution shows the cloudy appearance due to the lower solubility in water with increasing temperature (Puerto et al. 2012; Schramm and Kutay 2000). As the temperature approaches the surfactant's cloud point temperature, the turbidity increases in solution increases (Al-Ghamdi and Nasr-El-Din 1997; Puerto et al. 2012). In fact, the nonionic surfactant becomes less hydrophilic as the temperature increases (Hirasaki, Miller and Puerto 2011).

Besides many other chemical stability benefits, the addition of EO groups (i.e. the ethoxylation) enhances the nonionic surfactants thermal stability (Puerto et al. 2012) which is necessary to provide better foaming properties (Kuhlman, Lau, and Falls 2000).

Another method to increase the cloud point temperature of the nonionic surfactants is with the addition of the ionic surfactants. The increase in cloud point temperature depends on the mixed micelles that are formed by the interactions between the mixed surfactants in solution. In mixed surfactants systems, the mixed micelles have stronger electrostatic repulsive forces that prevent the micelles' coagulation (Schramm, Stasiuk, and Marangoni 2003). Also, Valaulikar and Manhour (1985) concluded that mixing nonionic with ionic surfactants increases the cloud point temperature of the nonionic surfactant by increasing the electrostatic repulsive forces between the new mixed micelles.

Figure 68 shows an example of how mixing anionic with nonionic surfactants enhances the solubility of the nonionic surfactant in water by increasing the cloud point temperature. The nonionic N25-3 surfactant appeared completely cloudy (insoluble) in

water) at room temperature at 0.5-wt% in DI water, see **figure 68A**. However, **figure 68B**, **C** and **D** are showing J071 with N25-3 mixtures at 0.5-wt% total concentrations at 1:1, 2:1, and 4:1 mixing ratios, respectively. Each image has 4 samples in DI water, 1, 2, and 3-wt% NaCl saline water. At 1:1 mixing ratio, the solubility in DI enhanced significantly, but not in saline solutions. Increasing the J071 concentration in mixture such as in 2:1 and 4:1 mixing ratios, **figure 68C** and **D**, in NaCl solutions enhanced the solubility significantly.

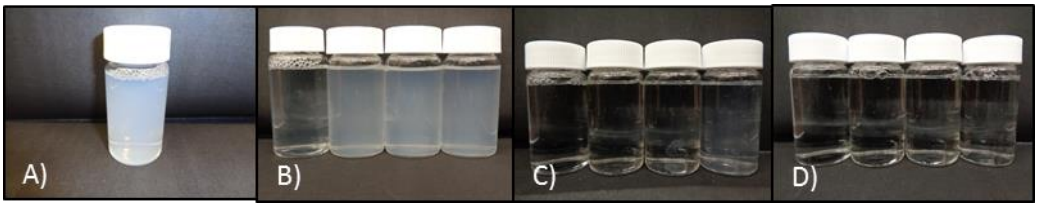

Figure 68: A) N25-3 in DI water, B) J071/N25-3 1:1, C) J071/N25-3 2:1, and D) J071/N25-3 4:1. All mixtures in DI water, 1, 2, and 3-wt% NaCl

V.3.2 Static Foam Tests

In this test, the individual nonionic surfactants and J071 were prepared at 0.05-wt% concentrations and tested in absence and presence of oil in DI water only. Interms of foamability, initial foam heights (hfi) in **figure 69** show that J071 was the best in absence and presence of crude oil (i.e. longer hfi). However, the nonionic surfactants performed well in terms of foam stability in absence of oil, but failed to generate foam in presence of oil except N91-8 surfactant.

Figure 70 compares the foamability and foam stability of the individual surfactants and mixtures of J071 with the nonionic surfactants in absence of oil at 0.05-wt% concentrations. The mixtures were prepared at 1:1 mixing ratio and the test was conducted in DI water only. Moreover, N25-3 nonionic surfactant was not tested individually because of its insolubility in DI water. As shown in **figure 70**, some of the mixtures provided better foam stability than J071, but slightly less in terms of foamability (i.e. shorter initial foam half-lives). The mixtures that enhanced the J071 FHL were: J071/N25-7, J071/N45-7, and J071/N25-3.

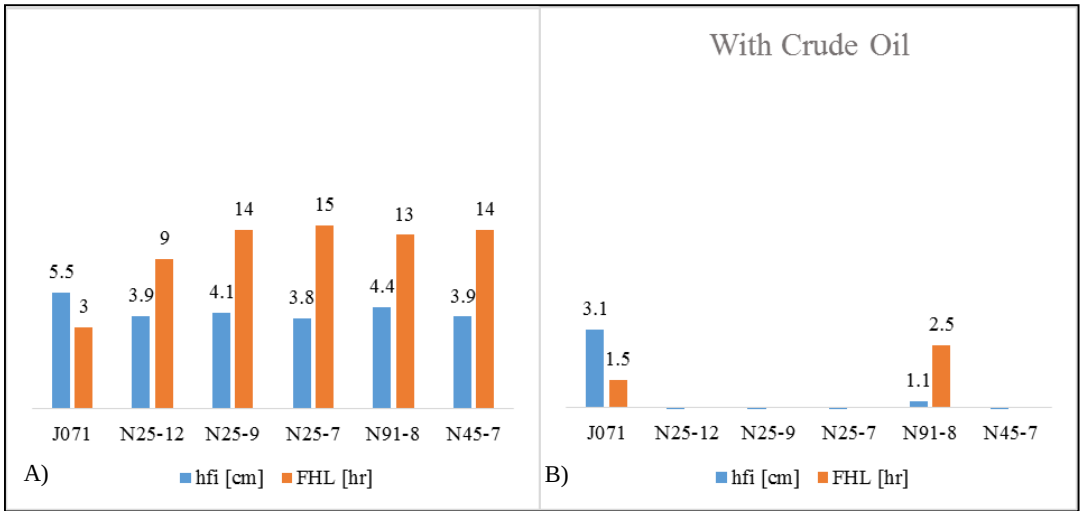

Figure 69: A) Foamability and foam stability in absence of oil and B) Foamability and foam stability in presence of oil. Both at 0.05-wt%

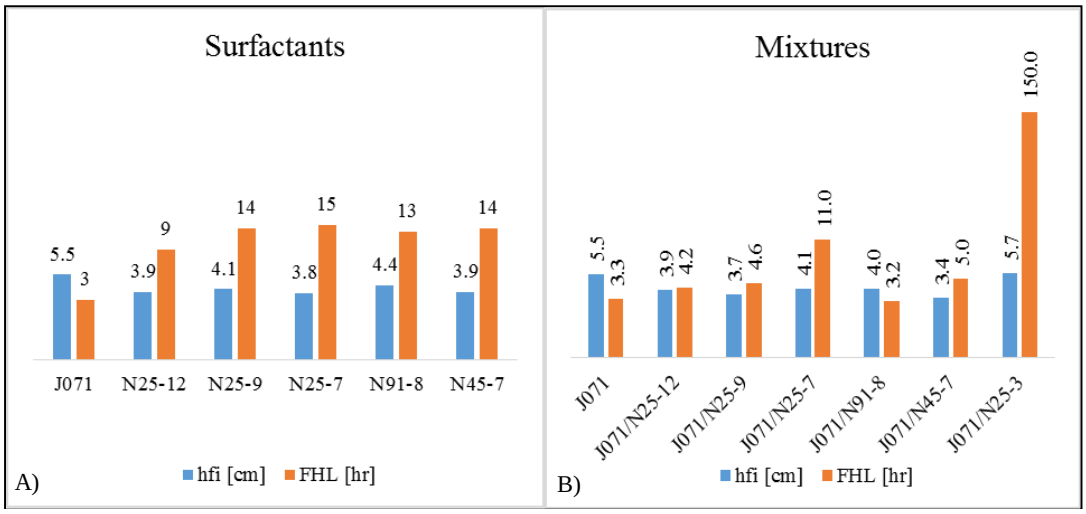

Figure 70: Foamability and foam stability at 0.05-wt% of A) Individual surfactants and B) Mixtures at 1:1 mixing ratio, both in absence of oil in DI water

More obviously, **figure 70** shows that J071/N25-3 mixture resulted in a significant enhancement in foam stability which was the highest FHL through the entire study. For instance, J071 had 3.3-hr FHL in DI water, but J071/N25-3 at 1:1 mixing ratio resulted in

150-hr FHL (approximately 6 days to lose half of the initial foam column height). There are few mechanisms that were mentioned in literature on foam stability enhancement by anionic-nonionic surfactants mixtures as follows:

1. The attachment of the nonionic surfactant on the palisade layer of the anionic surfactant's micelles (Schick and Fowkes 1957).
2. Mixing nonionic with anionic surfactant were found effective in enhancing the micellar stability for the anionic surfactants. As mentioned previously, less foamability and higher foam stability were observed when the micellar stability was increased (Patist et al. 2000, Patist et al. 2001). The less foam volume produced (i.e. lower initial foam height) by the nonionic surfactants in comparison with the anionic J071 implies the differences in micellar stabilities of these surfactants. Unlike anionic surfactants, nonionic surfactants hold no charge on their heads, and the lack of charge indicates lack of the repulsive forces between the surfactants molecules, and consequently, they feature high micellar stabilities than anionic surfactants (Patist et al. 2001). Ross and Haak (1958) found that the foam stability can be improved by lowering the rate of the surfactant migration to the G/W interface. Lowering the rate of surfactant migration to the G/W interface suggests increasing the micellar stability of the surfactants or less monomeric activity.
3. In some cases, it was found that mixing a small amount of nonionic surfactant with an anionic surfactant leads to the formation of liquid-crystalline phase which provides high foam stability (Schramm and Wassmuth 1994).

Figure 71 shows the salinity effect on foam stability for the individual surfactants and the chosen mixtures at 0.05-wt%. As shown, the FHL of the mixtures J071/N25-7 and J071/N25-3 dropped from 11 and 150-hr in DI water to 8.3 and 6-hr in 1-wt% NaCl, respectively. However, the salinity actually enhanced the foam stability of J071/N45-7 mixture. This could be related to the turbidity of this mixture at 1-wt% NaCl which increased the solution's viscosity. The increase in viscosity of the bulk solution could enhance the foam stability with unstable solution (Rosen and Kunjappu 2004).

Figure 72 shows the effect of mixing ratio on foam stability of J071/N25-3 mixtures at 1:1, 2:1, and 4:1 mixing ratios at 0.5-wt% concentrations. The main conclusion drawn from **figure 72** was that all mixing ratios showed better foam stabilities than J071 in DI water and in saline solutions. It should be noted that J071/N25-3 at 1:1 mixing ratio appeared cloudy as shown in **figure 86**. Such turbidity in solution could increase the viscosity and induce higher foam stability (Rosen and Kunjappu 2004). However, if the turbidity appears in saline solutions at ambient conditions, it must be avoided when using a solution at reservoir conditions.

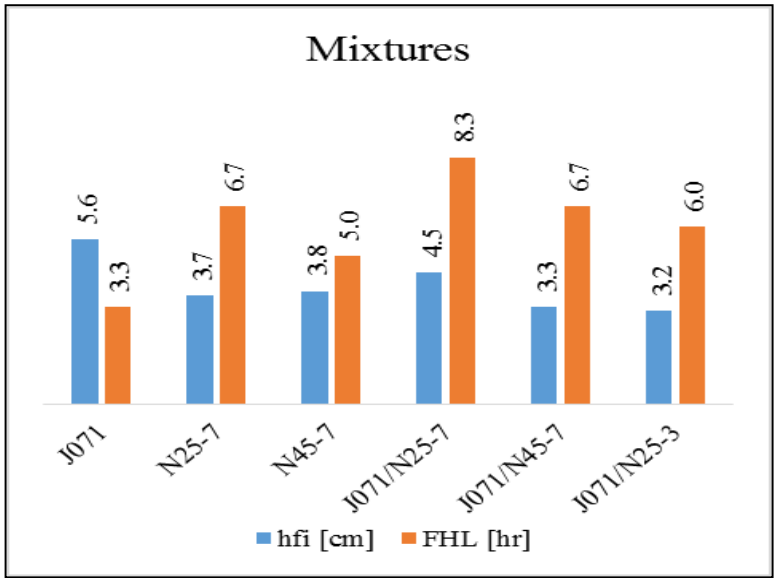

Figure 71: Foamability and foam stability of 0.05-wt% of individual surfactants and mixtures in 1-wt% NaCl

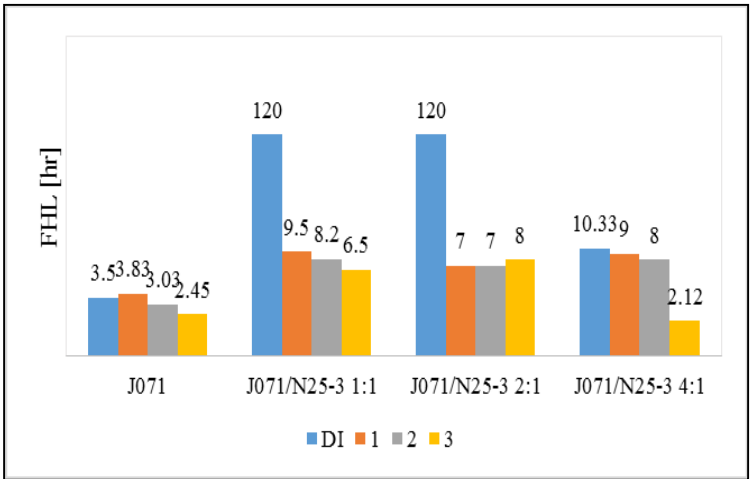

Figure 72: Foam half-lives for J071 and J071/N25-3 mixtures at 1:1, 2:1, and 4:1 mixing ratios at 0.5-wt% surfactant concentration in DI water, 1, 2, and 3-wt% NaCl salinities

V.3.3 Interfacial Properties

To understand the foam stability enhancements better, this section is to provide the interfacial properties for J071 vs. J071/N25-3 mixtures. **Figure 73** shows the $\sigma_{g/w}$ at different concentrations for J071 and the mixtures in DI water and **table 29** lists the CMC values for these surfactants.

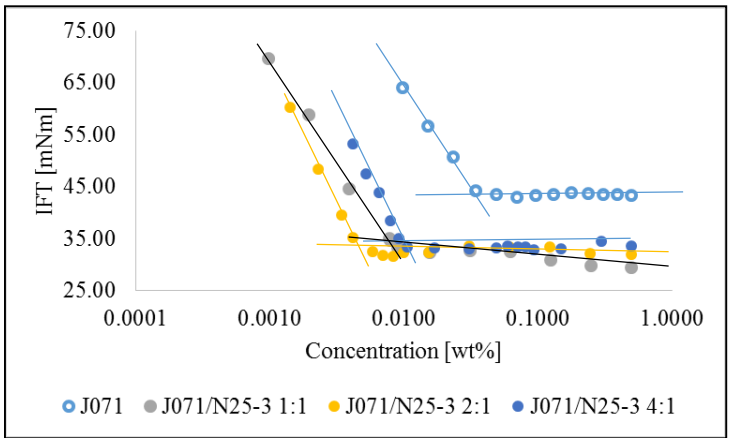

Figure 73: $\sigma_{g/w}$ at different concentrations in DI water for J071 and mixtures of J071/N25-3

Table 29: CMC values for J071/N25-3 mixtures

Surfactant	CMC [wt%]
J071	0.036
J071/N25-3 1:1	0.0080
J071/N25-3 2:1	0.0050
J071/N25-3 4:1	0.01

The mixtures reduced the $\sigma_{g/w}$ lower than that of J071 alone according to **figure 73**. Thus, the mixtures are expected to be more effective in terms of foam generation

(Rossen and Kunjappu 2004). Therefore, mixing J071 with N25-3 enhanced the foam stability with lowering the CMC for J071. Such observations are in line with the correlation between the CMC reduction and foam stability enhancement according to Schick and Fowkes (1957).

V.3.4 Effect of Oil

J071/N25-3 mixtures' foam-oil tolerance were investigated by shaking tests and using the foam-oil tolerance coefficients (E, S, B and lamella number). **Tables 30** and **31** show the $\sigma_{o/w}$ and $\sigma_{g/w}$ for J071 and the mixtures at 0.5-wt% concentration in DI water and at all NaCl salinities.

For 2:1 and 4:1 mixing ratios at 2 and 3-wt% salinities, they have negative entering coefficients, see **table 32**. For those with negative entering values, spreading coefficient in **table 33** shows negative values too. However, the spreading coefficient is showing that all the mixing ratios have negative values which means that these mixtures have good foam-oil tolerance. For the positive entering but negative spreading coefficients, the oil is expected not to be able to destabilize the lamellae. This is because after entering the lamellae, the oil will not spread at the G/W interface.

Table 30: $\sigma_{o/w}$ measurements, 0.5-wt% concentration, at 25°C temperature

Surfactant	DI water	1-wt% NaCl	2-wt% NaCl	3-wt% NaCl
J071	3.48	0.62	0.5	0.458
J071/N25-3 1:1	5.88	1.29	0.84	0.4
J071/N25-3 2:1	5.57	1.59	0.63	0.48
J071/N25-3 4:1	5.33	1.01	0.8	0.62

Table 31: $\sigma_{g/w}$ measurements, 0.5-wt% concentration, at 25°C temperature

Surfactant	DI water	1-wt% NaCl	2-wt% NaCl	3-wt% NaCl
J071	43.6	39.55	38.59	36.51
J071/N25-3 1:1	29.48	31.78	31.77	31.7
J071/N25-3 2:1	31.46	30.6	30.71	30.13
J071/N25-3 4:1	33.37	30.94	30.31	30.51

Table 32: J071 vs. J071/N25-3 2:1 entering coefficients at 0.5-wt% surfactant concentration at room temperature

Surfactant	DI water	1-wt% NaCl	2-wt% NaCl	3-wt% NaCl
J071	15.58	8.67	7.585	5.468
J071/N25-3 1:1	3.86	1.57	1.11	0.6
J071/N25-3 2:1	5.53	0.69	**-0.16**	**-0.89**
J071/N25-3 4:1	7.2	0.45	**-0.39**	**-0.37**

Table 33: J071 vs. J071/N25-3 2:1 spreading coefficient at 0.5-wt% surfactant concentration at room temperature

Surfactant	DI water	1-wt% NaCl	2-wt% NaCl	3-wt% NaCl
J071	8.62	7.43	6.60	4.55
J071/N25-3 1:1	**-7.9**	**-1.01**	**-0.57**	**-0.2**
J071/N25-3 2:1	**-5.61**	**-2.49**	**-1.42**	**-1.85**
J071/N25-3 4:1	**-3.46**	**-1.57**	**-1.99**	**-1.61**

Bridging coefficient interpretations in **table 34** reconcile with the entering and spreading coefficients interpretations for both 2:1 and 4:1 mixing ratios with salinity and for 1:1 in DI water only. These coefficients indicate that both 2:1 and 4:1 are predicted to generate stable foam in saline solutions in presence of oil, whereas 1:1 mixing ratio foam is expected to be stable with oil in DI water only.

Table 34: J071 vs. J071/N25-3 2:1 bridging coefficients at 0.5-wt% surfactant concentration at room temperature

Surfactant	DI water	1-wt% NaCl	2-wt% NaCl	3-wt% NaCl
J071	920.82	572.34	497.18	340.94
J071/N25-3 1:1	**-88.61**	19.38	17.79	12.80
J071/N25-3 2:1	28.51	**-53.36**	**-48.75**	**-84.20**
J071/N25-3 4:1	149.72	**-33.95**	**-72.91**	**-61.01**

Table 35: J071 vs. J071/N25-3 2:1 lamellae number at 0.5-wt% surfactant concentration at room temperature

Surfactant	DI water	1-wt% NaCl	2-wt% NaCl	3-wt% NaCl
J071	1.88	9.57	11.69	11.96
J071/N25-3 1:1	0.75	3.70	5.61	11.89
J071/N25-3 2:1	0.85	2.89	7.31	9.42
J071/N25-3 4:1	0.94	4.60	5.68	7.38

Table 35 shows the lamellae numbers values. The mixtures are better than J071 with stable foam in DI water (L<1), semi stable in saline solutions up to 2-wt% NaCl where L<7, and unstable in 3-wt% NaCl. In general, both theories: E, S and B and lamellae number indicates that mixtures have better foam-oil tolerance than J071 alone.

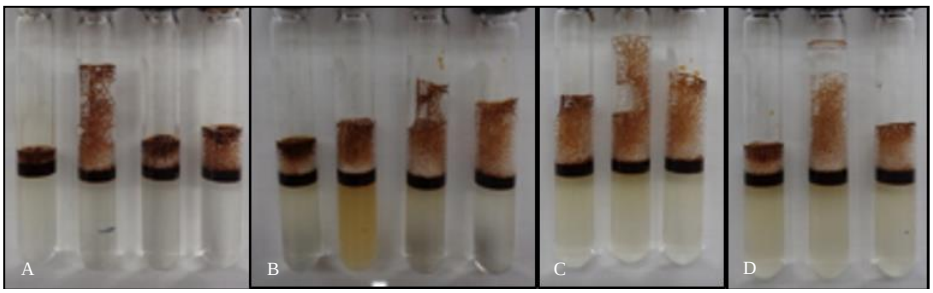

Figure 74: Foam columns with oil for J071 and J071/N25-3 at 1:1, 2:1 and 4:1 mixtures at 0.5-wt%. A) DI water after 1-hr., B) 1-wt% NaCl after 20-min; and C) and D) J071, 2:1 mixture and 4:1 mixture in 2 and 3-wt% NaCl after 20-min.

Figure 74 shows the foam columns with oil from the shaking tests as an example of foam-oil tolerance. **Figure 74A** and **B** include 4 samples for J071, 1:1, 2:1, and 4:1. However, **figure 74C** and **D** are missing 1:1 mixing ratio because it failed to generate foam in presence of oil at and beyond 2-wt% NaCl salinity. For timing, **figure 74A** was taken after 1-hr., while **B**, **C**, and **D** were taken after 20-min due to the low FHL in saline solutions. These images show obviously that J071/N25-3 at 2:1 and 4:1 mixing ratios perform better than J071 at higher salinities in presence of oil in agreement with the coefficients and lamellae number interpretations. Moreover, 2:1 outweighed 4:1 foam-oil tolerance at 2 and 3-wt% NaCl salinities.

V.3.5 Foam Dynamic Tests

Tables 36 and **37** show the experimental conditions and results for all dynamic foam experiments for J071/N25-3 at 2:1 mixing ratio in comparison with the previous experiments of J071 surfactant. Two runs were conducted in high permeability glass beads pack at high shear rate ~455-sec^{-1}, and other two runs were conducted in Bentheimer sandstone at low shear rate ~9-sec^{-1}. According to the objectives in this study, the mixture was compared with J071 in terms of mobility, effective foam viscosity and MRF. One baseline experiment was conducted using N_2 injection and was used to calculate the MRF for foam runs. Moreover, 1 pore volume of surfactant solutions were injected before the onset of surfactant-nitrogen simultaneous injection for in-situ foam generation in Bentheimer sandstone. The steady state pressure data was collected and used to calculate the mobility, foam effective viscosity and MRF.

Table 36: Experimental conditions for J071 vs. J071/NA25-3 at 2:1 mixture

Run #	Surfa-ctant	C [wt%]	Salinity NaCl [wt%]	Porous Media	k [Darcy]	φ [%]	Gas	P [psi]	T [°C]	Q [ml/min]	Injection Quality [%]	Velocity [ft/D]	Shear rate [sec]
1	J071	0.5	DI water	Glass beads	17.1	30	N_2	850	50	0.5	70	--	454.7
2	J071/ N25-3 (2:1)	0.5	DI water	Glass beads	17.1	30	N_2	850	50	0.5	70	--	454.7
3	J071	0.5	1	Sandstone	1.62	21.84	N_2	850	50	0.117	90	5	9.15
4	J071/ N25-3 (2:1)	0.5	1	Sandstone	1.61	21.52	N_2	850	50	0.107	90	5	9.15
5	--	0.5	1	Sandstone	1.62	21.84	N_2	850	50	0.117	90	5	9.15

Table 37: Results for J071 vs. J071/N25-3 at 2:1 mobility evaluation

Run #	Surfactant	Porous media	Shear rate [1/sec]	Permeability [Darcy]	Injection Quality [%]	ΔP_{ss} [psi]	Mobility [md/cp]	μ_{eff} [cp]	MRF
1	J071	Glass beads	454.74	17.1	70	481	72	334	1200
2	J071/N25-3 (2:1)	Glass beads	454.74	17.1	70	325	76	225	813
3	J071	Sandstone	9.15	1.62	90	5.27	33	50	13
4	J071/N25-3 (2:1)	Sandstone	8.84	1.61	90	18	9.54	170	45
5	--	Sandstone	9.15	1.62	--	0.4	431	3.8	--

The pressure drop profiles for J071 and J071/N25-3 at 2:1 mixing ratio in glass beads pack at high shear rate are shown in **figure 75**. At high shear rate, J071 showed higher pressure drop indicating higher flow resistance than the mixture. This also indicates that J071 at high shear rate is a better foaming agent for foam mobility control. However, this conclusion is in a disagreement with the static tests results where it was found that the mixture was always providing better foaming properties than J071 alone. In a disagreement with high shear rate results in **figure 75**, the mixture showed higher flow resistance at low shear rate in Bentheimer sandstone as shown in **figure 76** where the pressure drop profile of the mixture is higher than J071 alone.

As explained previously, J071 surfactant has low micellar stability. The micelles, with low stability in high shear rate, disintegrate into monomers and supply the newly created interfaces during foam generation (high surfactant flux to the interfaces). These phenomenon leads to higher foam viscosity as shown in **figure 75**. On the other hand, the low shear rate, **figure 76**, slows down the foam generation (i.e. slower rate to create the G/W interfaces) providing enough time for the mixture with higher micellar stability to approach the surface tension equilibrium to generate higher foam viscosity (Patist et al. 2001; Patist et al. 2000; Rosen and Kunjappu 2004). Another suggestion is that the low shear rate disturbance was not enough for J071 micelles to disintegrate into monomers leaving the newly created G/W interfaces to collapse due to the lack of monomers supply. This was also supported by the observations in shaking tests where the mixtures had lower foamability and higher foam stability than J071 alone. Therefore, mixing the anionic J071

surfactant with the nonionic N25-3 surfactant increased the micellar stability which induced lower foamability and higher foam stability (Patist et al. 2000).

J071/N_2 simultaneous injection in Bentheimer sandstone at 90% injection quality generated 50-cp foam viscosity and resulted in 13-times reduction in mobility of N_2 injection according to the results in **table 37**. On the other hand, the mixture reduced the mobility by 45-times at low shear rate compared with 13 times with J071 foam.

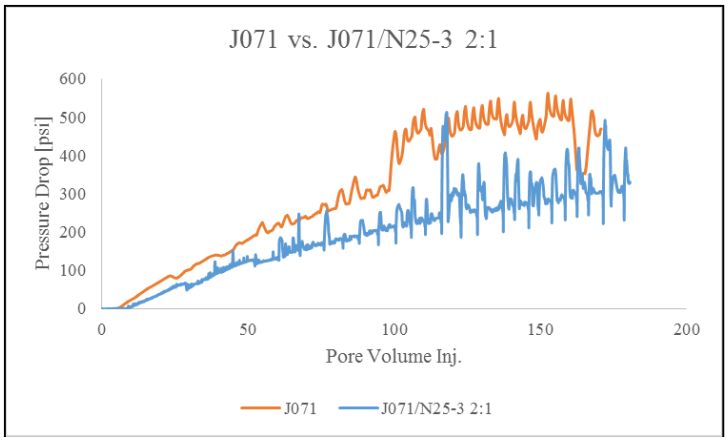

Figure 75: J071 vs. J071/N25-3 (2:1) in glass beads pack at high shear rate

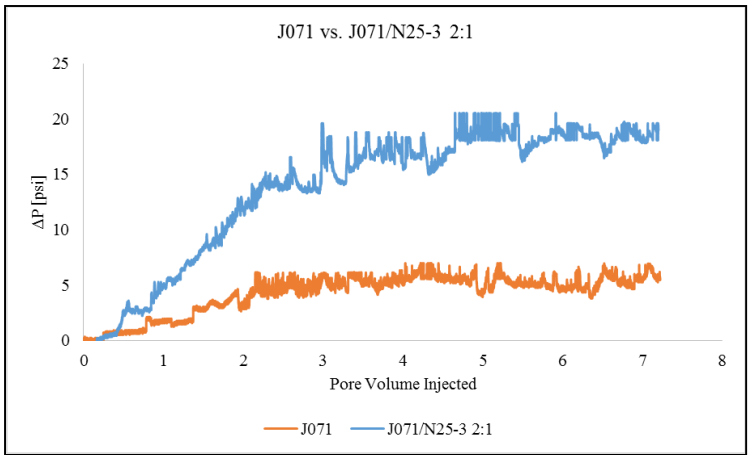

Figure 76: J071 vs. J071/N25-3 (2:1) in Bentheimer sandstone at low shear rate

To summarize, all the results above are in line with Sharma et al. (1984) and all studies conducted at the center of surface science and engineering at the University of Florida (Patist et al. 2001). Their studies on mixing SDS with alcohols of different carbon chain lengths resulted in the following: when the hydrophobic tails of both surfactants in mixture match, it results in higher micellar stability, lower foamability, and higher foam stability.

V.4 AOS vs. CNF

This section is to provide the results for two surfactants: AOS, CNF and their use for $ScCO_2$ mobility control during miscible flooding EOR process.

CNF is a new surfactant developed specifically for foam applications with CO_2 gas. It is a complex nanofluid defined as an anionic surfactant and supplied in liquid form with citrus odor. It is thermally stable with a flash point temperature more than 93.3°C. According to the manufacturer, CNF is thermally and hydrolytically suitable for utilization with CO_2 in gas state and at super critical $ScCO_2$ condition.

Being insensitive to the acidic environment (i.e. ScCO2), the main objective of this study to evaluate and compare the foaming agent AOS with the newly developed foaming agent CNF in terms of mobility reduction of carbon dioxide at supercritical state, interfacial properties, and oil recovery at reservoir conditions.

V.4.1 Interfacial Properties

Surface tension measurements were conducted first for both surfactants at different concentrations. **Figure 77** shows the interfacial measurements of both AOS and CNF at different concentrations in DI water. CNF has lower CMC than AOS, 0.011-wt% and 0.028-wt%, respectively. In foam systems, the lower the surfactant's CMC is the higher the efficiency to generate foam (Rosen and Kunjappu 2004).

Moreover, **figure 77**, for the concentrations below the CMC, shows that CNF has sharper sloped straight line than AOS. This also demonstrates that CNF has higher adsorption which results in smaller area/molecule at the G/W interface. Furthermore, CNF

reduces the $\sigma_{g/w}$ more than AOS at concentrations above the CMC. For example, at 0.5-wt%, CNF $\sigma_{g/w}$ is around 30.7 mN/m in comparison with 32.5 mN/m with AOS at the same concentration, see **tables 38** and **39**. The lower CMC, the lower surface tension, the higher adsorption and smaller area/molecule at the G/W interface show clearly that CNF is better than AOS in terms of foamability and foam stability as well.

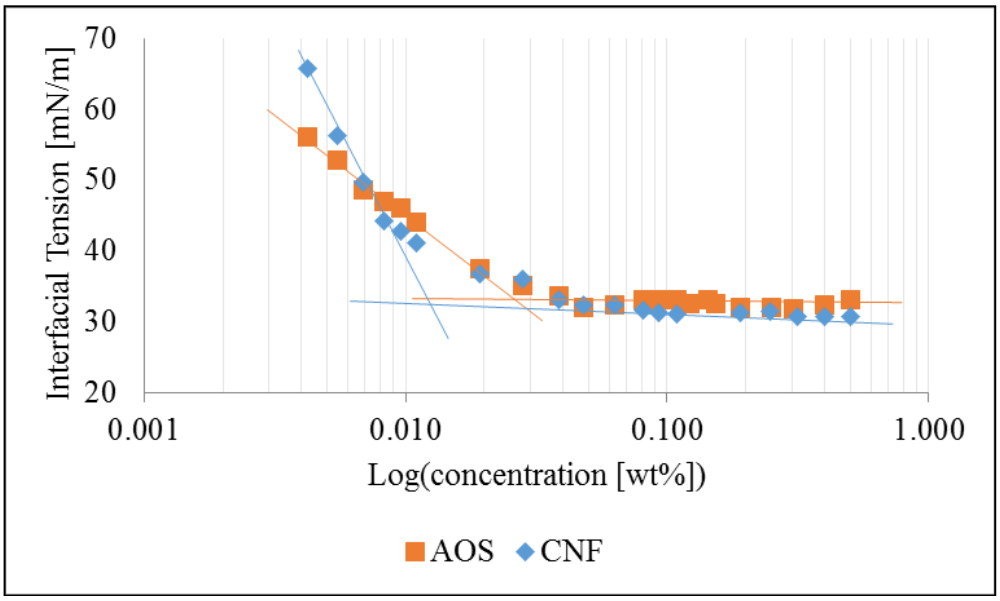

Figure 77: Interfacial measurements for AOS and CNF (Reprinted from Almobarky, Al-Yousef and Schechter (2017))

Table 38: $\sigma_{g/w}$ and $\sigma_{o/w}$ for AOS surfactant concentration at 23°C (Reprinted from Almobarky, Al-Yousef and Schechter (2017))

	Salinity			
	DI Water	1-wt% NaCl	2-wt% NaCl	3-wt% NaCl
$\sigma_{g/w}$ [mN/m]	32.5	32.3	32.1	32.15
$\sigma_{o/w}$ [mN/m]	1.4	0.52	0.44	0.38

Table 39: $\sigma_{g/w}$ and $\sigma_{o/w}$ for CNF at 0.5-wt% surfactant concentration at 23°C (Reprinted from Almobarky, Al-Yousef and Schechter (2017))

		Salinity		
	DI Water	1-wt% NaCl	2-wt% NaCl	3-wt% NaCl
$\sigma_{g/w}$ [mN/m]	30.7	31	31.25	31.11
$\sigma_{o/w}$ [mN/m]	5.88	3.94	3.51	3.11

V.4.2 Effect of Crude Oil

The stability of foam with crude oil can be predicated by the ability of the surfactant to reduce the $\sigma_{o/w}$ in saline solutions. According to the $\sigma_{o/w}$ in **tables 38** above, CNF foam-oil tolerance is expected to be significantly better than AOS. This is because the lower $\sigma_{o/w}$ with the addition of salts in comparison with AOS. For example, AOS reduced the $\sigma_{o/w}$ from 1.4 in DI water to 0.52 mN/m, whereas CNF had 5.88 in DI water and 3.94 mN/m in 1-wt% NaCl brine. Unlike AOS, the remaining $\sigma_{o/w}$ measurements at higher salinities confirm the same observation that CNF is not good at reducing the $\sigma_{o/w}$.

Table 40 shows positive entering coefficients that strongly imply the ability of crude oil to enter the lamellae between the bubbles to destroy the foam for both surfactants. However, the spreading coefficient in **table 41** shows negative values for CNF at all conditions and AOS at DI water only. Furthermore, the negative values of bridging coefficients for CNF and positive for AOS in **table 42** confirm the better foam-oil tolerance of CNF foam in comparison with AOS. According to these coefficients, the CNF foam stability is stronger than AOS at all conditions, while AOS foam-oil tolerance is good in DI water only.

Table 40: AOS vs. CNF entering coefficients (Reprinted from Almobarky, Al-Yousef and Schechter (2017))

Surfactant	DI water	1-wt% NaCl	2-wt% NaCl	3-wt% NaCl
AOS	2.4	1.32	1.04	1.03
CNF	5.08	3.44	3.26	2.72

Table 41: AOS vs. CNF spreading coefficients (Reprinted from Almobarky, Al-Yousef and Schechter (2017))

Surfactant	DI water	1-wt% NaCl	2-wt% NaCl	3-wt% NaCl
AOS	-0.4	0.28	0.16	0.27
CNF	-6.68	-4.44	-3.76	-3.5

Table 42: AOS vs. CNF bridging coefficients (Reprinted from Almobarky, Al-Yousef and Schechter (2017))

Surfactant	DI water	1-wt% NaCl	2-wt% NaCl	3-wt% NaCl
AOS	65.96	51.31	38.35	41.52
CNF	-15.19	-15.73	-3.37	-14.75

In addition, according to the lamellae numbers in **table 43**, CNF foam is stable in DI water and semi-stable in NaCl saline solutions. On the other hand, AOS is semi-stable in DI water but unstable in saline solutions.

Figure 78 shows samples from shaking tests with oil for CNF and AOS. The foam-oil columns with CNF in **figure 78A** did not collapse after 24-hr, whereas AOS in **figure 78B** shows either shorter or collapsed foam-oil columns after 18-hr.

Table 43: AOS vs. CNF lamellae number (Reprinted from Almobarky, Al-Yousef and Schechter (2017))

Surfactant	DI water	1-wt% NaCl	2-wt% NaCl	3-wt% NaCl
AOS	3.48	9.32	10.94	12.69
CNF	0.78	1.18	1.34	1.50

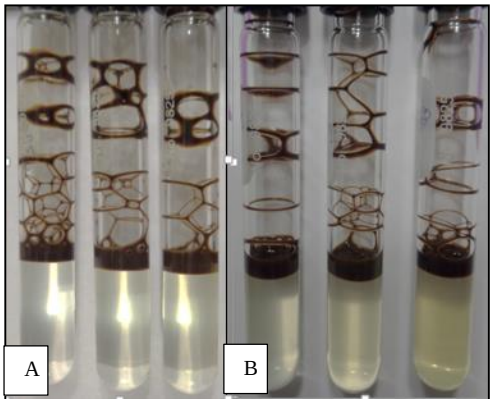

Figure 78: A) 0.5-wt% CNF in DI water, 1, and 2-wt% NaCl after 24-hr and B) 0.5-wt% AOS in DI water, 1, and 2-wt% NaCl after 18-hr (Reprinted from Almobarky, Al-Yousef and Schechter (2017))

V.4.3 Foam Dynamic Tests in Glass Beads Pack

Both AOS and CNF surfactants were assessed dynamically in high permeability glass beads pack porous media at high shear rates with the use of ScCO2. These experiments were conducted in the glass beads pack with 17.1 Darcy permeability and 30% porosity. The surfactants were prepared at 0.5-wt% concentrations for all experiments and the mobility reduction assessment were conducted in DI water and at different NaCl salinities 1, 2, and 3-wt%. Moreover, different injection qualities were used 50, 70, and 90% and different shear rates 317, 634, and 1268-sec^{-1} that are equivalent to

0.5, 1, and 2-ml/min flow rates. The conditions were chosen to ensure the existence of CO_2 at supercritical state at 1800-psi and 50°C.

In these tests, the foam generation was applied using the simultaneous injection of surfactant and $ScCO_2$. Moreover, the pressure drop across the porous media was measured and recorded. The rapid increase in pressure drop was recognized as the onset of strong foam generation (Dicksen, Hirasaki, and Miller 2002). If the strong foam generation was observed, the test continued until the steady state pressure drop was attained. This steady state pressure drop was used to calculate the mobility, foam effective viscosity, and MRF. **Table 44** shows the experimental conditions and results for all experiments. In addition, two runs for both surfactants were conducted at low shear rate to investigate the effect of shear rate on foam viscosity in porous media using $ScCO_2$.

Table 44: Experimental Conditions and results for AOS and CNF with CO_2 in glass beads pack (Modified from Almobarky, Al-Yousef and Schechter (2017))

Run #	Surfac-tant	NaCl Salinity [wt%]	Injection Quality [%]	Q [ml/min]	Shear rate [1/sec]	ΔP_{ss} [psi]	Mobility [md/cp]	μ_{eff} [cp]	MRF
1	AOS	--	90	0.5	317	208	118	144	5225
2	AOS	--	90	1	634	246	200	85	6150
3	AOS	--	90	2	1268	379	262	65	9475
4	AOS	1	90	0.5	317	164	150	114	4100
5	AOS	1	90	1	634	209	237	72	5225
6	AOS	1	90	2	1268	300	329	52	7500
7	AOS	2	90	0.5	317	161	156	109	4025
8	AOS	3	90	0.5	317	145	170	101	3625
9	AOS	3	90	1	634	170	290	59	4250
10	AOS	3	90	2	1268	216	459	37	5400
11	AOS	--	70	0.5	317	175	142	121	4375
12	AOS	1	70	0.5	317	99	249	69	2475
13	AOS	2	70	0.5	317	93	265	64	2325
14	AOS	3	70	0.5	317	91	273	63	2275
15	AOS	--	50	0.5	317	122	202	85	3050
16	AOS	1	90	0.015	9.51	9.97	74.15	230	250
17	CNF	--	90	0.5	317	162	153	112	4050
18	CNF	--	70	0.5	317	207	120	143	5175
19	CNF	--	50	0.5	317	225	110	154	5625
20	CNF	3	90	0.5	317	118	209	82	2950
21	CNF	1	90	0.015	9.51	16.09	46.00	371	402
22	--	1	--	0.015	9.51	0.04	616,270	0.03	--

V.4.3.1 Effect of Injection Quality

As observed, the foam viscosity was significantly affected by the injection quality. The dependence of foam viscosity and injection quality was found contradictory for AOS and CNF. **Figure 79** shows the foam viscosities for both surfactants at different injection qualities in DI water at 317- sec^{-1} in glass beads pack. As the injection quality decreases, AOS foam viscosity increases and CNF foam viscosity decreases. Accordingly, the maximum foam viscosity for AOS was 145-cp at 90% injection quality at which CNF provided 112-cp. Moreover, the maximum CNF foam viscosity was 154-cp at 50% injection quality at which AOS provided the minimum foam viscosity 85-cp.

These results disagree with the conclusions from the interfacial tension measurements. The interfacial tension measurements demonstrated that CNF has lower CMC, lower surface tension, higher adsorption and smaller area/molecule at the G/W interface. Such properties are indicators for a better foam stability that would presumably lead to higher foam viscosity. However, the interfacial properties were measured at atmospheric conditions and with air, whereas the dynamic foam experiments were conducted with $ScCO_2$ at 50°C and extremely higher pressure. The surfactants solubilities and performances as foaming agents in air differ significantly from that in $ScCO_2$. Therefore, predicting foam behaviors in $ScCO_2$ with interfacial properties that were measured with air is not accurate due to the different behaviors of the surfactants at G/W and C/W interfaces (Adkins et al. 2010). Moreover, foam viscosity relationship with injection quality is contradictory in literature. For example, Marsden and Khan (1966)

found that foam viscosity increases as the quality increases which is the opposite of what was found by Lee and Heller (1990).

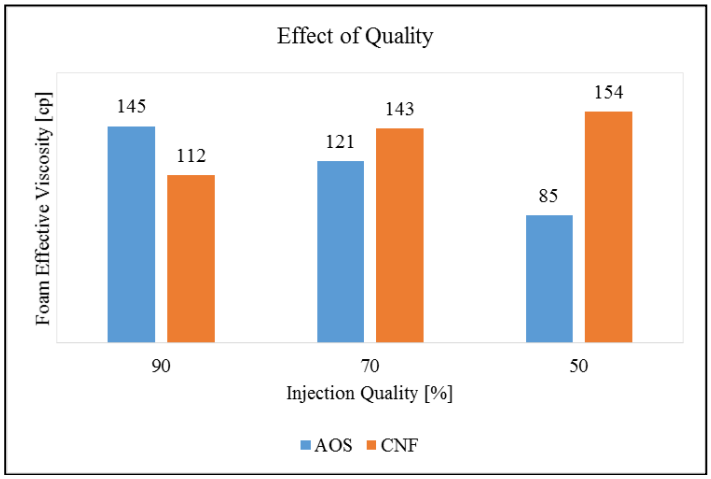

Figure 79: Effect of Quality of AOS and CNF in glass beads pack at 317-sec^{-1} (Reprinted from Almobarky, Al-Yousef and Schechter (2017))

V.4.3.2 Effect of Shear Rate

The high shear rates are not representative for the actual shear rates at reservoir conditions. Further dynamic tests were conducted at lower shear rate 9.51-sec^{-1} in the glass beads pack. The foam viscosities at 1-wt% NaCl salinity, 90% injection quality, and shear rates 317 and 9.51-sec^{-1} are shown in **figure 80**. Clearly, the foam is of shear thinning nature, the viscosity increased significantly for both surfactants at low shear rate. Moreover, CNF foam viscosity at low shear rate was higher with 371-cp compared with 230-cp for AOS.

Figure 81 shows the results for both surfactants at low shear rate in glass beads pack. In fact, these results are strong evidence that both surfactants are able to control the mobility of $ScCO_2$ inside the porous media, and CNF is stronger than AOS surfactant.

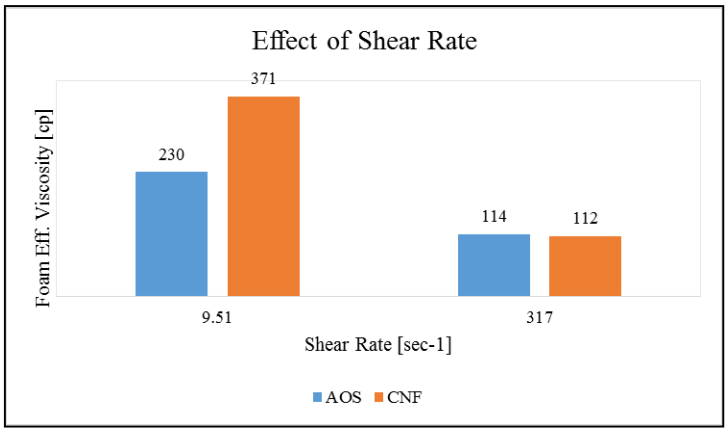

Figure 80: High vs. low shear rate foam viscosities for AOS and CNF at 0.5-wt% surfactant concentration, 1-wt% salinity, and 90% injection quality (Reprinted from Almobarky, Al-Yousef and Schechter (2017))

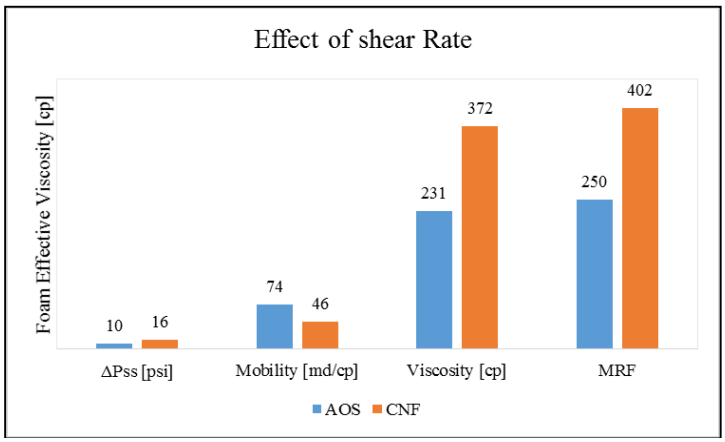

Figure 81: The low shear rate results at 0.5-wt% surfactant concentration at 90% injection quality (Reprinted from Almobarky, Al-Yousef and Schechter (2017))

V.4.4 Foam Dynamic Tests in Bentheimer Sandstone

This section is to show the results for mobility reduction at lower permeability Bentheimer sandstone at low shear rates, 8.92 to 9.51-sec^{-1} that corresponds to 4 to 5 ft/day velocity inside the porous media. In Bentheimer sandstone experiments, the mobility reduction evaluation was investigated using N_2 gas at 850-psi and $ScCO_2$ at 1800-psi and both at 50°C. **Table 45** lists the conditions for all experiment and **table 46** shows the results. In addition, two baseline experiments were conducted using N2 gas and $ScCO_2$. The results are also shown in **table 46** for runs 10 and 11.

Table 45: Experimental Conditions for AOS and CNF in sandstone (Modified (Reprinted from Almobarky, Al-Yousef and Schechter (2017))

Run #	Surfac-tant	Concentr-tion [wt%]	Salinity	P [psi]	Velocity [ft/day]	Shear Rate [sec^{-1}]	Injection Quality [%]	Gas	K [Darcy]
1	AOS	0.5	1-wt% NaCl	1800	5	8.92	90	$ScCO_2$	1.7
2	AOS	0.5	1-wt% NaCl	1800	5	8.92	70	$ScCO_2$	1.61
3	CNF	0.5	1-wt% NaCl	1800	5	8.92	90	$ScCO_2$	1.98
4	CNF	0.5	1-wt% NaCl	1800	5	8.92	70	$ScCO_2$	1.78
5	AOS	0.5	1-wt% NaCl	850	5	9	90	N_2	1.61
6	AOS	0.5	1-wt% NaCl	850	10	18	90	N_2	1.61
7	CNF	0.5	1-wt% NaCl	850	5	9.	90	N_2	1.68
8	CNF	0.5	1-wt% NaCl	850	10	18	90	N_2	1.68
9	CNF	0.5	DI water						
10	N_2 Gas injection	--	1-wt% NaCl	850	5	9	--	N_2	1.62
11	$ScCO_2$ injection	--	1-wt% NaCl	1800	5	9	--	$ScCO_2$	1.62

Table 46: Results for foam dynamic tests of AOS and CNF in sandstone (Modified from Almobarky, Al-Yousef and Schechter (2017))

Run #	Surfactant	Gas	ΔP_{ss} [psi]	Mobility [md/cp]	Foam Viscosity [cp]	MRF
1	AOS	$ScCO_2$	0.4	411	4.13	1.67
2	AOS	$ScCO_2$	25.42	6.79	237.11	105.92
3	CNF	$ScCO_2$	0.60	301.06	7.21	2.50
4	CNF	$ScCO_2$	2.00	89.00	20.00	8.33
5	AOS	N_2	1.35	129.33	12.5	3.38
6	AOS	N_2	3.46	101.5	16	8.7
7	CNF	N_2	12.89	13.6	123.4	32.23
8	CNF	N_2	34.4	10.2	164.7	86
9	CNF	N_2				
10	N_2 Gas injection	N_2	0.4	446	0.28	--
11	$ScCO_2$ injection	$ScCO_2$	0.24	680	0.46	--

V.4.4.1 Effect of Permeability

The effect of permeability on $ScCO_2$ mobility control was investigated using both glass beads pack and Bentheimer sandstone. However, there is a slight difference in the Bentheimer sandstone permeabilities for AOS and CNF, 1.71 and 1.98-Darcy, respectively. Results are listed in **table 44** and **46** where runs No. 16 and 1 for high and low permeability for AOS, and runs No. 21 and 3 for CNF. The foam generation was tested at low shear rate and 90% injection quality with 0.5-wt% surfactant concentrations prepared at 1-wt% NaCl brine.

Figure 82 shows the significant effect of permeability on foam viscosity. It is a fact that foam favors the high permeability porous media where foam generation is easier and stronger than that of low permeability porous media. As shown, 10 times reduction in permeability approximately induced a reduction in foam viscosities from 230 to 4.1-cp for

AOS and 372 to 7.2-cp for CNF. However, CNF foam viscosities are higher than that of AOS regardless of the permeability.

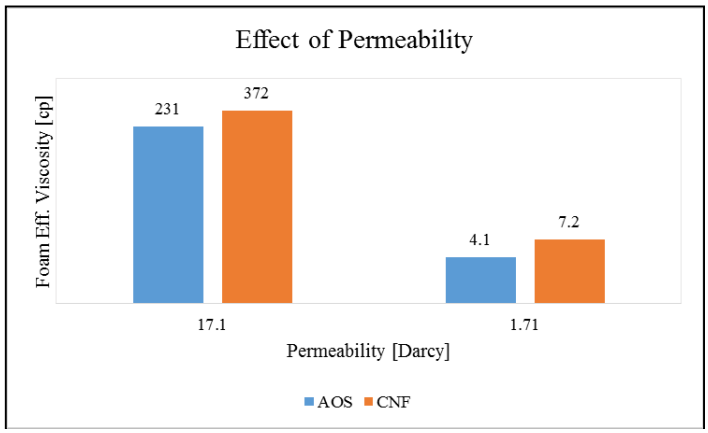

Figure 82: CNF and AOS foam viscosity at different permeability (Reprinted from Almobarky, Al-Yousef and Schechter (2017))

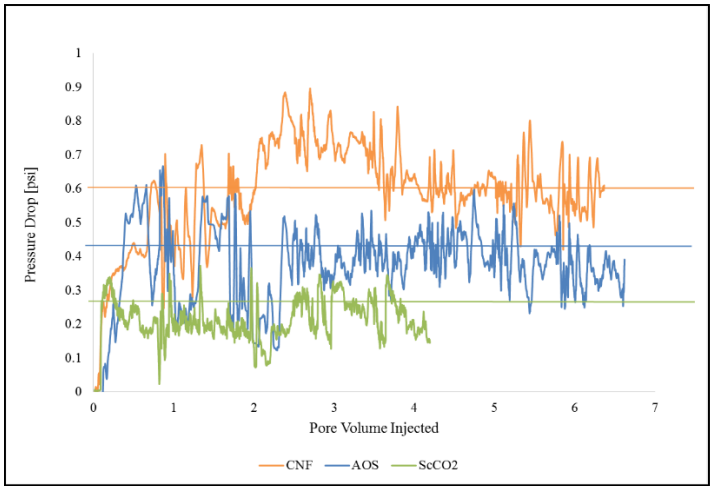

Figure 83: AOS and CNF at $ScCO_2$ at 90% injection quality (Modified from Almobarky, Al-Yousef and Schechter (2017))

Figure 83 compares the pressure profiles in Bernheimer sandstone at low shear rate, runs No. 1 and 3 in **table 45** for AOS and CNF, respectively. The baseline experiment for $ScCO_2$ injection was also included for comparison purposes. As shown, CNF foam approached 0.6-psi steady state pressure drop in comparison with 0.4-psi with AOS form, whereas the $ScCO_2$ injection provided lower steady state pressure drop 0.24-psi. Both surfactants lowered the ScCO2 mobility significantly. However, CNF was stronger with 2.5 MRF compared with 1.67 MRF with AOS.

V.4.4.2 Effect of Injection Quality

Runs 4 and 2 pressure profiles are shown in **Figure 84** for both surfactants with $ScCO_2$ at 70% quality at low shear rate in Bentheimer sandstone. In this case, AOS foam provided higher flow resistance with 25-psi steady state pressure drop compared with 2-psi with CNF. Calculations showed that AOS provided 106 MRF compared with 8.33 MRF only with CNF. These results are in disagreement with the high permeability glass beads pack results where AOS foam favored the higher injection quality and CNF foam favored the lower injection quality. Moreover, they are in disagreement with the literature where the steady state pressure drop for surfactant co-injection with $ScCO_2$ are believed extremely lower than 25 psi. Moreover, surfactant/$ScCO_2$ co-injection is known to be lower than surfactant/N_2 co-injection due to the different solubilities of surfactants in $ScCO_2$ and N_2. The next investigation was for both surfactants with N_2 gas to compare with the $ScCO_2$ results.

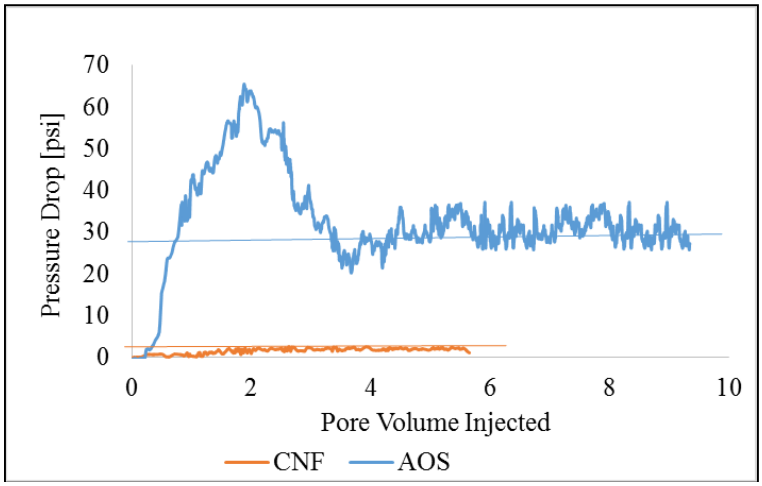

Figure 84: AOS and CNF at ScCO2 at 70% injection quality in sandstone (Reprinted from Almobarky, Al-Yousef and Schechter (2017))

V.4.4.3 Mobility Reduction Using N_2 Gas

The gas effect was investigated for 0.5-wt% surfactants in 1-wt% NaCl brine using N_2 at 850-psi and 50°C. These runs were conducted at 90% injection quality at two shear rates: 9 and 18-sec^{-1} corresponding to 5 and 10 ft/day. After approaching the steady state at 5 ft/day, the experiments were continued with higher velocity 10 ft/day. **Figure 85** shows the pressure drop profiles for runs 5, 6, 7, and 8 in **table 45** and results in **table 46**. With N_2, the pressure profiles confirm that CNF is able to provide higher flow resistance at both velocities more than that of AOS. Moreover, foam viscosities of using CNF/N_2 co-injection were 123.4 and 164.7-cp in comparison with 12.5 and 16-cp with AOS/N_2 co-injection at 5 and 10 ft/day, respectively, see **figure 86**.

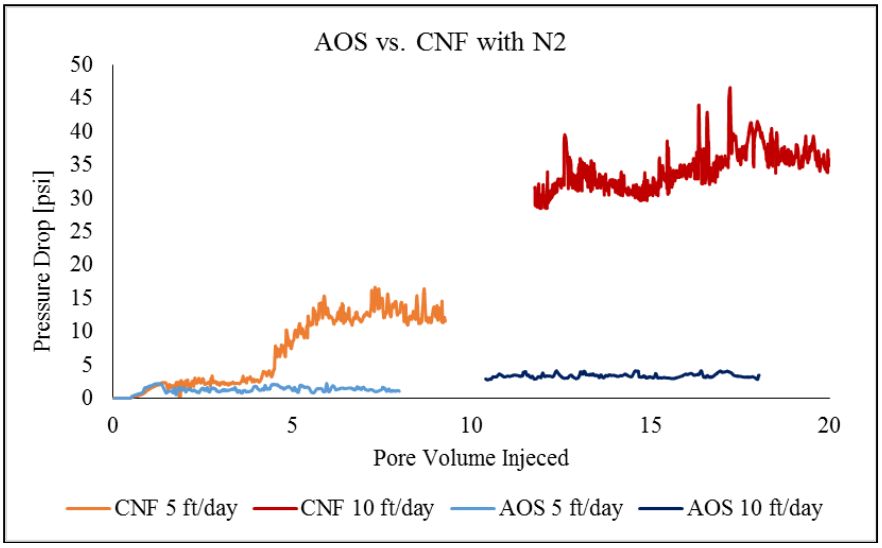

Figure 85: AOS and CNF with N_2 at 850-psi at 5 and 10 ft/day velocities at 90% injection qualities (Reprinted from Almobarky, Al-Yousef and Schechter (2017))

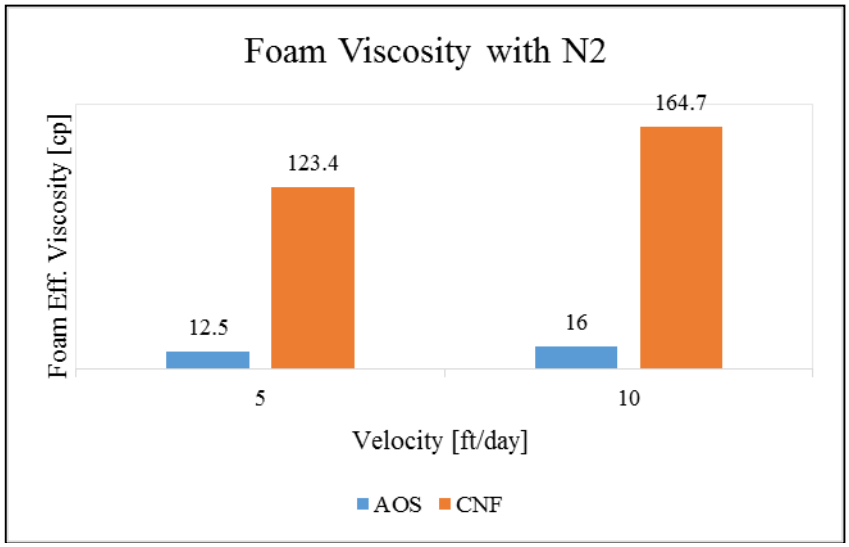

Figure *86*: Foam viscosity at 5 and 10 ft/day for 0.5-wt% of CNF and AOS in 1-wt% NaCl brine solution at 90% injection quality with N_2 gas (Reprinted from Almobarky, Al-Yousef and Schechter (2017))

Another observation from **figure 86** is that the viscosities increased as the velocity increased. Foam is a non-Newtonian fluid of a shear thinning nature, as the shear rate increases, the foam viscosity decreases (Schramm and Wassmuth 1994). However, these results disagree with this fact because the viscosities increased as the shear rate increased exhibiting shear-thickening behavior.

Foam shear thickening behavior was reported in many studies in literature. Adkins et al. (2010) measured the foam viscosity for nonionic surfactants with $ScCO_2$ and found that foam rheology depends on the foam texture. They observed shear thickening behavior when the bubbles sizes changed, whereas foam shear thinning behavior was observed when there was no change in bubble sizes. Farajzadeh et al. (2015) experimentally found that foam exhibited shear-thickening nature and attributed this to the effect of rock permeability. Sanders et al. (2010) related the foam shear-thickening behavior to the permeability contrasts inside the porous media. Also, there might be a chance that such behavior was caused by a technical error. Both velocities, 5 and 10 ft/day, were conducted in one experiment. The 10 ft/day velocity was applied after the foam was generated successfully during the 5 ft/day injection. This means that the gas relative permeability in the porous media was reduced already due to the gas blockage effect by the foam that was generation during the 5 ft/day injection. Therefore, the following 10 ft/day velocity promoted more foam generation and provided lower mobility (i.e. higher foam viscosity) in an unclean lower permeability rock. Thus, the observed foam viscosity of 10 ft/day might be less than the correct viscosity if it were conducted in a clean rock.

Figure 87 shows the effect of $ScCO_2$ at 1800-psi on foam viscosity in comparison with N_2 at 850-psi for both surfactants at the same conditions. Foam with $ScCO_2$ provides lower flow resistance (i.e. lower pressure drop across the porous media) than that with N_2 gas as reported in (Du et al. 2008). Therefore, the results of AOS/$ScCO_2$ at 70% injection quality where the steady state pressure drop exceeded 30-psi, in **figure 84**, is highly questionable.

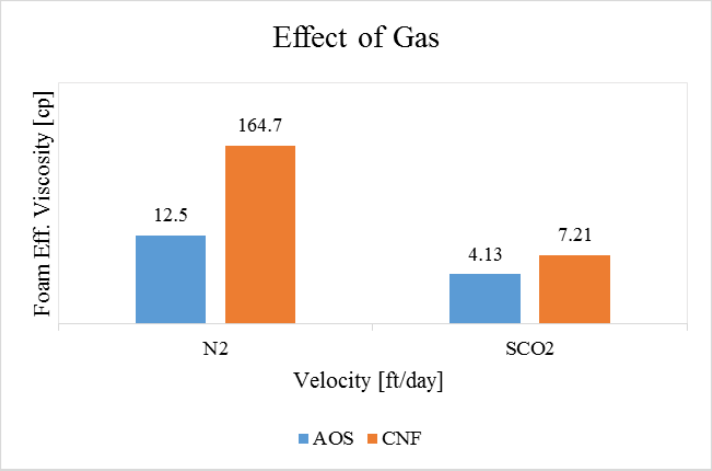

Figure *87*: Effect of gas on foam viscosity of AOS and CNF with $ScCO_2$ at 1800-psi and N_2 at 850-psi at the same conditions

V.4.5 Core Flooding Experiments

Three core flooding experiments were conducted for $ScCO_2$ continuous injection as a baseline experiment, CNF and AOS foam floods with $ScCO_2$. Both surfactants were used at 0.5-wt% and prepared in 1-wt% NaCl. These core floods were conducted in three oil recovery stages at 1450-psi and 50°C. The overburden pressure was at least 500-psi more than the experiment pressure.

The first stage in all experiments was water flooding in which 5 pore volumes of 1-wt% saline water were injected at constant flow rate equivalent to 5 ft/day velocity. For the baseline experiment, 5 pore volumes of $ScCO_2$ were injected at 5 ft/day velocity. For the foam core flood experiments, the second stage was to inject 1 pore volume of surfactant at 5 ft/day. This is to mitigate the effect of surfactant adsorption on rock surfaces. Then, 5 pore volumes of surfactant and $ScCO_2$ simultaneous injection at a total flow rate equivalent to 5 ft/day velocity at 90% injection quality for 24-hr foam flood. **Table 47** shows the experimental conditions and rocks properties used in these experiments.

Table 47: Core flooding experimental conditions and sandstone properties (Modified from Almobarky, Al-Yousef and Schechter (2017))

Run #	Surfactant	Velocity [ft/day]	Injection Quality [%]	Rock	Length [in]	Diameter [in]	Pore Volume [cc]	Porosity [%]	Permeability [Darcy]
1	$ScCO_2$ injection	5	--	Bentheimer Sandstone	12	1	33.52	21.71	1.87
2	AOS/$ScCO_2$	5	90	Bentheimer Sandstone	12	1	34.74	22.5	1.71
3	CNF/$ScCO_2$	5	90	Bentheimer Sandstone	12	1	33.74	21.85	1.91

Figures 88 shows the results for the baseline core flood experiment in which $ScCO_2$ was injected without surfactant. Water flooding resulted in 39.66% oil recovery. Moreover, injecting 5 pore volumes of $ScCO_2$ produced 27.54% of the OOIP. The total oil recovery in the baseline experiment was 76.2% of the OOIP.

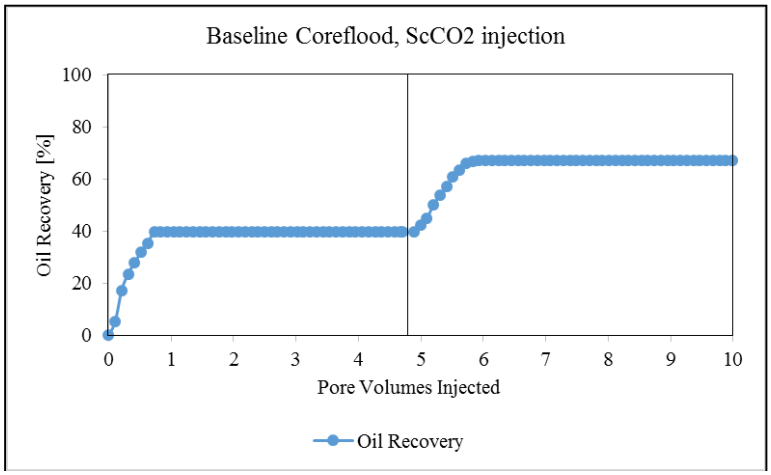

Figure *88*: Baseline experiment $ScCO_2$ injection (Reprinted from Almobarky, Al-Yousef and Schechter (2017))

Figure 89 shows the results of AOS/$ScCO_2$ core flood experiment. Injecting 4.56 Pore Volumes (PV) of water flooding resulted in ultimately 35.42% of the OOIP. Then, 1.62 PV of surfactant solution were injected as a pre-flush in which an insignificant amount of oil (4.75% of the OOIP) was observed during AOS pre-flush stage. This insignificant amount of oil production is not expected to be related to the reduction in capillary forces but a result of a technical error while performing the experiment. Maintaining the pressure stabilization at the beginning of co-injection was considered very important due to the pressure surge that is normally expected at the beginning of the gas

injection. Consequently, the co-injection was deliberately started thorough the bypass until the stabilization is maintained after which the flow (i.e. co-injetion) was diverted into the core. In this experiment, perhaps the co-injection was diverted to the core before the stabilization which caused the pressure surge at the sand face leading to surfactant injection into high and low permeable zones where the remaining oil exists. This pressure surge could be the reason for the surfactant pre-flush oil recovery. Another supporting evidence is that AOS showed less ability to reduce the $\sigma_{o/w}$ than that of J071 mixtures that were tested previously. However, those mixtures did not produce oil during the pre-flush stage, while AOS did.

Finally, 5 PV of AOS/$ScCO_2$ simultaneous injection for foam application resulted in 28.5% additional oil recovery. The total oil recovery of AOS foam core flood was 68.67% of the OOIP. Moreover, AOS foam flooding resulted in around 1% additional oil recovery at 28.5% compared with 27.54% oil recovery in the baseline experiment.

Figure 90 shows the results for CNF foam core flood. The ultimate oil recovery of water flooding was 39.66% of the OOIP. Surfactant pre-flush, the second stage, resulted in no oil recovery whatsoever. Then, the foam was applied by injecting CNF and $ScCO_2$ simultaneously which resulted in 36.37% additional oil recovery. The total oil recovery of this experiment was 76.03%. In fact, CNF foam flood produced 7.87% more oil recovery than AOS foam flood and 8.83% more than that of the baseline experiment. Therefore, CNF surfactant proved better than AOS in terms of mobility reduction and enhanced oil recovery.

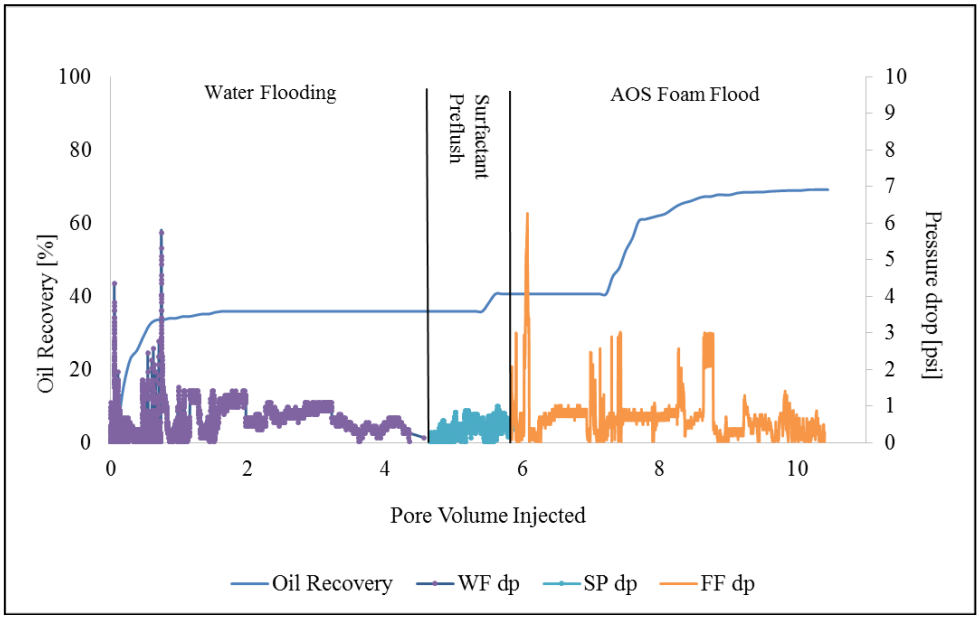

Figure *89*: AOS foam flood experiment (Reprinted from Almobarky, Al-Yousef and Schechter (2017))

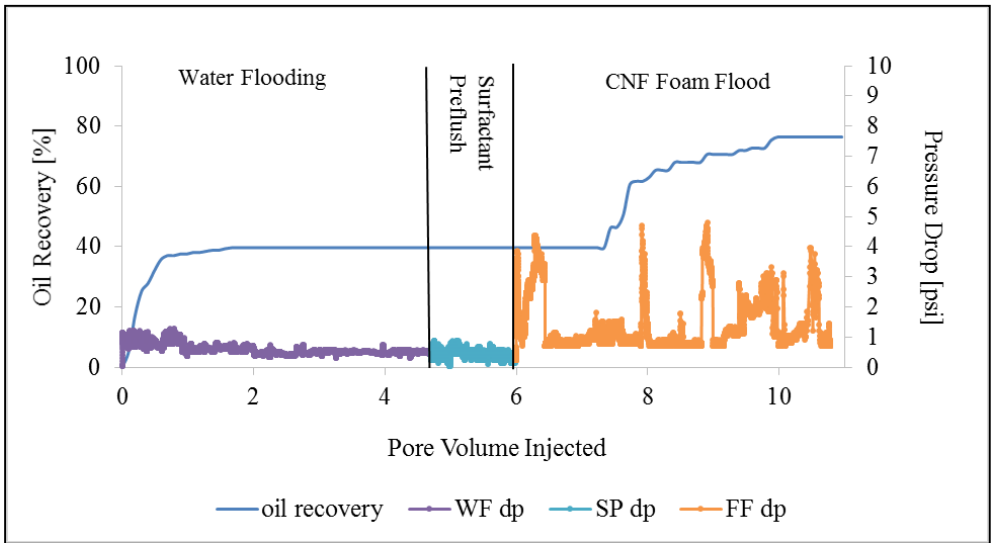

Figure *90*: CNF foam flood experiment (Reprinted from Almobarky, Al-Yousef and Schechter (2017))

CHAPTER VI
CONCLUSIONS AND RECOMMENDATIONS

VI.1 Results

The study objectives were mainly concerned about enhancing the oil recovery by the application of foam for mobility control in chemical as well as CO_2 miscible flooding. Also, the other objective is to enhance the foamability and foam stability in absence and presence of crude oil by the use of surfactants mixtures. The mixtures were prepared by mixing commercially available individual surfactants.

Experimental investigations were achieved by conducting different types of tests using different devices to acquire the parameters that helped to compare the individual surfactants and their mixtures in terms of foaming properties. Experimental work was divided into four categories: preliminary work for finding the suitable surfactants for mixtures based on foam-oil tolerance, foam static tests or shaking tests, interfacial properties measurements, and foam dynamic tests that included mobility control evaluation and core flooding experiments at reservoir conditions.

Shaking tests included the investigation of foamability which defines the tendency of the foaming agent to produce the foam, and foam stability which defines the ability of the foaming agent for foam stabilization. Both foamability and foam stability were investigated in absence and presence of crude oil. This study used NBU light crude oil (33.7°API at 23°C) for all experiments. Combining the shaking tests results with the

measurements of interfacial properties was important to understand and describe the thin-film stability mechanisms.

Also, static tests were paired with bubble sizes measurements using from micro-images. The smaller the bubbles with time is the better foam stability.

Foam dynamic tests were mainly conducted for mobility reduction evaluation of the surfactants and their mixtures without oil at reservoir conditions. They were conducted in two different porous media: high permeability, in-house built, glass beads pack and Bentheimer sandstone for lower permeability investigations. Moreover, the mobility reduction evaluation was conducted using high and low shear rates to provide a better understanding for the mechanisms by which the mixtures enhance the foam stability.

Finally, core flooding experiments were conducted using Bentheimer sandstone at reservoir conditions to compare the oil recovery efficiency.

The main conclusions are:

- The criteria proposed for surfactants screening proved successful to determine the suitable surfactants for mixing. Finding the mixtures that enhances the foam-oil tolerance resulted in mixtures with better foaming properties in absence and presence of oil;
- The high foamability in presence and absence of crude oil does not necessarily result in high foam stability.
- For anionic-anionic surfactants mixtures, salinity has no impact on foamability, but dramatically affected the foam stability in presence of oil.

- The best foam-oil stabilizers in deionized water, in this study, were impacted dramatically with the addition of salts. In fact, they turned to poor foaming agents with the addition of salts in presence of crude oil.
- Mixing the best surfactants in terms of foamability with the best foam-oil stabilizers provided mixtures with better foaming properties such as better foam stability in DI water, saline water, in absence and presence of crude oil. Moreover, mixtures generated higher foam viscosity in porous media, and produced higher oil recovery than that of the individual surfactants.
- Shaking tests, in general, indicated that anionic surfactants and their mixtures produce the same foam volume, whereas anionic-nonionic mixtures produced less foam volume than the individual anionic surfactant they were compared with. This is because of the higher micellar stability of the mixtures in comparison with the individual anionic surfactant.
- Observations suggested that mixing anionic with nonionic surfactants resulted in mixtures with higher micellar stability than the individual surfactants. Therefore, higher foam stability.
- Comparing foam dynamic tests at high and low shear rate was adopted from Patist et al. (2001) where they compared high and low shear rate in static tests. In this study, the individual surfactant produced higher foam viscosity than the mixtures at high shear rates. This is in disagreement with the previous shaking tests results where mixtures performed better than the individual surfactant. However, at lower shear rates in lower permeability

porous media, the mixtures performed better than the individual surfactant. The lower micellar stability of J071 was the reason for such behavior as discussed. Therefore, the micellar stability might be a major factor in enhancing the foam stability in static as well as dynamic tests in porous media.

- J071-IOS mixtures showed that the longer the carbon chain length of the IOS surfactant in mixture resulted in better foam stability. This is in a disagreement with Shiao et al. (1998) where it was found that the SDS mixture with a nonionic alcohol of the same carbon chain length gave the best foam stability and lower mobility. It should be noted that this study used commercially available surfactants that might be mixtures of different types of surfactants, whereas Shiao et al. (1998) used pure surfactants.
- The anionic-nonionic mixtures are in agreement with Shiao et al. (1998). Both surfactants mixed were approximately possessing the same carbon chain lengths.
- Those mixtures showed better foam stability were also found with lower CMC than the individual surfactant. This is line with Schick and Fowkes (1957) experimental work where lowering the CMC was correlated with enhancing the foam stability for anionic-nonionic alcohol mixtures.
- This study also compared 2 anionic surfactants: AOS and a newly developed surfactant CNF. This investigation concluded that CNF might

be one of the best commercially available anionic surfactants for $ScCO_2$ mobility control in miscible flooding process.

- AOS surfactant is also a powerful foaming agent, and none of the mixtures with AOS were able to provide better foam stability than AOS itself.

VI.2 Recommendations

- Correlating the dynamic surfactant tension with the static foam tests results is crucial and recommended for more understanding of the ability of the mixtures to enhance the foam stability better than the individual surfactants;
- Calculating the β interaction parameters to investigate the interactions between the surfactants might provide more understanding on the behaviors of the mixtures in comparison with the individual surfactants in terms of their foaming properties.
- For better comparison between mixtures and individual surfactants in terms of thin-film stability mechanisms, it is recommended to perform shaking tests, bubble size micro-imaging, and interfacial tension measurements at higher pressure and temperature.
- Micellar stability measurements and correlating them with the low/high shear rate dynamic foam testing (i.e. foam viscosity) will definitely provide significant insights for foam stability in porous media.

REFERENCES

Adkins, S. S., Chen, X., Chan, I., Torino, E., Nguyen, Q. P., Sanders, A. W., & Johnston, K. P. 2010. Morphology and Stability of CO_2-in-Water Foams with Nonionic Hydrocarbon Surfactants. *Langmuir.* **26** (8): 5335-5348.

Adkins, S. S., Chen, X., Nguyen, Q. P., Sanders, A. W., & Johnston, K. P. 2010. Effect of Branching on the Interfacial Properties of Nonionic Hydrocarbon Surfactants at the Air–Water and Carbon Dioxide–Water Interfaces. *Journal of Colloid and Interface Science.* **346** (2): 455-463.

Ahmed, T. 2000. Minimum Miscibility Pressure from EOS. Canadian International Petroleum Conference, Calgary, Alberta. PETSOC-2000-001.

Al-Ghamdi, A. M., & Nasr-El-Din, H. A. 1997. Effect of Oilfield Chemicals on the Cloud Point of Nonionic Surfactants. Colloids and Surfaces A: *Physicochemical and Engineering Aspects*. **125** (1): 5-18.

Ali, S. M. F. 2003. Heavy Oil—Evermore Mobile. *Journal of Petroleum Science and Engineering,* **37** (1): 5-9.

Almobarky, M. A., AlYousef, Z., & Schechter, D. 2017. A Comparison between Two Anionic Surfactants for Mobility Control of Super Critical CO_2 in Foam-Assisted Miscible EOR. Carbon Management Technology Conference, Houston TX, USA, July 2017, http://carbonmanagement.org/cmtc/2017.

Almobarky, M. A., AlYousef, Z., & Schechter, D. 2017. A Comparison between Two Anionic Surfactants for Mobility Control of Super Critical CO_2 in Foam-Assisted Miscible EOR. *Society of Petroleum Engineers*. https://doi.org/10.7122/486486-MS. CMTC-486486-MS.

AlYousef, Z. A., M. A. Almobarky, and D. S. Schechter.2017. The Effect of Nanoparticle Aggregation on Surfactant Foam Stability. *Journal of Colloid and Interface Science.* **511**:365-373.

Amro, M., Mohammed A. Al Mobarky, and E. S. Al-Homadhi. 2007. Improved Oil Recovery by Application of Sound Waves to Water Flooding. 15th SPE Middle East Oil & Gas Show and Conference. International Exhibition Center, Kingdom of Bahrain. *Society of Petroleum Engineers*. SPE-105370-MS.

Andrianov, A., R. Farajzadeh, M. Mahmoodi Nick, M. Talanana, and P. L. J. Zitha. 2012 Immiscible Foam for Enhancing Oil Recovery: Bulk and Porous Media Experiments. *Industrial & Engineering Chemistry Research.* **51** (5): 2214-2226.

Aveyard, R., Binks, B. P., Fletcher, P. D. I., Peck, T. G., & Rutherford, C. E. 1994. Aspects of Aqueous Foam Stability in the Presence of Hydrocarbon Oils and Solid Particles. *Advances in Colloid and Interface Science*. **48**: 93-120.

Bera, A., Ojha, K., & Mandal, A. 2013. Synergistic Effect of Mixed Surfactant Systems on Foam Behavior and Surface Tension. *Journal of Surfactants and Detergents, **16*** (4): 621-630.

Bikerman, J.J.; Perry, J. M.; Booth, R. B.; Currie, C. C. 1953. Foams: Theory and Industrial Applications, Reinhold Publishing Corporation, New York.

Boeije, C. S., Bennetzen, M., & Rossen, W. 2017. A Methodology for Screening Surfactants for Foam Enhanced Oil Recovery in an Oil-Wet Reservoir. *SPE Reservoir Evaluation & Engineering.* SPE-185182-PA.

Bond, D.C. and O.C. Holbrook. 1958. Gas drive oil recovery process. US. Patent No. 3529668.

Borchardt, J. K., Bright, D. B., Dickson, M. K., & Wellington, S. L. 1985. Surfactants for CO_2 Foam Flooding. The 60th Annual Technical Conference and Exhibition, Las Vegas, USA. *Society of Petroleum Engineers.* SPE-14394-MS.

BP Global. 2016. The BP Statistical Review of World Energy. *British Petroleum Global.*

Casteel, J. F., & Djabbarah, N. F. 1988. Sweep Improvement in CO_2 Flooding by Use of Foaming Agents. *SPE Reservoir Engineering.* **3** (4). SPE-14392-PA.

Chang, S.-H., & Grigg, R. B. 1999. Effects of Foam Quality and Flow Rate on CO_2-Foam Behavior at Reservoir Conditions. *SPE Reservoir Evaluation and Engineering.* **2** (3). SPE-56856-PA.

Chen, Qing, Margot Geertrui Gerritsen, and Anthony Robert Kovscek. 2010. Improving Steam-Assisted Gravity Drainage Using Mobility Control Foams: Foam Assisted-Sagd (Fa-Sagd). *SPE Improved Oil Recovery Symposium*. Tulsa, Oklahoma. Society of Petroleum Engineers. SPE-129847-MS.

Dicksen, T., Hirasaki, G. J., & Miller, C. A. 2002. Conditions for Foam Generation in Homogeneous Porous Media. *Society of Petroleum Engineers.* SPE-75176-MS.

DOE. Enhanced Oil Recovery. 2017. https://energy.gov/fe/science-innovation/oil-gas-research/enhanced-oil-recovery.

Dong, M., S. Huang, R. Srivastava. 2000. Effect of Solution Gas in Oil on CO_2 Minimum Miscibility Pressure. *Journal of Canadian Petroleum Technology.* **39** (11): 53-61.

Du, D.-X., Beni, A. N., Farajzadeh, R., & Zitha, P. L. 2008. Effect of Water Solubility on Carbon Dioxide Foam Flow in Porous Media: an X-ray Computed Tomography Study. *Industrial & Engineering Chemistry Research*. **47** (16): 6298-6306.

Eastoe, J., Gold, S., & Steytler, D. C. 2006. Surfactants for CO_2. Langmuir. **22** (24): 9832-9842.

EIA. 2016. International Energy Outlook 2016 With Projections to 2040. *U.S. International Energy Administration.*

Enick, Robert Michael, David Kenneth Olsen, James Robert Ammer et al. 2012. Mobility and Conformance Control for CO_2 EOR via Thickeners, Foams, and Gels -- A Literature Review of 40 Years of Research and Pilot Tests. SPE Improved Oil Recovery Symposium, Tulsa, Oklahoma, USA. SPE-154122-MS.

Falls, A. H., G. J. Hirasaki, et al. 1988. Development of a Mechanistic Foam Simulator: The Population Balance and Generation by Snap-Off. *SPE Reservoir Engineering*. **3** (03). SPE-14961-PA.

Farajzadeh, R., A. Andrianov, and P. L. J. Zitha. 2010. Investigation of Immiscible and Miscible Foam for Enhancing Oil Recovery. *Industrial & Engineering Chemistry Research.* **49** (4): 1910-1919.

Farajzadeh, R., Andrianov, A., Krastev, R., Hirasaki, G. J., & Rossen, W. R. 2012. Foam–oil interaction in porous media: Implications for Foam Assisted Enhanced Oil Recovery. *Advances in Colloid and Interface Science*. **183**: 1-13.

Farajzadeh, R., Lotfollahi, M., Eftekhari, A. A., Rossen, W. R., & Hirasaki, G. J. H. (2015). Effect of Permeability on Implicit-Texture Foam Model Parameters and the Limiting Capillary Pressure. *Energy & Fuels*. **29** (5), 3011-3018.

Farzaneh, S. A., & Sohrabi, M. 2013. A Review of the Status of Foam Application in Enhanced Oil Recovery. *The EAGE Annual Conference & Exhibition incorporating SPE Europec*. Society of Petroleum Engineers. SPE-164917-MS.

Feldman, D. 1987. Surfactants in Consumer Products, Theory, Technology and Application, (J. Falbe, Ed.), Springer-Verlag, Berlin, 1987 547. *Journal of Polymer Science Part C: Polymer Letters*, **25** (11): 461-462.

Fredd, C. N., Miller, M. J., & Quintero, B. W. 2004. Impact of Water-Based Polymer Fluid Characteristics on CO_2 Foam Rheology. SPE International Symposium and Exhibition on Formation Damage Control, Lafayette, Louisiana, USA. SPE-86493-MS.

Fried, A. N. The Foam-Drive Process for Increasing the Recovery of Oil. 1961. U.S. Bureau of Mixes, Rep. Inv., 5866, Washington, D. C.

Garrett, P. 1993. Defoaming: theory and industrial applications, Volume 45. CRC Press.

Gauglitz, P. A., F. Friedmann, S. I. Kam, and W. R. Rossen. 2002. Foam Generation in Porous Media. *SPE/DOE Improved Oil Recovery Symposium*. Tulsa, Oklahoma: Society of Petroleum Engineers. SPE-75177-MS.

Green, D.W. and Willhite, G.P. 1998. *Enhanced Oil Recovery*.Vol. 6, *SPE Textbook Series*, Richardson, Texas: SPE.

Guo, H., Zitha, P. L. J., Faber, R., & Buijse, M. A Novel Alkaline/Surfactant/Foam Enhanced Oil Recovery Process. doi: 10.2118/145043-pa

Hadlow, R. E. 1992. Update of Industry Experience With CO_2 Injection. Paper presented at the SPE Annual Technical Conference and Exhibition, Washington, D.C. SPE-24928-MS.

Haugen, Åsmund, Martin A. Fernø, Arne Graue, and Henri J. Bertin. 2012. Experimental Study of Foam Flow in Fractured Oil-Wet Limestone for Enhanced Oil Recovery. *SPE Reservoir Evaluation & Engineering.* **15** (02). SPE-129763-PA.

Healy, R. N., Holstein, E. D., & Batycky, J. P. 1994. Status of Miscible Flooding Technology. 14th World Petroleum Congress, Stavanger, Norway. *Society of Petroleum Engineering*. WPS-26169.

Heller, J. P., Lien, C. L., & Kuntamukkula, M. S. 1985. Foamlike Dispersions for Mobility Control in CO_2 Floods. Society of Petroleum Engineers Journal, **25** (04). SPE-11233-PA.

Hill, R. M. 1993. Applications of surfactant mixtures. In *Mixed Surfactant Systems*, Chapter 11: 317-336. *Surfactant Science Series. Volume 46*. Marcel Dekker, Inc.

Hirasaki, G. J. "Supplement to SPE 19505, the Steam-Foam Process--Review of Steam-Foam Process Mechanisms." SPE-19518-MS: Society of Petroleum Engineers, 1989.

Hirasaki, George, Clarence A. Miller, and Maura Puerto. 2011. Recent Advances in Surfactant EOE. *SPE Journal*. **16** (04). SPE-115386-PA.

Hoefner, M. L., E. M. Evans, J. J. Buckles, and T. A. Jones. "CO_2 Foam: Results from Four Developmental Field Trials." *SPE Reservoir Engineering* 10, no. 04 (1995).

Holland, P. M., & Rubingh, D. N. 1992. Mixed Surfactant Systems. In *Mixed Surfactant Systems, Volume 501*: 2-30. American Chemical Society.

Huh, D. G., and L. L. Handy. 1989. Comparison of Steady and Unsteady-State Flow of Gas and Foaming Solution in Porous Media. *SPE Reservoir Engineering* **4** (01). SPE-15078-PA.

Kovscek A R and C J Radke. 1994. Fundamentals of From Transport in Porous Media. In *Foams Fundamentals and Applications in the Petroleum Industry*, Chap. 3, 115-163. *Advances in Chemistry*, Americam Chemical Society.

Kuhlman, M. I., Lau, H. C., & Falls, A. H. 2000. Surfactant Criteria for Successful Carbon Dioxide Foam in Sandstone Reservoirs. *SPE Journal*. SPE-60855-PA.

Lai, K. Y., & Dixit, N. 1996. Additives for foams. In *Foam Theory, Measurements, and Applications*, Chapter 8: 315-338. Surfactants Science Series. Volume 57.

Lawson, Jimmie B., and Joseph Reisberg. 1980. Alternate Slugs of Gas and Dilute Surfactant for Mobility Control During Chemical Flooding. *SPE/DOE Enhanced Oil Recovery Symposium*. Tulsa, Oklahoma: Society of Petroleum Engineers. SPE-8839-MS.

Lee, H. O., & Heller, J. P. (1990). Laboratory Measurements of CO_2-Foam Mobility. doi: 10.2118/17363-pa

Lee, H. O., J. P. Heller, and A. M. W. Hoefer. 1991. Change in Apparent Viscosity of CO_2 Foam with Rock Permeability. *SPE Reservoir Engineering.***6 (**04). SPE-20194-PA.

Li, Robert F., George Hirasaki, Clarence A. Miller, and Shehadeh K. Masalmeh. 2012. Wettability Alteration and Foam Mobility Control in a Layered, 2d Heterogeneous Sandpack. *SPE Journal.* **17** (04). SPE-141462-PA.

Llave, F. M., and D. K. Olsen. 1994. Use of Mixed Surfactants to Generate Foams for Mobility Control in Chemical Flooding. *SPE Reservoir Engineering*. **9** (02). SPE-20223-PA.

Lunkenheimer, K. and K. Malysa. 2003. Simple and Generally Applicable Method of Determination and Evaluation of Foam Properties. *Journal of Surfactants and Detergents*. **6** (1): 69-74.

Maini, B. B. 1986. Laboratory Evaluation Of Foaming Agents For High Temperature Applications -III. Effect Of Residual Oil On Mobility Reduction Performance. Annual Technical Meeting, Calgary, Alberta. *Petroleum Society of Canada.* PETSOC-86-37-01.

Manev, E. D., S. V. Sazdanova, and D. T. Wasan. 1984. Stratification in Emulsion Films. *Journal of Dispersion Science and Technology* **5** (2): 111-117.

Mannhardt, K., Novosad, J., & Schramm, L. 2000. Comparative evaluation of foam stability to oil. SPE Reservoir Evaluation & Engineering. **3** (01): 23-34.

Manrique, E. Jose, C. P. Thomas, Ravi Ravikiran et al. 2010. EOR: Current Status and Opportunities. SPE Improved Oil Recovery Symposium. Tulsa, Oklahoma, USA. SPE-130113-MS.

Marsden, S. S., and Suhail A. Khan. 1966. The Flow of Foam through Short Porous Media and Apparent Viscosity Measurements. *Society of Petroleum Engineers Journal* **6** (01).

Nikolov, A. D., P. A. Kralchevsky, I. B. Ivanov, and D. T. Wasan. 1989. Ordered Micelle Structuring in Thin Films Formed from Anionic Surfactant Solutions. *Journal of Colloid and Interface Science* **133** (1): 13-22.

Nikolov, A., Wasan, D., Huang, D., & Edwards, D. 1986. The Effect of Oil on Foam Stability: Mechanisms and Implications for Oil Displacement by Foam in Porous Media. The 61st Annual Technical Conference and Exhibition. Society of Petroleum Engineers, New Orleans, LA. SPE-15443-MS.

Oh, S. G., & Shah, D. O. 1991. Relationship Between Micellar Lifetime and Foamability of SDS and Sodium Dodecyl Sulfate/1-Hexanol Mixtures. *Langmuir*. **7** (7): 1316-1318.

Patist, A., Axelberd, T., & Shah, D. O. 1998. Effect of Long Chain Alcohols on Micellar Relaxation Time and Foaming Properties of Sodium Dodecyl Sulfate Solutions. *Journal of Colloid and Interface Science,* **208** (1), 259-265.

Patist, A., Devi, S., & Shah, D. O. 1999. Importance of 1:3 Molecular Ratio on the Interfacial Properties of Mixed Surfactant Systems. *Langmuir*. **15** (21): 7403-7405.

Patist, A., Jha, B. K., Oh, S.-G., & Shah, D. O. (1999). Importance of micellar relaxation time on detergent properties. *Journal of Surfactants and Detergents*. **2** (3): 317-324.

Patist, A., Oh, S. G., Leung, R., & Shah, D. O. 2001. Kinetics of Micellization: its Significance to Technological Processes. *Colloids and Surfaces A: Physicochemical and Engineering Aspects.* **176** (1): 3-16.

Patist, A., Oh, S.-G., Shiao, S., Ling, T., Lee, K., Sharma, M., . . . Shah, D. 2000. Unity in Diversity in Interfacial Phenomena. In *Emulsions, Foams and Thin Films.* Chapter 2: 31-59. Marcel Dekker Inc., New York.

Porter, M. R. 1994. Handbook of Surfactants. *Blackie Academic & Professional*. Second ed.. Galsgow. United Kingdom.

Prud'homme, & Khan, R. 1995. Foams: Theory, Measurements, and Applications, Volume 57, CRC Press.

Puerto, M., Hirasaki, G. J., Miller, C. A., & Barnes, J. R. 2012. Surfactant Systems for EOR in High-Temperature, High-Salinity Environments. *SPE Journal.* **17** (1). SPE-129675-PA.

R. Fink., E.J. Beckman. 2000. Phase Behavior of Siloxane-Based Amphiphiles in Supercritical Carbon Dioxide. Journal of Supercritical Fluids. **18** (2): 101-110.

Rafati, R., Hamidi, H., Idris, A. K., & Manan, M. A. 2012. Application of sustainable foaming agents to control the mobility of carbon dioxide in enhanced oil recovery. *Egyptian Journal of Petroleum.* **21** (2): 155-163.

Ransohoff, T. C., and C. J. Radke. 1988. Mechanisms of Foam Generation in Glass-Bead Packs. *SPE Reservoir Engineering* **3 (**02). SPE-15441-PA.

Rider, E. and International Energy Agency IEA. 1993. *Collaborative Project on Enhanced Oil Recovery 14th International Workshop and Symposium*. Vienna, Austria: IEA.

Rosen, M. J. 2004. Molecular Interactions and Synergism in Mixtures of Two Surfactants. In *Surfactants and Interfacial Phenomena*. Chapter 11, 379-414. John Wiley & Sons, Inc.

Rosen, M. J. Surfactants and Interfacial Phenomena. 3 ed. Hoboken, New Jersey, USA: John-Willey & Sons Inc., 2004.

Rosen, M. J., & Kunjappu, J. T. 2004. Foaming and Antifoaming by Aqueous Solutions of Surfactants. In *Surfactants and Interfacial Phenomena.* Chapter 7, 308-335. *John Wiley & Sons, Inc*.

Rosen, M. J., & Solash, J. 1969. Factors Affecting Initial Foam Height in the Ross-Miles Foam Test. *Journal of the American Oil Chemists' Society*. **46** (8): 399-402.

Rosen, M. J., & Zhu, Z. H. (1988). Synergism in binary mixtures of surfactants. 7. Synergism in foaming and its relation to other types of synergism. Journal of the American Oil Chemists' Society, 65(4), 663-668.

Rosen, M., Surfactants and Interfacial Phenomena, A John-Willey & Sons, 2000 get the page and the chapter)

Ross, S., & Bramfitt, T. H. 1957. Inhibition of Foaming. VIII. Changes in Electrical Conductivity of Colloidal Electrolyte Solutions on Addition of Non-ionic Foam Stabilizers and Foam Inhibitors. *The Journal of Physical Chemistry*. **61** (10): 1261-1265.

Ross, S., & Haak, R. 1958. Inhibition of Foaming. IX. Changes in the Rate of Attaining Surface Tension Equilibrium in Solutions of Surface-active Agents on Addition of Foam Inhibitors and Foam Stabilizers. *The Journal of Physical Chemistry*. **62** (10): 1260-1264.

Rossen, W. R., and P. A. Gauglitz. 1990. Percolation Theory of Creation and Mobilization of Foams in Porous Media. *AIChE Journal* **36** (8): 1176-1188.

Sahimi M., Rasaei M. R., Haghighi M. 2006. Gas Injection and Fingering in Porous Media. *Theory and Application of Transport in Porous Media* **(20)**. Springer: 133–168.

Salehi, M. M., Safarzadeh, M. A., Sahraei, E., & Nejad, S. A. T. (2013). Experimental study of surfactant alternating gas injection versus water alternating gas and water flooding enhanced oil recovery methods. Journal of Petroleum and Gas Engineering, 4(6), 160-172.

Sanchez, J. M., and R. D. Hazlett. 1992. Foam Flow through an Oil-Wet Porous Medium: A Laboratory Study. *SPE Reservoir Engineering* **7 (**01).

Sanders, A., Nguyen, Q. P., Nguyen, N., Adkins, S., & Johnston, K. P. (2010). Twin-Tailed Surfactants for Creating CO_2-in-Water Macroemulsions for Sweep Enhancement in CO_2-EOR.

Schick, M. J., & Fowkes, F. M. 1957. Foam Stabilizing Additives for Synthetic Detergents. Interaction of Additives and Detergents in Mixed Micelles. *The Journal of Physical Chemistry.* **61** (8): 1062-1068.

Schramm, L. L., & Wassmuth, F. 1994. Foams: Basic Principles. In *Foams: Fundamentals and Applications in the Petroleum Industry.* Volume **242**. Chap. 1, 3-45. American Chemical Society.

Schramm, L.L. and J.J. Novosad, Micro-visualization of foam interactions with a crude oil. Colloids and Surfaces, 1990. 46(1): p. 21-43.

Schramm, L.L. and Kutay, S. M.. 2000. Emulsions and Foams in Petroleum Industry. In *Surfactants: Fundamentals and Applications in the Petroleum Industry*, Chap. 3, 79-121. Cambridge University Press.

Shah, D. O. (1971). Significance of the 1:3 Molecular Ratio in Mixed Surfactant Systems. *Journal of Colloid and Interface Science*. **37** (4): 744-752.

Sharma, M. K., Shah, D. O., & Brigham, W. E. 1984. Correlation of Chain Length Compatibility and Surface Properties of Mixed Foaming agents with fluid displacement efficiency and effective air mobility in porous media. *Industrial & Engineering Chemistry Fundamentals*. **23** (2): 213-220.

Shiao, S. Y., Chhabra, V., Patist, A., Free, M. L., Huibers, P. D. T., Gregory, A., . . . Shah, D. O. (1998). Chain length compatibility effects in mixed surfactant systems for technological applications. Advances in Colloid and Interface Science, 74(1–3), 1-29. doi: https://doi.org/10.1016/S0001-8686(97)00005-5

Simjoo, M., Rezaei, T., Andrianov, A., & Zitha, P. (2013). Foam stability in the presence of oil: Effect of surfactant concentration and oil type. Colloids and Surfaces A: Physicochemical and Engineering Aspects, 438, 148-158.

Syahputra, Andy Eka, Jyun-Syung Tsau, and Reid B. Grigg. 2000. Laboratory Evaluation of Using Lignosulfonate and Surfactant Mixture in CO_2 Flooding. *SPE/DOE Improved Oil Recovery Symposium*. Tulsa, Oklahoma. Society of Petroleum Engineers. SPE-59368-MS.

Taber, J.J., Martin, F.D. and Seright, R.S. 1997. EOR Screening Criteria Revisited - Part 1: Introduction to Screening Criteria and Enhanced Recovery Field Projects. SPERE 12 (3): 189-198. doi: 10.2118/35385-PA.

Talebian, S. H., Masoudi, R., Tan, I. M., & Zitha, P. L. J. 2013. Foam assisted CO_2-EOR; Concepts, Challenges and Applications. *SPE Enhanced Oil Recovery Conference*. Society of Petroleum Engineers. SPE-165280-MS.

Talley, L. D. Hydrolytic Stability of Alkylethoxy Sulfates. 1988. SPE Reservoir Engineering. **3** (1). SPE-14912-PA.

Theander, K., & Pugh, R. J. 2003. Synergism and Foaming Properties in Mixed Nonionic/Fatty Acid Soap Surfactant Systems. *Journal of Colloid and Interface Science*, **267** (1): 9-17.

Torino, E., Reverchon, E., & Johnston, K. P. 2010. Carbon Dioxide/Water, Water/Carbon Dioxide Emulsions and Double Emulsions Stabilized With a Nonionic Biocompatible Surfactant. *Journal of Colloid and Interface Science*. **348** (2): 469-478.

Tsau, Jyun-Syung, and J. P. Heller. 1992. Evaluation of Surfactants for CO_2-Foam Mobility Control. *Permian Basin Oil and Gas Recovery Conference*. Midland, Texas: Society of Petroleum Engineers. SPE-24013-MS.

Tsau, Jyun-Syung, Andy Eka Syahputra, Hossein Yaghoobi, and Reid B. Grigg. 1999. Use of Sacrificial Agents in CO_2 Foam Flooding Application. *SPE Annual Technical Conference and Exhibition*. Houston, Texas, USA. Society of Petroleum Engineers. SPE-55563-MS.

Turta, A. T., & Singhal, A. K. 2002. Field Foam Applications in Enhanced Oil Recovery Projects: Screening and Design Aspects. *Journal of Canadian Petroleum Technology*. **41** (10). PETSOC-02-10-14.

Valaulikar, B. S.; Manohar, C. *J. Colloid Interface Sci*. **1985**,*108*, 403.

Varadaraj, R., Bock, J., Zushma, S., Brons, N., & Colletti, T. 1991. Effect of Hydrocarbon Chain Branching on Interfacial Properties of Monodisperse Ethoxylated Alcohol Surfactants. *Journal of Colloid and Interface Science*. **147** (2): 387-395.

Vikingstad, A. K., & Aarra, M. G. 2009. Comparing the Static and Dynamic foam properties of a fluorinated and an alpha olefin sulfonate surfactant. *Journal of Petroleum Science and Engineering*. **65** (1): 105-111.

Vikingstad, A. K., Skauge, A., Høiland, H., & Aarra, M. 2005. Foam–oil Interactions Analyzed by Static Foam Tests. *Colloids and Surfaces A: Physicochemical and Engineering Aspects*, **260** (1): 189-198.

Wasan, D. T., Koczo, K., & Nikolov, A. D. 1994. Mechanisms of Aqueous Foam Stability and Antifoaming Action with and without Oil Foams. In *Fundamentals and Applications in the Petroleum Industry*. Chap. 2, 3-47. Advances in Chemistry Series **242.** American Chemical Society.

Whorton, L. P., W. F. Kieschnick. 1950. A Preliminary Report on Oil Recovery by High-Pressure Gas Injection. Drilling and Production Practice, New York, USA. API-50-247.

Wilson, A. J. 2013. Foams: physics, chemistry and structure. Springer Science and Business Media.

Xing, D., Wei, B., McLendon, W. J., Enick, R. M., McNulty, S., Trickett, K., Mohamed, A., Cummings, S., Eastoe, J., Rogers, S., Candall, D., Tennant, B., McLendon, T., Romanov, V., Soong, Y. 2011. CO_2-Soluble, Nonionic, Water-Soluble Surfactants That Stabilize CO_2-in-Brine Foams. *SPE Journal.* **17** (4). SPE-129907-PA.

Zhang, Z. F., V. L. Freedman, and L. Zhong. 2009. Foam Transport in Porous Media - a Review. *U. S. Department of Energy*.